The Development of Large-Area Fast Photo-detectors

April 22, 2009

John Anderson, Karen Byrum, Gary Drake, Edward May, Alexander Paramonov, Mayly Sanchez, Robert Stanek, Hendrik Weerts, Matthew Wetstein[1], Zikri Yusof
High Energy Physics Division
Argonne National Laboratory, Argonne, Illinois 60439

Bernhard Adams, Klaus Attenkofer
Advanced Photon Source Division
Argonne National Laboratory, Argonne, Illinois 60439

Zeke Insepov
Mathematics and Computer Sciences Division
Argonne National Laboratory, Argonne, Illinois 60439

Jeffrey Elam, Joseph Libera
Energy Systems Division
Argonne National Laboratory, Argonne, Illinois 60439

Michael Pellin, Igor Veryovkin, Hau Wang, Alexander Zinovev
Materials Science Division
Argonne National Laboratory, Argonne, Illinois 60439

David Beaulieu, Neal Sullivan, Ken Stenton
Arradiance Inc., Sudbury, MA 01776

Mircea Bogdan, Henry Frisch[1], Jean-Francois Genat, Mary Heintz, Richard Northrop, Fukun Tang
Enrico Fermi Institute, University of Chicago, Chicago, Illinois 60637

Erik Ramberg, Anatoly Ronzhin, Greg Sellberg
Fermi National Accelerator Laboratory, Batavia, Illinois 60510

James Kennedy, Kurtis Nishimura, Marc Rosen, Larry Ruckman, Gary Varner
University of Hawaii, 2505 Correa Road, Honolulu, HI, 96822

Robert Abrams, Valentin Ivanov, Thomas Roberts
Muons,Inc 552 N. Batavia Avenue, Batavia, IL 60510

Jerry Va'vra
SLAC National Accelerator Laboratory, Menlo Park, CA 94025

Oswald Siegmund, Anton Tremsin
Space Sciences Laboratory, University of California, Berkeley,CA 94720

Dmitri Routkevitch
Synkera Technologies Inc., Longmont, CO 80501

David Forbush, Tianchi Zhao
Department of Physics, University of Washington, Seattle, WA 98195

[1] Joint appointment Argonne National Laboratory and Enrico Fermi Institute, University of Chicago

The Development of Large-area, Fast, Time-of-Flight Detectors

PROJECT SUMMARY

We propose a program to develop a basic family of economical robust large-area photo-detectors that can be tailored for a wide variety of applications that now use photomultipliers. Advances in materials science and nano-technology, complemented by recent innovations in microelectronics and data processing, give us an opportunity to apply the basic concept of micro-channel plate detectors to the development of large-area economical photo-detectors with quantum efficiencies and gains similar to those of photo-tubes, and with inherent good space and time resolution. The new devices are designed to cover large areas economically, being a sandwich of simple layers rather than an assembly of discrete parts. The plan of R&D that follows is intended to solve the critical technical issues and to deliver proto-types that are ready to be commercialized within 3 years.

The initial use of glass capillary MCP substrates and conventional photo-cathode technology provides a proven solution for each of these components on the critical path. Mechanical assembly and the extension of existing photo-cathode technology to large area planar applications, while formidable tasks, are within the scope of current industrial practice. We have the capabilities and facilities at Argonne, the Space Sciences Laboratory (SSL), and our industrial partners to extend the known technologies.

We have also identified three areas in which new technologies have the potential for transformational developments. First, the development of higher quantum efficiency photo-cathodes based on nano-science morphology with customized work-functions and the adaptation of techniques from the solar-energy sector would allow large area detectors and possibly cheaper assembly techniques. Second, Atomic Layer Deposition (ALD) provides a powerful technique for control of the chemistry and surface characteristics of new photo-cathodes. ALD also can be used to form the secondary emission surfaces of the channels one molecular layer at a time, including controlling the geometry of the electron cascade itself, to enable functionalization of channel-plate substrates with high gain and low noise. This capability allows the separation of the properties of the substrate material from the amplification functionality. We have experience in self-organized nanoporous ceramic (Anodic Aluminum Oxide, AAO) that would provide low-cost batch-produced substrates, and also are investigating substrates made from glass capillaries. Lastly, we have already demonstrated that fast waveform sampling using CMOS ASICs at both ends of transmission line anodes allows the coverage of large areas with small numbers of channels, permitting excellent time and space resolution and a built-in noise identification and reduction mechanism. Design work has started on an ASIC with 2-4 times the number of channels per chip than present chips.

Large-area, robust, and affordable photo-detectors would be transformational in a wide variety of areas. Possible applications include cheaper and more precise Positron Emission Tomography (PET) cameras in medical imaging, scanners for transportation security, and particle detectors in high-energy neutrino and collider physics, astrophysics, and nuclear physics. There would also be many possibilities for new products and spin-off technologies. Because the new devices are planar, relatively thin, and physically robust, they will require less volume and infrastructure in large-area applications for which photomultipliers are presently the current solution, providing additional economies and offering new measurement opportunities.

To meet the challenges we have assembled an experienced cross-disciplinary team that integrates expertise and facilities of national laboratories, universities, and industry, and that includes expertise in both the basic and the applied sciences.

The Development of Large-area, Fast, Time-of-Flight Detectors

PROJECT DESCRIPTION

Contents

1 Introduction **6**
- 1.1 Technical and Scientific Motivation . . . 6
- 1.2 Societal Context . . . 7
- 1.3 The 'Frugal' MCP Concept . . . 7
- 1.4 Organization of the Proposal . . . 8

2 The Critical-Path to Large-Area Fast Detectors: the Needed Three Developments **9**
- 2.1 Photo-cathodes . . . 9
  - 2.1.1 Conventional Bialkali Photo-cathodes . . . 9
  - 2.1.2 R&D on Nano-scale Photo-cathodes . . . 10
  - 2.1.3 Characterization Facilities . . . 11
- 2.2 The First Strike Problem . . . 12
  - 2.2.1 Introduction to Amplification in Micro-Channels . . . 12
  - 2.2.2 Functionalization of MCP's with Atomic Layer Deposition . . . 14
    - 2.2.2.1 Capillary Glass Channel Substrates . . . 14
    - 2.2.2.2 Self-Organized Channel Substrates . . . 16
    - 2.2.2.3 Aerogel Substrates . . . 17
    - 2.2.2.4 Testing of the Functionalized Substrates . . . 17
- 2.3 The Charge Collection and Digitization Problem . . . 17
  - 2.3.1 System Issues: Readout, Calibration, and Clock Distribution . . . 18

3 Mechanical Assembly **18**
- 3.1 Scaling Conventional Ceramic Technology . . . 18
- 3.2 All-Glass Detector Modules . . . 20

4 Deliverables **20**

5 Summary **22**

6 Acknowledgements **22**

7 Work Plans **22**
- 7.1 Overview . . . 22
- 7.2 Characterization of Photo- and Secondary-Emitting Materials . . . 22
- 7.3 Simulation . . . 23
- 7.4 Device Testing . . . 23
- 7.5 Photocathode . . . 23
- 7.6 Amplification Stage: Substrates, Coatings, Scaling . . . 24
- 7.7 Anode . . . 24
- 7.8 Front-End Electronics . . . 24
- 7.9 Mechanical Assembly . . . 24
- 7.10 Integration . . . 24

8 Management **24**
- 8.1 Overview . . . 24
- 8.2 Industry/Lab Partnerships . . . 24
- 8.3 Reviews . . . 24
- 8.4 Transparency/Dissemination . . . 25

9 Milestones **26**
9.1 Year 1 . . . 26
9.2 Year 2 . . . 28
9.3 Year 3 . . . 29

10 Budget **30**

11 Budget Justification **31**

12 Appendix A: Applications **36**
12.1 Overview . . . 36
12.2 Collider Physics: Strange, Charm, Bottom, Top Quark, and Tau Lepton Identification; Photon Vertexing . . . 36
12.3 Medical Imaging . . . 39
12.4 Neutrino Physics . . . 41
12.5 Non-proliferation and Transportation Security . . . 42
12.6 Accelerator Diagnostics . . . 42

13 Appendix B: Simulation of Front-End Electronics **44**

14 Appendix C: Advanced Photo-cathodes **45**

15 Appendix D: Anodized Aluminum Oxide Plates **53**

16 Appendix E: Atomic Layer Deposition for the Fabrication of Microchannel Plates **60**

17 Appendix F: Biographical Sketches **68**

GOAL

The goal of this R&D program is to develop a family of large-area robust photo-detectors that can be tailored for a wide variety of applications for which large-area economical photon detection would be transformational. Progress in modern micro-electronics, materials science, and nano-technology gives us an opportunity to apply micro-channel plate technology to produce large-area photo-detectors with excellent space and time resolution.

In addition to having excellent resolution, the new devices should be relatively economical to produce in quantity, being a simple sandwich of layers rather than an assembly of discrete parts. Because the proposed new devices are planar, relatively thin, and physically robust, there will be additional economies associated with the overall system design for applications such as precision time-of-flight measurements at particle accelerators such as the LHC, RHIC, JPARC, Super-B, and the ILC; Positron-Emission Tomography; large-area detectors such as those being proposed for DUSEL; and non-proliferation security.

The plan of focused R&D that follows is intended to solve the basic technical issues and deliver working prototypes within 3 years.

1 Introduction

1.1 Technical and Scientific Motivation

Photomultipliers are truly remarkable devices, loved and admired by anyone who has worked with them. They are high-bandwidth, high-gain, current-source amplifiers, with high quantum efficiency (QE) for photons [1] and the ability to resolve single photo-electrons. Photomultipliers (PMT's) can have excellent time resolution [2], and multi-anode PMT's allow spatial resolution as well [3]. Specialized PMT's and hybrid variations can be tailored for specific high-precision uses [4, 5]. In addition, PMT's are robust, well-understood, easy to use, and can be quite inexpensive.

Micro-channel plate photo-multipliers (MCP-PMT 's) are an evolution from the basic principles of photo-multipliers, and have been developed to be a robust and mature technology [6, 7, 8, 9, 10, 11] The carefully crafted planes of small pores, which form the amplification sections of the complete MCP-PMT device, have been thoroughly characterized [12, 13, 14, 15], and sophisticated simulation programs and an extensive literature exist to predict their performance[16, 17, 18].

Micro-channel plate photomultipliers combine many of the virtues of photo-multipliers with a relatively simple planar package construction that lends itself to scaling to large-area detectors. In addition, MCP-PMT 's employ a local amplification construction with very small path-lengths for the photon conversion and electron multiplication, resulting in exceptionally fast rise times [19]. Initially driven by the desire to do particle identification at colliders, we have asked the question whether can one make a photo-detector that has all these characteristics at once- in particular both large area and good time resolution. In the process we have solved one of the fundamental problems, the complementarity between time resolution and large transverse dimensions. Two other fundamental problems remain, the production and assembly into devices of planar large-area photocathodes, and the economical large-scale production of amplification sections, as discussed below. However, we believe that there are no 'show-stoppers' for either of these, and a concerted attempt will solve these as well.

The solution to the first problem, which has allowed us to move to the next two, is an anode design that uses transmission lines digitized on both ends by waveform sampling to get position (from the difference in times on the two ends) and time (from the average). The solution is economical as the number of electronics channels goes as L, the transverse size of the MCP-PMT , rather than L^2, as would a pixel detector. The solution also scales well to large transverse sizes, up to many feet in a single panel. There is extensive successful experience with wave-form sampling integrated circuits [20, 21, 22, 23]; sampling chips exist now for many applications, and work is now underway to develop designs in silicon processes with a feature size half that of present chips, allowing up to four times as many channels per chip and the capability of reaching resolutions of a few psec [24].

Some applications motivating the proposal are briefly listed below, with more detail given in Appendix A and in the talks at our biannual workshops, available on the group web page [25].

- High-precision time-of-flight systems, with resolutions below a few pico-seconds, for new or upgraded detectors in particle and nuclear physics. Such a system would provide photon vertexing, multiple-interaction separation, and charge-particle identification. Possible candidates are the LHCb upgrade, the ATLAS upgrade, ALICE, Super-B, future detectors at a muon collider or ILC, and experiments at the precision frontier such as $K_L \to \pi^0 \nu \bar{\nu}$ at JPARC.
- Utilizing the thin planar geometry of these photo-detectors to construct a Positron Emission Tomography (PET) camera employing thin crystals in a sampling-calorimeter configuration, giving depth-of-interaction information as well as superb energy and time resolution. In addition this design would cut system costs as well as the cost of the photo-devices, resulting in a highly economical all-digital design of a clinical PET scanner with depth-of-interaction and TOF measurement [26, 27, 28, 29, 30].
- A large water Cherenkov detector with active photon coverage over essentially 100% of the surface area, using large-area planar MCP-PMT's [31]. Photo-detectors with complete coverage and 100-psec-time and 1"-position resolution on each photon may allow new capabilities, such as increased fiducial volume, π^0-electron separation, track reconstruction, and possibly even the introduction of a low magnetic field for charge determination.
- Diagnostics at accelerators and in beam lines, such as the MANX muon cooling experiment, or the Advanced Photon Source (APS) at Argonne.
- Nuclear non-proliferation and transportation security. MCP's can be optimized for neutron or photon detection; large area panels would allow economical scanners for containers and trucks.

The different applications have different cost targets, as the areas covered and resolution requirements are so different. For example, the surface area of the typical collider solenoid to be tiled by MCP-PMT 's [32],

or of a precision time-of-flight (TOF) plane at LHCb [33], is 30 m^2; at \$100,000 per square meter the cost for a transformational [1] time-of-flight system would be 3M\$. Similarly, for Positron Emission Tomography, one planar $8'' \times 8''$ MCP would typically replace 64 photo-tubes and bases [34], with additional reduced electronics costs, so that a target price of even as high as \$1000 per MCP-PMT would result in an order-of-magnitude lower photo-device cost as well as increased capability. For use in a large water Cherenkov detector, to economically achieve 'hermetic' (close to 100%) coverage, which may allow sub-radiation-length vertex resolution for π^0-electron separation and tracking capability [2] requires the ability to integrate the individual components into large panels.

1.2 Societal Context

Figure 1 lists the priorities of Steven Chu, the new Secretary of Energy, as quoted by Deputy Secretary Patricia Dehmer to HEPAP [35]. The development of new photo-detector devices by a consortium of national laboratories, universities, and industry seems precisely what Secretary Chu is talking about. He points out that undertaking risks on long-term technical developments with high pay-offs is indeed the role of the national labs, which should be less risk-averse than industry. We will not get everything right, and as this is R&D, we cannot forsee every eventuality or plan the out-years in detail. But a great deal of work has been done in industry and universities over the last several decades, and consequently a number of technologies have matured substantially, [3] giving us hope that a concerted effort can advance them to the point where they can come together to produce a device with transformational capabilities [36]. In addition, we have spent the last 5 years developing a new and essential capability [24, 37]. We believe that if this group of labs, universities, and industry cannot successfully complete this development in three years, then it is likely that nobody can, at least not in the US. The goal has an exceptionally high payoff in spin-off applications as well as in the science we want to do with it, and we believe we have a very high chance of success.

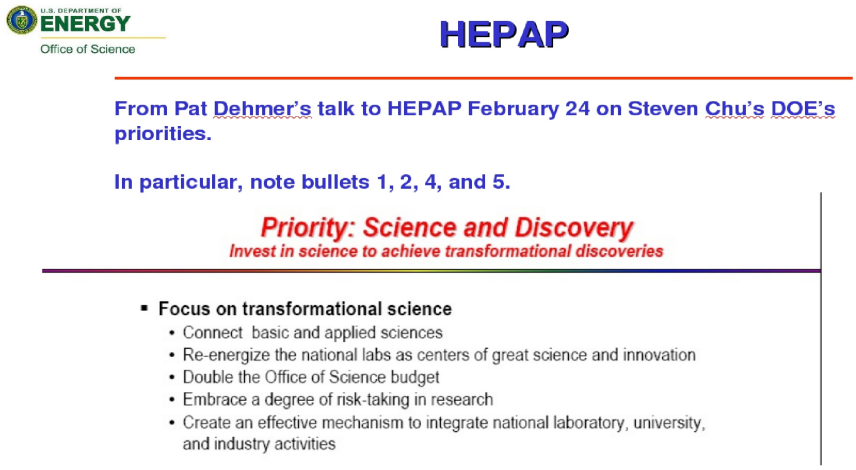

Figure 1: The priorities of the DOE as quoted from Secretary Chu by Patricia Dehmer, Deputy Director for Science Programs, DOE Office of Science [35].

1.3 The 'Frugal' MCP Concept

Up to this point we have done our development R&D using commercial MCP-PMT 's, which are typically a factor of 10 to 100 more expensive per unit area than a typical PMT [6]. However, it has been an instructive exercise to consider a 'strawman' design for a simple MCP-PMT, to be used as a test-bed for scaling up the interior pieces to larger areas. Figure 2 shows a 'cartoon' of the concept of an economical large-area prototypical MCP-PMT module, which in principle could be the basis for a much larger mosaic of either complete modules,

[1] Resolution < 10 psec for charged particles and photon-vertexing to 3mm in the direction of flight

[2] Simulation studies of the effects of light-scattering and multiple scattering of the charged particles on these tracking capabilities are beginning inside the DUSEL collaboration with joint members of our group.

[3] For a notable example, see Ref. [1].

or only the active layers in a single common shell (4-foot-long anode transmission lines that span multiple 8" panels will a bandwidth over 1 GHz). We are exploring the costs for scaling up a conventional ceramic body, used with immense success for many years at SSL [9, 10, 11] and industry, and also for an all-glass design, for which there exists an industrial base for televisions, monitors, and other displays [38], and also extensive expertise at Argonne. The glass alternative is attractive in principle for size and cost considerations, but we will need to solve a set of problems for MCP-PMT production already solved in the ceramic solution: applying transmission lines to the anode plane, internal electrical connections, getting the signals out without too much loss of fidelity, glass-to-glass seals, mechanical integrity, implementation of getters, and bake-out, among others.

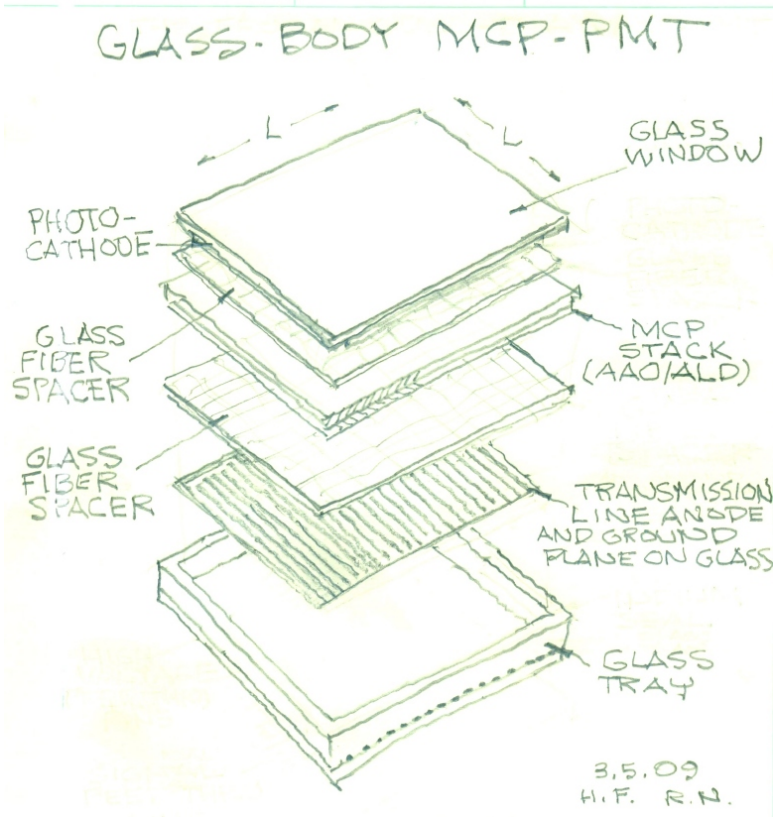

Figure 2: A 'cartoon' of the concept of a glass 'frugal' MCP-PMT , used as the basis for discussion of design choices and costs. The goal is to reduce the cost of each of the components and of the overall assembly. We are considering construction both with ceramic, for which there is extensive experience [9, 10, 11], and glass, such is used in flat-panel televisions. The interior pieces lend themselves to 'tiling' large areas within a panel, and would be integrated into a single monolithic detector sub-assembly. The development of a robust nano-structured photo-cathode material would allow bypassing vacuum assembly, making the assembly of large panels feasible. Note that the pattern and layout of the anode transmission line is easily optimized to the desired granularity and geometry, with the number of channels variable from one to many.

1.4 Organization of the Proposal

The proposal is organized as follows:

Section 1 has given a brief introduction to the motivation for considering micro-channel plate technology for large-area photo-detectors, and briefly summarized several of the applications in science and medicine for which the technology would be transformational. Section 2 describes three developments that are on the critical path to the development: photo-cathodes, the amplification section, and charge collection and digitization. Plans for mechanical assembly are presented Section 3. Section 4 describes the three 'deliverables', a developmental size,

a stand-alone module of a typical size for collider or medical imaging applications, and a large panel for low-rate large-area applications. A brief summary and acknowledgments are given in Sections 5 and 6, respectively.

The work plans for each of the sub-areas of development are described in Section 7. Section 8 describes the management structure. The milestones, organized by task and effort, are presented in Section 9. The budget for each of the three years is presented in Section 10, and Section 11 contains the budget justification.

Appendix A describes several applications for which large-area photo-detectors with good space and time resolution would be transformational. Additional detail on the front-end electronics, photo-cathodes, MCP substrates, and Atomic Layer Deposition is given in Appendices B-E. Lastly, biographical sketches are presented in Appendix F.

2 The Critical-Path to Large-Area Fast Detectors: the Needed Three Developments

We see three areas in which our expertise can be applied to develop economical large-area MCP-PMT 's. They are: 1) the scale-up and modification of photo-cathode production technology for larger area planar devices; 2) implementing solutions to the 'first-strike' problem of developing substrates that satisfy the geometry for channel-plate amplification, are low cost and scalable to large areas, and that may also allow new geometries with higher photon detection efficiency and improved single photo-electron resolution; and 3) solving the time/amplitude/transverse-size complementarity problem. We have spent the last several years solving the third problem, and the solution, transmission-line anodes to preserve the signal amplitude and shape with cheap fast low-power waveform sampling on both ends, is the breakthrough that enables the creation of large-area photo-detectors[37, 24].

We bring to these efforts the resources of the Advanced Photon Source (APS), the Center for Nanoscale Materials (CNM), and the Electron Microscopy Center (EMC) at Argonne, as well as the expertise in the five Divisions. Each of the other institutions in the collaboration brings extensive experience in one of the three critical areas, with decades of experience with photo-cathodes at SSL, industrial expertise represented by Arradiance in emissive materials, Muons,Inc in MCP-PMT simulation, and Synkera in self-organized nanoporous ceramics, and long and successful track records by Chicago, Hawaii, and Argonne in electronics systems.

2.1 Photo-cathodes

2.1.1 Conventional Bialkali Photo-cathodes

There have been major advances in photo-cathode development in recent years [1]. Figure 3 shows the recent gains in quantum efficiency by Hamamatsu versus wavelength (left-hand panel), as well as the spectrum of Cherenkov light as observed through water [39] as a reference input spectrum. The technique is very advanced, giving QE of over 40% in the UV/visible spectral regions today. In addition, photocathode processing is low cost and has good yields [36].

We plan to use conventional bialkali photo-cathodes in an $8'' \times 8''$ format and a conventional transmission geometry as the primary choice. SSL has a long history of successfully producing photo-cathodes [40, 41, 42]. The SSL group has produced conventional photo-cathodes larger than 5" square,and has the facilities to go to 8" square, the size we are considering as our basic sub-assembly. The 8" size will also fit in process equipment routinely used by the semi-conductor industry.

The strategy for the bialkali photo-cathodes will be to optimize the SSL bialkali quantum efficiences on development-size (32.8mm) window samples to increase the present quantum-efficiency from $\sim$20% to 30% or more in small samples, and to achieve uniformity in large samples. Once we have achieved the required quantum-efficiency, we will extend the process to the $8'' \times 8''$ format. Work will continue in collaboration with the materials science efforts at Argonne in characterization and simulation, to improve the quantum-efficiency beyond 30%, which is now routinely available from industry(See Figure 3).

We will also explore the quantum-efficiency and stability of opaque photo-cathode geometries by putting cathodes directly on ALD treated substrates in the 32.8 mm development format (see Section 2.2. In principle, opaque photo-cathodes combined with anti-reflection coatings and photon internal capture techniques developed by the solar cell industry should give an increase in quantum-efficiency [43].

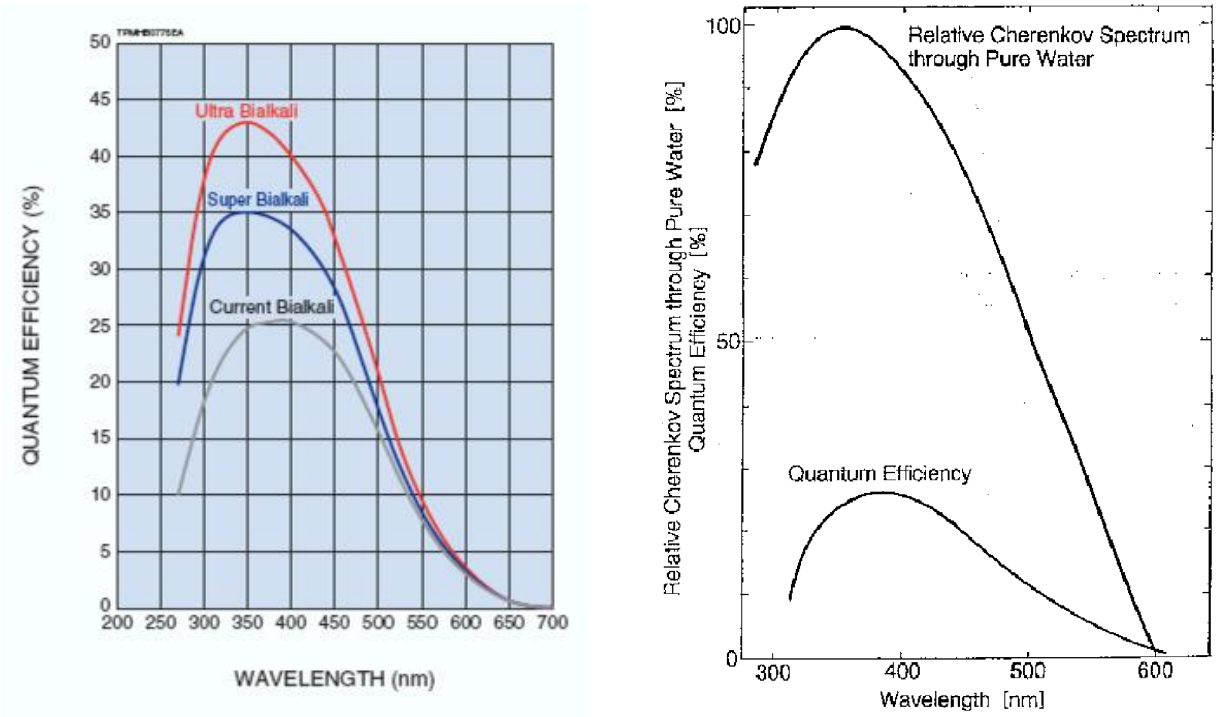

Figure 3: Left: Quantum efficiencies for Hamamatsu bialkali photocathodes, showing the recent developments. Right:The spectrum of Cherenkov light in water, and the quantum efficiency of the Hamamatsu 20" photo-tube used in Super-K (from Ref. [39])

2.1.2 R&D on Nano-scale Photo-cathodes

In parallel with getting our bialkali quantum-efficiency up to industry standards, we will devote effort to develop advanced photo-cathodes using the facilities and strengths in nano-materials at Argonne. The effort will share characterization and test facilities, standard substrates, standard measurement criteria, and expertise with the mainstream effort on bialkali photo-cathodes. The effort will be a coordinated effort between the Advanced Photon Source, Materials Science, Energy Systems, Math and Computer Science, and High Energy Physics Divisions at Argonne and which will take advantage of unique user facilities at the Argonne Advanced Photon Source (APS), Center for Nanoscale Materials (CNM), and Electron Microscopy Center (EMC). In particular, our goal is to develop novel photo-cathodes that appear 'black' to photons in the required spectral region, have high electron emissivity, and can be applied to large panels using Atomic Layer Deposition (ALD) or Chemical Vapor Deposition (CVD), as briefly described below and in Appendix C. A list of references is also attached to Appendix C.

The development of a radically new photocathode material based on nano-technology has the potential for comparable or higher quantum efficiencies (QE's) by optimizing the cathode surface morphology and dielectric constant, and thus tailoring the near-surface electric field so that it significantly enhances photo-electron emission. This approach can become an alternative to lowering the surface work-function of a conventional photo-cathode by fine (and expensive) tuning of its already complex chemical composition. Additional gains in overall detector efficiency may be obtained by using nano-engineered photon-trapping surface geometries with reduced reflection losses, thus benefiting from technologies now standard in the solar cell industry.

The goal for higher quantum efficiency using nano-technology is based on evading the fundamental limitations of conventional transmission photo-cathodes, which are that the electron escape depth is typically smaller than the photon absorption length. This leads to low photon-to-electron conversion eficiency, high energy spread, and a wide angular distribution. Using nano-technology one can optimize the surface technology as shown in Figure 4. What is attractive about nano-technology is that various methods exist to grow different morphologies so that there is a wide range of possibilities(See Figure 5). It is relatively cheap and scalable to large production quantities, and is inherently industrially compatible. Electronic properties can be widely manipulated. However electronic properties and structure are strongly dependent on specific growth conditions, and the basic understanding is not yet solid. A development program thus must have the ability for rapid throughput for

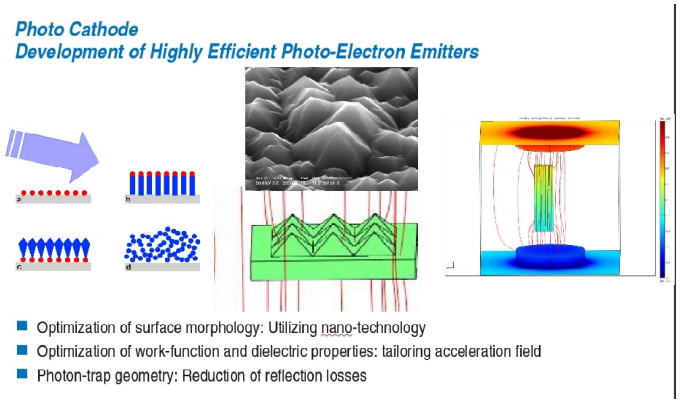

Figure 4: Some basic ideas for developing highly efficient cathodes [44]: using non-normal incidence, back reflectors, total internal reflection, tuning of feature size to minimize reflection and maximize absorption, and control of secondary emission by morphology.

testing many different parameters in parallel, facilities for hard-science characterization and measurement, and theoretical and simulation expertise for rational design. All of these have been developed in other contexts at Argonne, and the leaders of these programs have joined forces in the present effort.

Reproducible material synthesis is impossible without accurate characterization. Emission of photo- and secondary electrons is extremely sensitive to materials properties such as surface composition and structure, including contamination and aging. For characterization we will need structural and electronic probes, an automated fast test capability, local probes for work-function measurements, and the ability to make timing and emission angle measurements. For simulation we will need both static and dynamical models and band-structure calculations. We have access to the Center for Nanoscale Materials at Argonne for initial production.

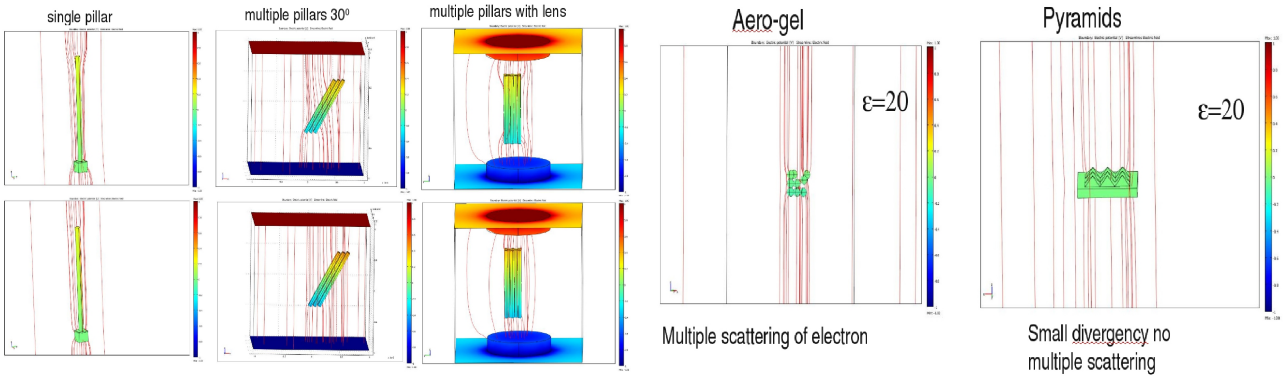

Figure 5: Examples of effects caused by morphology, from a simulation including both the emission characteristics (work-potential- chemistry) and electron optics, including dynamic effects (nano-technology and static/RF-electron simulation). The left-hand panel shows simulations of several geometries; the right-hand panel shows simulations of aerogel and surface pyramid morphologies.

2.1.3 Characterization Facilities

There are programs already underway at Argonne in the APS and HEP Divisions on the development of high-performance photo-cathodes. The authors of the present proposal include experts on the physics of photo-cathodes, the material fabrication and processing of the photo-cathodes, surface and material properties of the photocathode using various techniques such as x-ray diffraction and photo-emission, and the characterization of the photoelectrons generated from these photo-cathodes, such as the distributions in energy and angle. This will allow us to apply the revolution in surface chemistry due to the application of sophisticated surface analysis facilities and theoretical knowledge implemented in simulations to large-area MCP-PMT 's.

We are uniquely able to perform advanced characterization of efficiency vs composition using several highly-evolved facilities at Argonne. Figures 6 and 7 provide a succinct description of the facilities for sputter-depth profiling and sample volatilization, electron-microscope mapping, and nanometer-scale analysis.

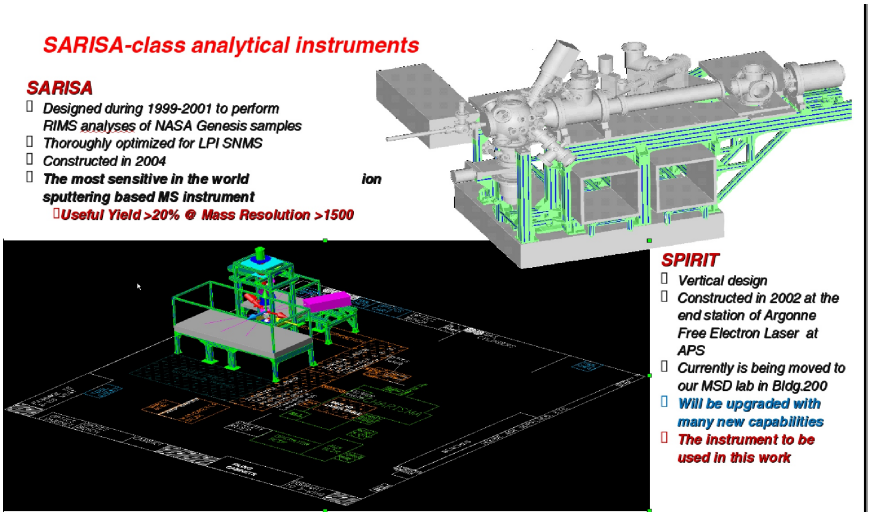

Figure 6: The SARISA-class instruments to be used for characterization and testing of photo-cathode and electron-emitting materials (from I. Veryovkin [45]).

2.2 The First Strike Problem

2.2.1 Introduction to Amplification in Micro-Channels

The second problem on the critical path is to make arrays of channels that have the required characteristics for high efficiency and gain, low noise, a good transit-time-spread, and good amplitude resolution for single photo-electrons. These characteristics include providing a well-defined surface for the first-strike for the incoming photo-electron, large open-area-ratios, and an interior surface with electrical and physical properties to sustain a cascade with enough gain and current capability, while maintaining an acceptable dark current.

We have strength and experience in the technologies needed to attack these problems at Argonne, Arradiance, SSL, and Synkera. Many of the problems have been studied by members of our team [46, 47, 48, 49,

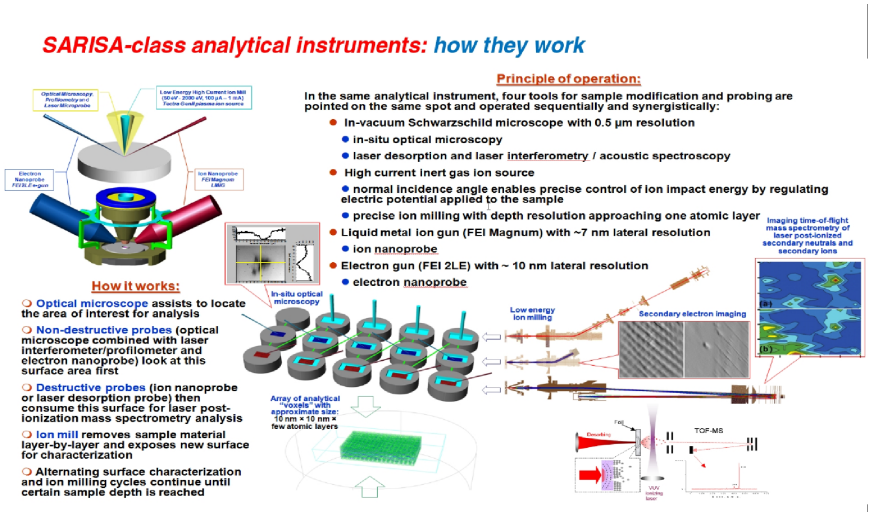

Figure 7: An explanation of how the SARISA-class instruments work (from I. Veryovkin [45]).

50, 51, 17, 52, 53] over the last several years; we bring this expertise to the table so as to be able to concentrate on new materials and the tailoring of the photo-cathode/channel geometry to produce high QE and gain with a well-understood electron shower.

Figure 8 shows the basics of channel geometry. First, the channel needs to provide a first strike for the incoming photo-electrons, followed by successive strikes which provide the amplification. The surface of the channel must provide a current-carrying layer that provides adquate charge, much as the dynode string in a photo-multiplier base does, and a functionalized complex surface layer that provides gain for each strike [54].

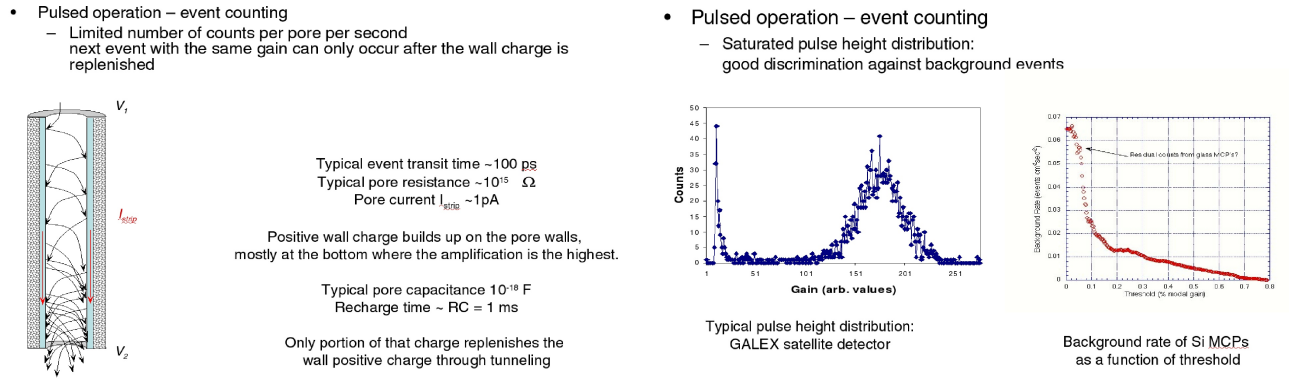

Figure 8: Left: The basics of amplification in a channel. The underlying current-carrying layer provides charge for the shower, and the functionalized complex surface layer provides gain for each strike; Right: A typical pulse height distribution and the rate from a glass MCP vs threshold showing the good separation of background in saturated mode. (from A. Tremsin [25])

Figure 9 is an example of the studies we are doing on the details of the showering inside the channel, with the goal of optimizing transit-time-spread, gain variations, and saturation [55]. However, these simulations are only as good as the input data on the materials, and so a parallel program to survey existing data has started. The emphasis on characterization in our group using the Argonne facilities is driven by this need to have input data that we can trust [56].

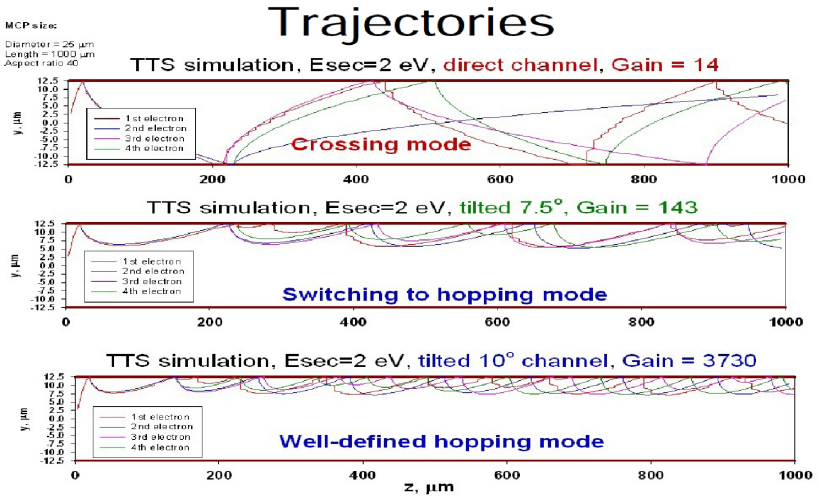

Figure 9: A slide from a study of transit-time-spread in pores (Z. Insepov and V. Ivanov), demonstrating the power of simulation [55]. This also demonstrates how critical it is to have correct input data characterizing the properties of materials.

2.2.2 Functionalization of MCP's with Atomic Layer Deposition

The availability of the technique of Atomic Layer Deposition, ALD, to functionalize MCP's revolutionizes the possibilities for MCP construction by separating the functions of the substrate, which provides the channel geometry, and the ALD surface layers, which provide the current and gain. The use of ALD for MCP's has been proven over the last several years [46], and a great deal of work has been done understanding the basic issues and exploring the multi-dimensional parameter space [46, 47, 48, 49, 50, 51, 17]. Appendix E gives more detail on the use of ALD for MCP's.

ALD also gives the possibility of eventually functionalizing the channels so that they have an internal structure similar to that of a photo-multiplier, with well defined first and second dynodes, for example, in this case implemented as bands of enhanced secondary emission [48]. It may be possible to use ALD to make a photo-cathode in an 'opaque' geometry on the surface of a funnel around the channel opening, as shown in Figure 14, giving a large open-area-ratio even with small channels. Since most of the time jitter is introduced in the photon-conversion and photo-electron drift and the first several strikes in the amplification process, this geometry, with its tight control over the shower development, is predicted to have a remarkable time resolution. In addition, defining the geometry of the shower evolution, much as it is defined by the discrete dynodes of a photo-multiplier, should improve the single photo-electron peak resolution (this is one of the areas we will be addressing using the Muons,Inc MCP simulation).

Fig. 10 shows curves of output current vs input current for an MCP functionalized with ALD [46] and a model that is in good agreement with observations. We start with access to this experience inside the collaboration, with channel performance better than with the standard commercial MCP's [46].

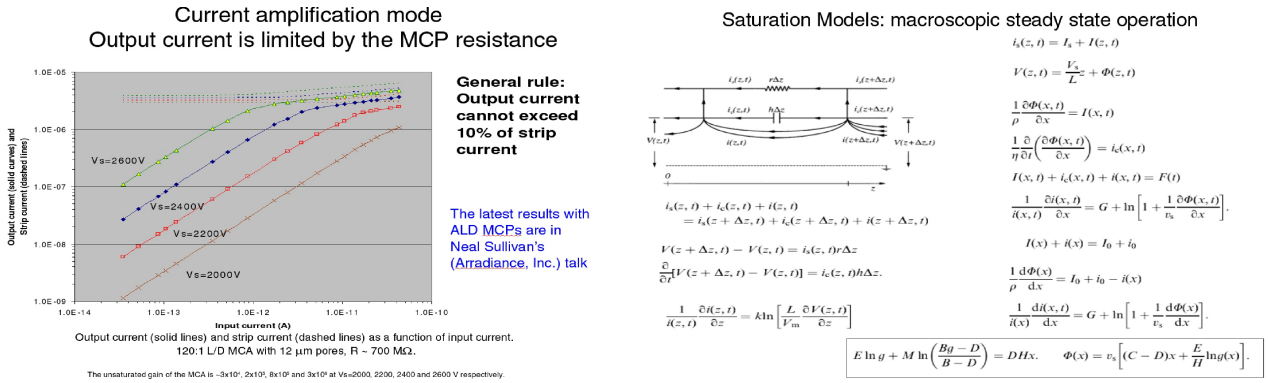

Figure 10: Left: Curves of output current vs input current for an MCP functionalized with ALD [46]. Right: A model of macroscopic steady state operation that is in good agreement with measurements [17], giving us confidence in the channel simulation (from A. Tremsin [25]).

Fig. 11 shows more predictions from the modeling of the channels, again giving us confidence that the ALD aspect of this proposal is under control, with the main issue being scale-up. At the same time, with the combined expertise in characterization and ALD of the group it is possible that we can find major improvements in gain and effective collection area that will translate directly into coverage.

2.2.2.1 Capillary Glass Channel Substrates

We are investigating an attractive solution for the amplification substrate using conventional technology [57]. We have recently located a supplier of glass capillary plates with the requisite properties for making MCP substrates at a cost of less than \$200 per $8'' \times 8''$ chevron plate-pair [58]. Plates are available with 20-40 micron channels, an aspect ratio of 40:1, and a bias angle of 8°, solving the first-strike problem. Presently available small pore plates have open area ratios of 65%, with 83% available for larger pore sizes. Figure 12 shows an array of 40-micron diameter capillaries with an open area ratio of 65%. The left-hand panel of Figure 13 shows a substrate with 50 micron pores. Development is underway to reduce the available pore size to 10 microns or below (see the right-hand panel of Figure 13 [59].)

The capillary glass plates we are considering are much simpler to produce than those used in commercial MCP's, and consequently are much cheaper to produce in large areas. Because the resistive and amplification layers are implemented by functionalizing with ALD rather than the many-step reducing treatment used in conventional MCP production,these substrates provide only the physical substrate geometry, with no special requirements on the type of glass or the surface treatment. In addition, the type of glass used is decoupled from

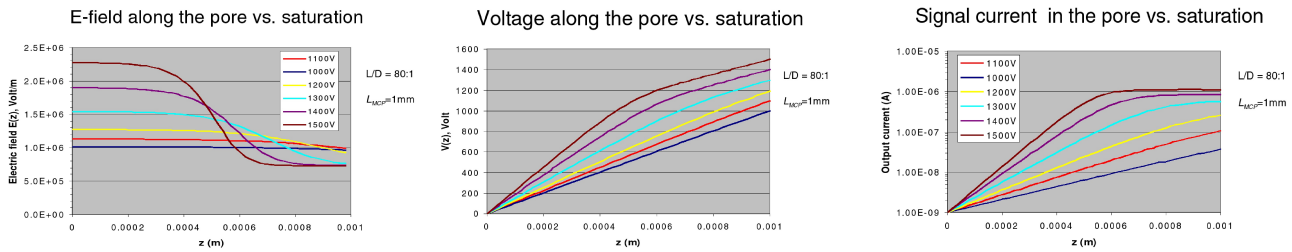

Figure 11: Left: The predicted electric field distribution along the channel for different operating voltages. Middle : The electric potential along the channel. Right: The current along the channel. These predictions match the data well, giving us confidence in our understanding of the operation of MCP and the field configuration even in the presence of saturation (from A. Tremsin [25])

.

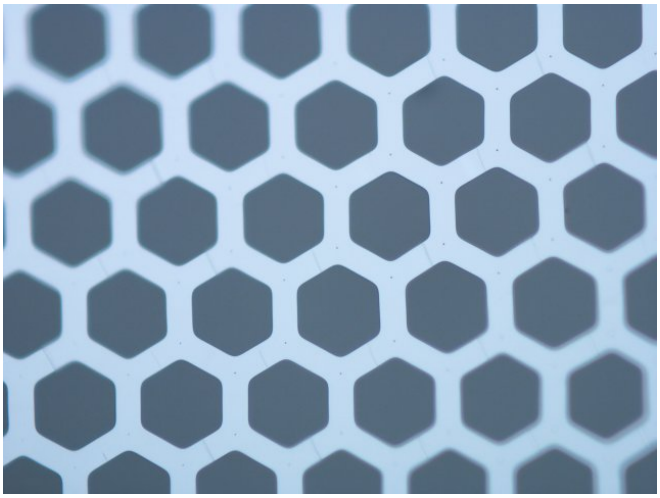

Figure 12: A microscope image of a glass 40-micron diameter capillary array with 65% open area from Incom,Inc.

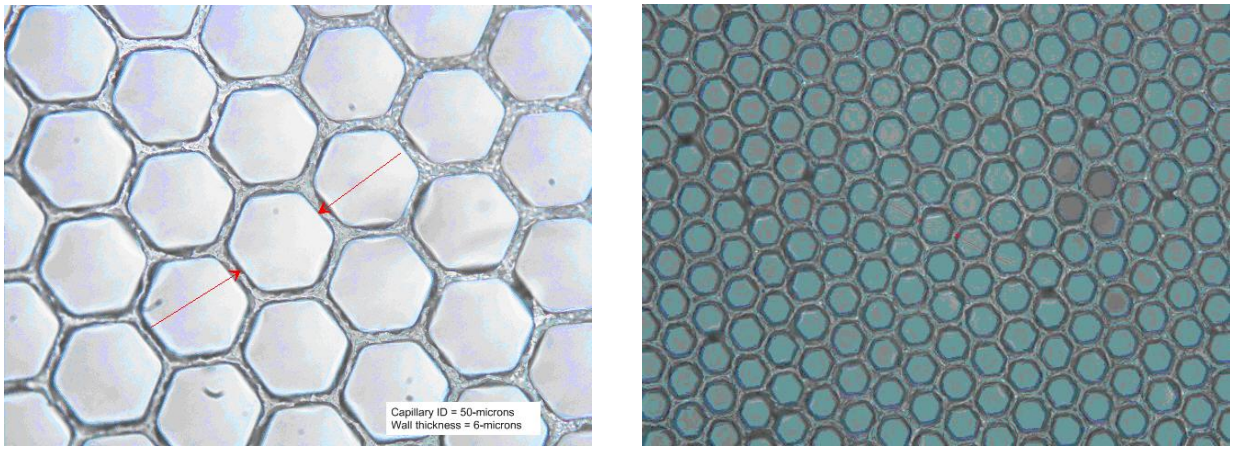

Figure 13: Left: A 500×-magnification microscope image of a capillary array from Incom,Inc. Wafer dimensions are 1" × 1" by 0.100" thick. The capillary ID measured flat-to-flat is 50-microns, with a wall thickness of 6-microns. Right:A 500×-magnification microscope image of a MCP array from Incom,Inc with 10-micron diameter channels, measured flat-to-flat. The wafer is 2" × 2" by 0.055" thick.

the amplification requirements, so that inexpensive and robust boro-silicate glasses able to withstand temperatures well above $700^{\circ}C$ (even up beyond $1500^{\circ}C$) can be used [59].

We are currently aggressively pursuing this path with 32.8mm samples to test the ALD and photo-cathode characterization. This path may prove to be a more-than-acceptable solution that is available now. The use of glass capillary substrates would also allow us to go ahead more quickly on the ALD optimization. We thus regard the capillary glass development path as the most-likely path to low-cost substrates. However we are also considering several more radical alternatives that have some attractive characteristics and that may lead to new applications or developments, and these are discussed below.

2.2.2.2 Self-Organized Channel Substrates Self-Organized substrates that can be produced in batch processes are attractive as possible economical alternatives to glasses. These alternative substrates may allow different capabilities, such as low background radiation compared to glass, or different geometries such as funnel entrances for opaque photo-cathodes. We plan on exploring these novel alternatives to glass capillaries until we understand the best solution for cost and mechanical properties.

One such substrate is Anodic Aluminum Oxide, AAO. AAO is a well-known self-organized material that contains highly uniform cylindrical nanopores, and can be made in a batch process. However, pores made in an intrinsic process (i.e. not micro-machined) are naturally small, typically a few hundred nanometers. To make MCP channels, pore diameters in intrinsic AAO of at least >0.5 μm , and preferably >1 μm , are needed. Synkera has demonstrated the feasibility of 0.5-0.6 μm channels with a funnel-like entrance on one face, and complementary research is going on at Argonne in the Materials Science Division. More details about the AAO developments at Argonne and Synkera are available in Appendix D.

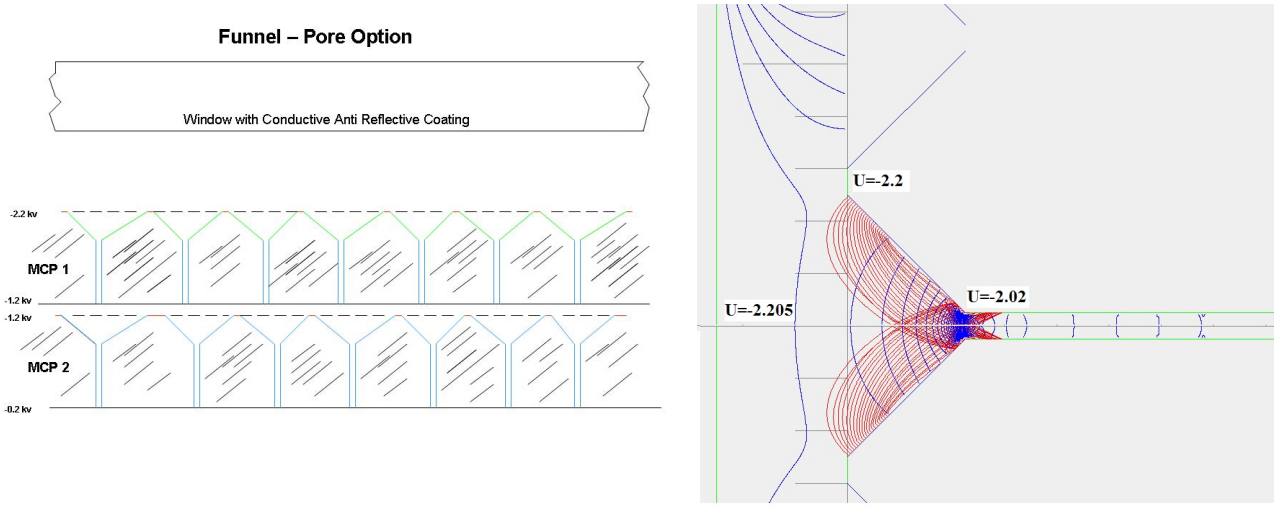

Figure 14: Left: A sketch showing the funnel solution to the first-strike problem. The funnel surface would be coated with a secondary emitter, either the photo-cathode or a first-strike surface (in the first case the window would be coated with a transparent conducting surface optimized for non-reflection; in the second the window coating would be the photo-cathode). By moving the photocathode out of the line of the channel one ameliorates the ion-aging problem, as well as possibly allowing for smaller (e.g. 1μm) channels with a large fractional coverage. Right: A simulation [16] of the equi-potentials (blue) and secondary electron trajectories (red) for a small-channel/large-open-area AAO design (the top window is on the left, and the channel runs to the right.)

We have several proposals for improving the open-area ratio and better determining the place of first strike, including making the entrance to the channel into a funnel, as shown in the left-hand panel of Figure 14, so that the electron strikes the surface of the funnel and secondary electrons are sucked into the channel (See Appendix D). Alternatively, the funnel could be directly coated with the photo-cathode material, with the photo-electron or electrons then initiating the shower in the channel, as shown in the simulation in the right-hand panel of Figure 14. The funnel solution is also attractive in that it hides the photo-cathode from ion feedback– ions that are created on the channel walls and accelerated back up the channel [60, 61]. These ions are a cause of aging of MCP's, and can be a problem at high gain.

The development of ALD and AAO will be done in the small 'development' format, which is 32.8 mm round, for speed and ease of testing. Static testing will be done at Argonne, Arradiance, SSL, and Synkera.

2.2.2.3 Aerogel Substrates

While the traditional architecture for electron amplifying channel plate's has been arrays of micron sized tubes, the only scaffold requirements are 1) a high surface area of electron amplifying media to provide gain, 2) a strong electric field gradient to guide electrons and recharge the surface, and 3) a large open porosity to allow electrons to traverse from front to back. Aerogels are relatively inexpensive materials that when functionalized by Atomic Layer Deposition can also provide these three requirements. When compared to conventional channel plates, aerogel-templated materials have larger open area ratios, larger surface areas, and are relatively easy to fabricate in large flat form factors. We have already demonstrated that aerogels can both be functionalized and work well as photo-anodes for solar cells [62, 63]. The on-going program involving Argonne on aerogels can be used to prepare samples for characterization and gain measurements with little additional investment of effort or funding.

2.2.2.4 Testing of the Functionalized Substrates

The dynamic response of the development MCP plates will be tested using an X-ray streak camera now in operation at Sector 7 of the APS. In this device, electrons are created by a laser striking a photocathode, and then focused on the sample MCP. The output pulse from the MCP is then streaked out to precisely determine its waveform. The current leaving the sample MCP may also be measured electronically by steering it statically onto an optional microwave strip line near the readout MCP, providing a measurement of the gain.

Facilities for the simpler static tests of gain can be performed at Arradiance, Synkera, SSL, and in multiple setups at Argonne.

2.3 The Charge Collection and Digitization Problem

In order to take advantage of large-area photo-detectors with good intrinsic space and time resolution, one has to solve the problems of building high-speed front-end electronics systems with low power and cost, and also collecting signal over distances large compared to the time resolution while preserving the fast time resolution inherent in the small feature size of the detectors themselves. [4] Since some of the applications such as large water Cherenkov detectors require thousands of square meters of photo-detector, the readout electronics have to be integrated with the photo-detector itself in order to provide adequate analog band-width and to reduce the channel count and power. The two problems require an integrated solution.

The physical design proposed here uses strip transmission lines [37] which serve as the MCP anodes, i.e. are inside the vacuum volume. Both ends of each line are sampled by a channel of the front-end waveform sampling chip (See Fig. 15). The time of a pulse is given by the average of the times measured at the two ends, and the position along the line by the difference, as shown in Figure 16. The orthogonal coordinate is given by which lines are hit and the relative pulse heights and shapes. Simulations of the integrated system for a 2-inch-square MCP give expected time resolutions down to several psec and spatial resolutions of 0.1mm [24].

We have recently made the corresponding measurements, shown in Fig. 17, and find a spatial resolution of 97 microns a relative time resolution between the two ends of several psec, which are also in excellent agreement with the simulation [5]

Simulations of 48-inch-long transmission lines, such as one might have in a large water Cherenkov detector at DUSEL, show the bandwidth remains above 1 GHz, as shown in Fig. 18. The combined solution of transmission lines with waveform sampling at each end allows covering large areas with a 1-dimensional array,

[4] Space and time resolution will probably be necessary in low-cost large-panel detector technologies as the noise rate from an emitter-based cathode or a batch-process MCP may integrate over large areas to be significant. Spatial resolution allows the identification of 'hot-spots' which then can be identified and eliminated in the local FPGA without ever entering the data stream. This is particularly important given our goal of very high QE photo-cathodes, which well may have locally high dark-currents due to occasional hot-spots of field-emission due to surface defects or impurities. We can suppress these in the front-end electronics automatically, with the FPGA itself keeping only an internal list of the areas that are bad actors. This would not be feasible while maintaining high efficiency without superb space and time resolution.

[5] We do not yet have the ability to measure absolute time resolutions below 6 psec, which is what we achieve with the laser test stand, and is presently limited by electronics and details of the test setup.

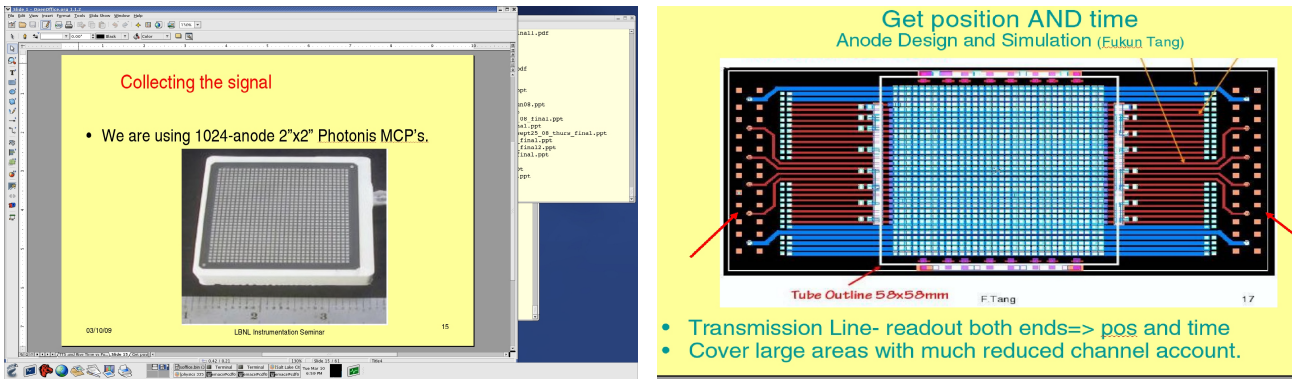

Figure 15: Left: The 32×32 array of anode pads on the Photonis Planacon MCP we are presently using to test the simulation and the transmission line boards. Right: The layout of the transmission line board showing the 32×32 array of pads which connect to the anode pads on the MCP. In the proposed devices the transmission lines will be inside the vacuum enclosure and will form the anodes directly, a simpler and more robust solution.

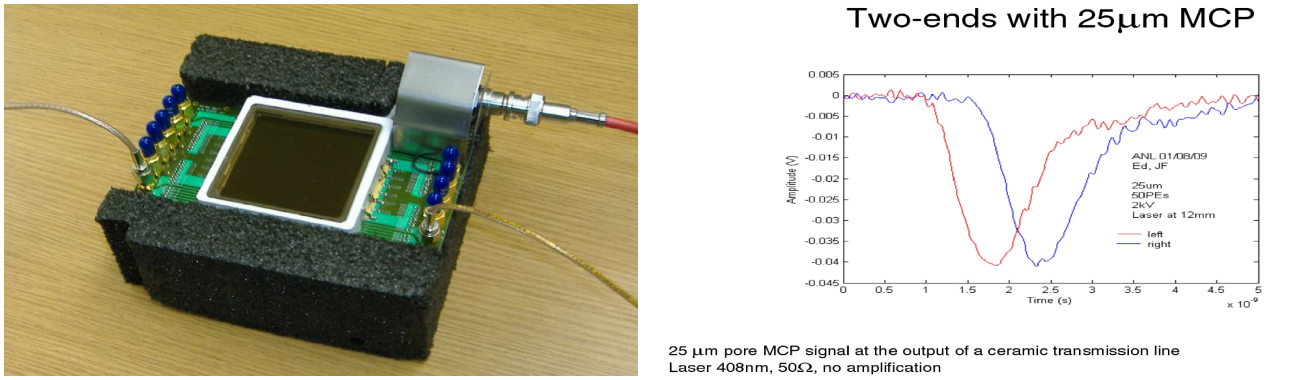

Figure 16: Left: The Photonis Planacon and transmission line readout anode card. Right: A scope trace of the two ends of the transmission line readout for a laser pulse equivalent to 50 photo-electrons incident on the Planacon.

with a greatly reduced channel count and expense. The system provides excellent temporal and 2-dimensional spatial resolution as an added bonus intrinsic to the design [6].

2.3.1 System Issues: Readout, Calibration, and Clock Distribution

The sampling chips require a non-trivial infrastructure to be a system. The Argonne HEP electronics engineering group has put substantial effort into investigating a clock distribution system with psec stability and control, and have a demonstration board that meets our initial specs. Preliminary designs of the interface to a XILINX FPGA to control and readout the front-end chips also exist.

3 Mechanical Assembly

3.1 Scaling Conventional Ceramic Technology

To get to larger size individual MCP's, an extension of the ceramic technology that is used in space exploration and night vision to larger detectors will be started at SSL. This is a proven technology that has high reliability and low cost, and is used by night vision vendors to provide assemblies at thousands of units per month with high reliability and low cost. Figure 19 shows the mechanical assembly for the ceramic technology used by SSL.

[6] The costs for large-area are dominated by other factors than readout; the differential savings in eliminating

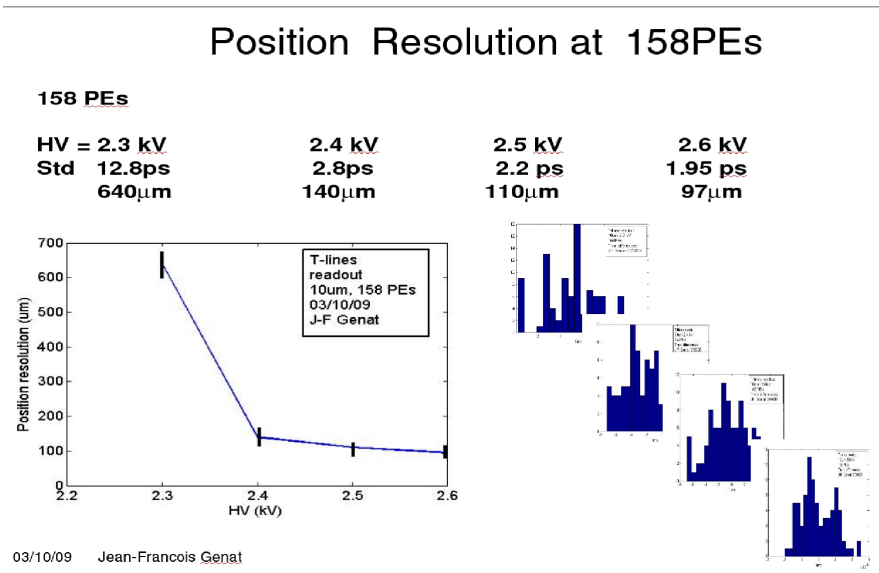

Figure 17: Measurements of the Planacon/transmission-line readout taken with the Argonne fast laser teststand, showing the spatial resolution vs signal size. At 2.6 KV the measured resolution is 97 microns.

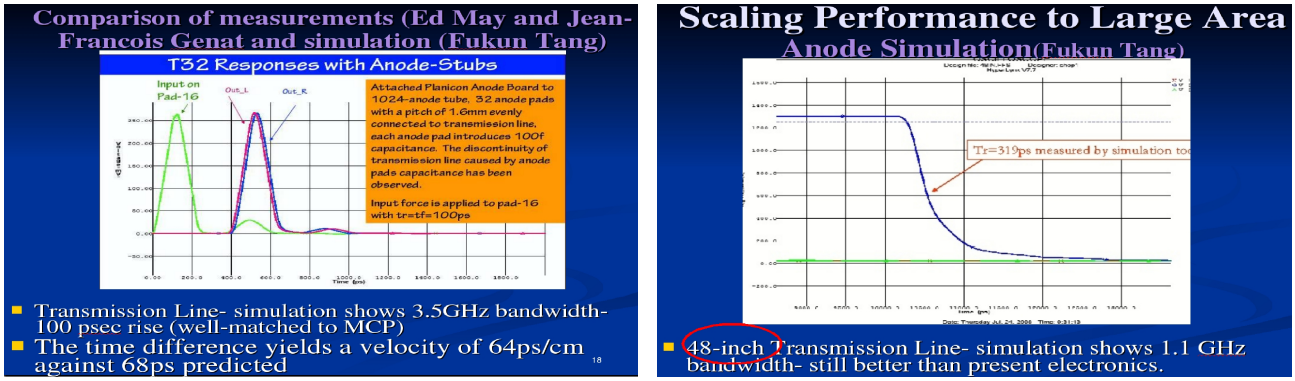

Figure 18: Left: A SPICE simulation of a linear model of the transmission line, extracted from the physical parameters of the printed-circuit card of Fig. 16; Right: The same simulation for a 48"-long transmission line. We find an analog bandwidth of 1.1 GHz, more than adequate for very large area applications such as a water Cherenkov counter for DUSEL. The performance of the $4' \times 2'$ module proposed here should be better than this result, as the anode lines are inside the vacuum, and there will be no 'stubs' connecting the line to the MCP.

The scale-up of the ceramic technology to the $8'' \times 8''$ module is relatively straight-forward, with a well-known set of possible problem areas: indium seal success ratios, design and braze success rates, window costs, and materials selection. A rough estimate of the cost of the assembly, including the anode, is less than \$500, ($\leq$\$12,500/m^2), i.e. much less than the \$100,000 target for the collider detector applications(ATLAS and LHCb, for example). The larger alumina anodes should not be a problem provided that the strip anode and ground planes are properly applied, the braze materials are chosen correctly, and the process is shaken down. Hydrogen contamination will be avoided by using vacuum brazing, in which LBNL has expert capabilities. We regard this path, which satisfies several of the highest priority applications, as low risk.

spatial resolution we believe to be small while greatly increasing the risk and diminishing the capabilities.

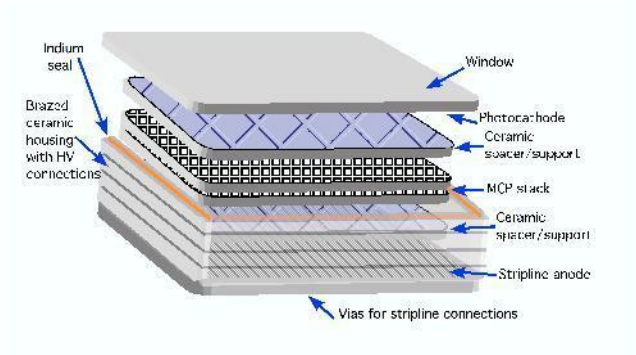

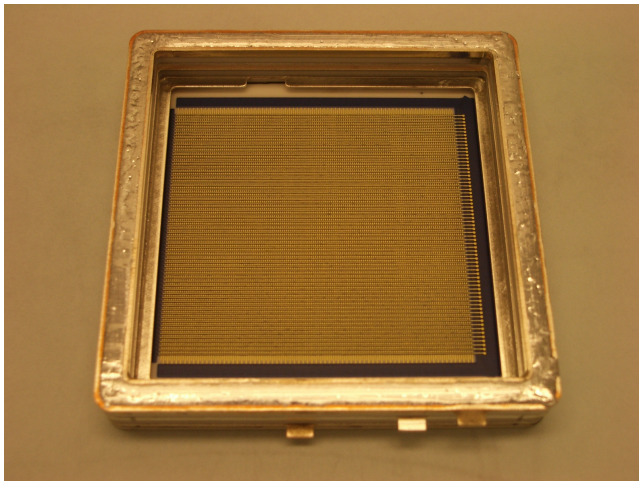

Figure 19: Left: The construction of a ceramic MCP-PMT . Right: A photograph of the mechanical assembly, showing the ceramic-substrate anode plane that forms an integral stack with ceramic spacers.

3.2 All-Glass Detector Modules

However, the mechanical assembly of *very* large-area photo-detectors, such as the $4' \times 2'$ panel, is a major challenge. There are issues of mechanical registration and connection of the internal planes to form a monolithic package, electrical connections both internal and external, vacuum transfer, and assembly. An assembly facility will need to provide the ability to process and seal the advanced cathodes, MCPs and the front face in vacuum and bake and hot-scrub the MCPs.

We will try to exploit advances in flat-panel and solar energy technology to make a flat all-glass design. We have recently recruited a leader for this effort, which will be based at Argonne, and who recently was the Project Leader at CERN on a highly successful project to build a large subsystem at the LHC involving 24 institutions. Argonne has extensive experience with glass, including a dedicated glass shop and a (now half-time) glass expert. The design would be based on thin glass technology with laser-cutting and welding; pressure resistance would be provided by glass lattice spacers, much as load-bearing walls in a house provide pressure transfer from top to bottom. We are investigating the use of glass for the anode transmission lines as well; a range of dielectric constants with acceptable loss angles (determined from our simulations) is available. Among the many concerns we are addressing are the mechanisms for making the internal layers into an integral amplification section, electrical charging of non-emitting surfaces, electrical connections and penetrations, and mechanical stability and robustness. We note 'it has been 30 years since the night vision guys tossed out their glass tube technology' [64]; it is worth revisiting given the changes in lasers and flat-panel glass technologies.

In the first year we will start with the $8'' \times 8''$ size module to get these issues under control, while planning the $4' \times 2'$ construction and fabrication facility. The out-year efforts will depend on the outcome of this R&D; if it is successful, construction of a fabrication facility will be begin at Argonne in the second year.

4 Deliverables

We plan to make as deliverables 3 separate designs of planar photo-detectors:

1. A 32.8 mm round format micro-channel plate, the 'Development' size, which we use as a testbed for characterizing new photo-emitting and secondary emitting materials. In addition to using the bare plates for characterization, this is a standard size used by SSL, and so we already have designs and parts for mechanical and electrical assembly to test the complete chain from photo-cathode to output, as shown in Figure 20.
2. A square glass-body 'Frugal' $8'' \times 8''$ MCP-PMT , schematically shown in Figure 2. The $8''$ size of the photocathode, amplification section, and anode forms the sub-unit out of which larger devices can be assembled. The assembled module is also a standalone device that replace a 10" tube, base, and front-end

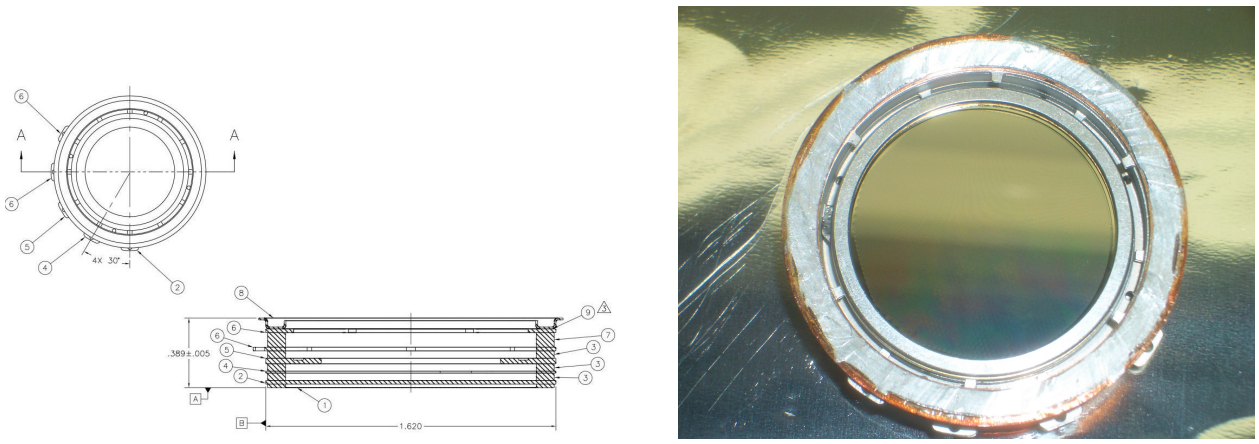

Figure 20: Left: The existing mechanical design for the Development 32.8 mm MCP-PMT , used for rapid photo-cathode and secondary emission development and characterization of materials. Right: An existing MCP-PMT in the Development format.

electronics assembly. [7]

3. A $4' \times 2'$ panel consisting of multiple $8'' \times 8''$ photo-cathodes and amplification sections, feeding a continuous common anode with 4-foot long strip transmission lines, as shown in Figure 21 (also see Figure 18 for a simulation of the anode performance). This is the proto-type for DUSEL and other very large-area applications.

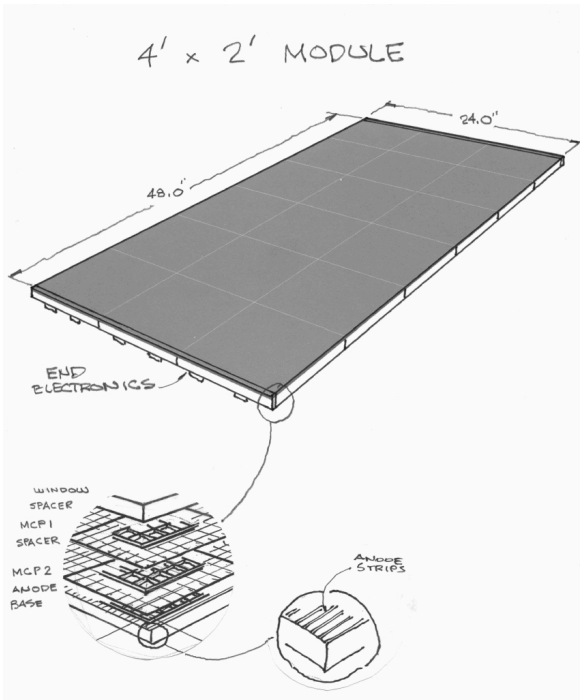

Figure 21: The $4' \times 2'$ panel, with a mosaic of photo-cathodes and AAO amplification plates, and a single anode consisting of 4-foot long transmission lines. Simulation results give an analog bandwidth of 1.1 GHz for the readout, more than adequate for DUSEL.

[7] We have settled on $8'' \times 8''$ from initial studies; it may be that a somewhat larger size (e.g. 12" square) will turn out to be optimum in terms of cost of tooling and assembly, but the principle and basic details remain the same.

5 Summary

While what we are proposing is not easy, there are demonstrated solutions to each of the individual pieces. Readout of MCP-PMT 's by transmission-line anodes with wave-form sampling on both ends has been demonstrated and a detailed simulation that predicts good performance for modules up to 4-feet long has been validated by measurements. Industry routinely makes bialkali photo-cathodes for PMTs and MCP-PMT 's; we need to improve the quantum-efficiency of the SSL photo-cathodes from $\sim 20\%$ up to typical industry values and scale up in size, and to solve the problems of mechanical assembly into large panels. Glass capillary substrates look very promising as an available and economical MCP substrate, with several nano-material alternatives under investigation. The superior performance of ALD-coated glass substrate MCP's has been demonstrated, and ALD is already used in industry at the scales we need. The problems of mechanical assembly of scale-up to large (e.g. $4' \times 2'$) panels are formidable, as they involve *in situ* photo-cathode production, ultra-high-vacuum transfer, bake-out and scrubbing, glass-to-glass and glass-to-metal seals, surface physics issues (e.g. dark-current, non-channel noise sources, and aging), ASIC design, electronics systems design, and integration. However we do not see any show-stoppers; just a lot of hard work. In parallel we will pursue synergistic programs of higher risk but very high pay-off to improve the single photo-electron energy resolution and the transit-time spread by optimizing the photo-cathode/channel geometry, and to improve photo-cathode quantum efficiencies using the expertise at Argonne in nano-scale materials, our advanced MCP simulations, and our facilities and experience for ALD.

6 Acknowledgements

We gratefully thank Alan Bross (Fermilab), Joseph Gregar (Argonne) Paul Hink (Photonis), Michael Minot (Incom), and Bill Moses (LBNL) for helpful comments, criticisms, and suggestions in the preparation of this proposal.

7 Work Plans

7.1 Overview

We have put together a collaboration of four national labs, three companies, and three universities, with overlapping as well as complementary strengths. There are several basic tenets that underlie our organization of the effort and allocation of resources and responsibilities. First, allocation of work flow is determined by the strengths of the individual institutions, examples being SSL's vast experience in making and using MCP's, Argonne's strength in characterization and testing of photo- and secondary-emitting materials and in wet chemistry, Synkera's and SSL's experience in developing AAO-based MCP's, and the strength in Arradiance, Argonne, and Synkera in ALD [8]. Second, in general we start from conventional values of working parameters (e.g. L/D=40, 10 micron pores, etc.) to evolve into innovative solutions in a controlled fashion, changing only one thing at a time on a given parallel path. Third, we use simulation validated at these starting points to explore parameter space, cutting development time and costs. Fourth, for the high-risk areas, such as new high-QE nano-structured photo-cathodes, we have as our primary path a parallel effort on conventional technology building on techniques and capabilities we already have in hand (e.g. photo-cathodes), or are extensions of known techniques (e.g. glass capillary substrates). Fifth, we emphasize the goal of the development of commercializable devices, with strong protection of the intellectual property (IP) and interests of the companies that are part of the effort. We believe that it is possible, with enough care, to use the complementary strengths and roles of the national labs, industry, and universities so that it is 'win-win' for everybody, and this is the fundamental tenet of the collaboration.

7.2 Characterization of Photo- and Secondary-Emitting Materials

The development of new photo-cathode materials and better secondary emitters is appropriate for a national lab, and there are existing efforts and remarkable facilities already at Argonne. The Directed Energy Interactions with Surfaces (DEIS) group of the MSD at Argonne will conduct characterization of electron emitting materials for photocathodes and MCPs. Characterization experiments will include high resolution measurements of kinetic energy spectra of photo- and secondary electrons, and of the elemental and isotopic composition of the surface

[8] This principle does not, however, preclude parallel efforts, which can be very efficient

and bulk of emitting materials. The DEIS group will use the following advanced analytical instrumentation: (1) an electron spectrometer equipped with X-ray, VUV light (HeI and HeII) and electron beam sources to generate electron emission and with a hemispherical energy analyzer to precisely determine energy spectra of these electrons (XPS/UPS); (2) three advanced time-of-flight mass spectrometers (TOF MS) optimized for laser post-ionization of neutral species volatilized from materials surfaces by focused ion, electron and photon beams. These mass spectrometers have parts-per-trillion sensitivity, and probe resolutions up to 10 nm for ion and electron beams, and 0.5 micron for laser beams. Both XPS/UPS and TOF MS instruments are equipped with dedicated ion sources for surface cleaning. The TOF MS instruments are capable of sputter depth profiling with a dynamic range of more than 5 orders-of-magnitude, and are equipped with in-vacuum optical microscopes with submicron resolution, precise sample positioning stages, and also can perform in a scanning electron microscope (SEM) mode thanks to built-in dedicated electron detectors. Tunable Ti:sapphire lasers, normally used for photo-ionization of sputtered or laser desorbed neutrals, will be used to probe both the front and back of the emissive materials samples so that photo-electrons are generated, extracted and detected. With these tools, the DEIS group can probe the secondary and photo-electron emission of photo-cathode materials in opaque and transmission geometries, probe the secondary electron emission of MCP-coating materials, and determine how their emissive properties depend on materials composition, surface morphology, structure, and geometry.

Dynamic tests of the pulse shape will be performed in the HEP and Advanced Photon Source Divisions of Argonne, which already are engaged collaboratively in investigations of photocathode QE and pulse shape, using a streak-camera setup with MCP-amplification [65]. The group has photocathode deposition systems and UHV vacuum transfer systems.

Arradiance, SSL, and Synkera also have extensive operational test and characterization facilities that will be used for tests of conventional emitters and of the favored novel candidates as they emerge from the broader and deeper testing at ANL.

7.3 Simulation

A parallel effort in simulation is essential for integrating the measurements into rational development program. There is a large literature on the simulation of MCP's [18]. However in the interests of building devices that are optimized for low cost, we would like to move into an area of parameter-space that is not fully explored. We are lucky to have access to two of the most advanced MCP simulations in the world through Arradiance [66] and Muons,Inc [16], which would be the lead institutions in this effort. In addition we have at Argonne access to sophisticated simulations of secondary emission processes through the MCS Division. We have already started to explore expanding the area coverage of pores, space charge and saturation as a function of L/D, smaller D as would be natural in intrinsic AAO plates, and high secondary emission first-strike geometries. As the simulations are only as good as the input data, simulation results would then be compared with measurements made at Argonne, Arradiance, Synkera, and SSL. [9]

7.4 Device Testing

Dynamic testing of the electron charge shower development would be measured in the 32.8mm-format MCP's at Argonne, using the streak camera setup at the Advanced Photon Source. Gain and pulse measurements of MCP-PMT 's (i.e. with photo-cathode and anode) would be done at Argonne, Arradiance, SLAC, SSL, and Synkera. Photo-cathode testing would be done in both of the two photo-cathode development programs at Argonne. Measurements for applications involving charged particles will be performed in the MTEST test-beam at Fermilab.

7.5 Photocathode

The improvements to the SSL bialkali photo-cathodes from $\sim 20\%$ up to industry standards will be a joint effort of SSL and Argonne. The development of novel nano-scale photo-cathodes would be centered at Argonne in the MS, APS, MCS, and ES Divisions and the Center for Nano-scale Materials, in conjunction with SSL.

[9] Comparisons of simulation with measurements of conventional MCP's in the Argonne laser test stand and Fermilab MTEST beam are already underway; see the collaboration Blog at hep.uchicago.edu/psec/.

7.6 Amplification Stage: Substrates, Coatings, Scaling

The adaptation of capillary-based glass substrates from industry is being coordinated through Argonne and Chicago. In parallel, the development of AAO substrates with funnel geometries will be a joint effort of Argonne, SSL, and Synkera. The ALD development for the substrate resistive and emissive coatings is the responsibility of Argonne, in collaboration with Arradiance and Synkera.

7.7 Anode

The basic R&D for the anode has been done in the last several years by a collaboration of Chicago, Argonne, and Fermilab. Extending this to larger areas, including possibly using glass as a cheaper substrate, will be done by the same group, in close consultation with the experts at SSL. RF simulations of the anode that have been developed at Chicago, and that agree very well with measurements made with the Argonne laser test stand [67], will be used to design and validate new anode designs.

7.8 Front-End Electronics

The front-end wave-form sampling electronics is relatively advanced based on the work at Chicago, Hawaii, Orsay, PSI, Saclay, and SLAC. Work has started at Chicago and Hawaii to move the design of the waveform sampling chip to the more modern 130 nm IBM CMOS process that will support up to 32 channels per chip. The development of the FPGA-based control and DAQ system will be done at Argonne, Chicago, and SSL. The clock distribution system work will be also done at Argonne in a collaboration of the HEP and APS Divisions.

7.9 Mechanical Assembly

We are pursuing two parallel paths for the mechanical package. The first is the logical extension of widely-used and well-understood ceramic package, with metal-to-ceramic seals. This work will be done at SSL, where there is tooling and extensive experience. A second effort to develop an all-glass mechanical assembly using techniques developed for large flat panel screens is being started at Argonne, Chicago, and Fermilab, with consultation by SSL. As different applications will have different requirements on robustness (the SSL experience in successfully making devices that withstand rocket launchings is one example), required area, and cost, we foresee pursuing both these paths to the completion of a ($8'' \times 8''$) prototype.

7.10 Integration

Integration of these efforts, including managing the budgets, schedule, and reviews, will be the responsibility of Argonne.

8 Management

8.1 Overview

The management of this program will be done through the HEP Division of Argonne.

8.2 Industry/Lab Partnerships

We see the efforts in ALD and AAO as a partnership between the national laboratories and industry. We are in the process of establishing the formal protocols on IP and deliverables, with one NDA in place with Synkera, one being negotiated with Arradiance, and a joint SBIR submitted with Muons,Inc.

8.3 Reviews

We expect regular reviews of the program by the DOE. We will also establish internal review committees ('god-parents' [68]) from inside the collaboration, with outside experts added as needed, with the responsibility to regularly review progress in the individual areas.

8.4 Transparency/Dissemination

We aim for a unified, transparent effort with built-in reviews and documentation. We have already put a structure in place, with a web page (http://hep.uchicago.edu/psec/), a regular weekly meeting, a blog for results and presentations, two broadly-attended workshops per year since 2005 [25], and several formal collaborations and MOU's. We report our work at IEEE, Real-Time, and other technical conferences, with papers in the proceedings [69].

9 Milestones

9.1 Year 1

1. **Photo-cathode Group** *Siegmund,Attenkofer,Insepov,Pellin,Yusof*
   (a) Demonstrate a quantum efficiency $\geq$ 25 % with a bialkali photo-cathode on a solid glass plate, with acceptable dark current;
   (b) Produce a $8'' \times 8''$ conventional photo-cathode with photo-cathode quantum efficiency. $\geq$ 25 %.
   (c) Screen and test flat and morphology-based negative-electron-affinity materials and compare to simulation.

2. **Glass Substrate Group** *Tremsin,Frisch,Siegmund,Hau,Pellin,Sullivan*
   (a) Develop and characterize 32.8mm glass substrates with 10-40 micron pores diameters L/D of 40, a bias angle of 8 degrees, and an open area ratio $\geq$ 80% suitable for an MCP;
   (b) Acquire and test $8'' \times 8''$ plates;
   (c) Evaluate the process economics.

3. **Advanced Substrate Group** *Wang,Routkevitch,Pellin*
   (a) Achieve straight pores in AAO with diameter $\geq$ 0.7 microns (no-funnel option), 40 <L/D< 100, and open-area ratio $\geq$ 60 %;
   (b) Demonstrate the feasibility of making AAO funnels suitable for photo-cathode deposition;
   (c) Produce blanks of 32.8mm AAO plate for tests and MCP development.
   (d) Evaluate the process economics.

4. **Atomic Layer Deposition Group** *Elam,Insepov,Sullivan,Libera,Wang*
   (a) Systematically characterize the leading ALD materials for Photo-emission and Secondary Electron Emission (SEE);
   (b) Demonstrate gain > 1000, non-uniformity to < 25% with ALD on a 32.8mm glass capillary substrate MCP, with acceptable dark current;

5. **Testing Group** *Adams,Veryovkin,Attenkofer,Genat,May,Nishimura,Ramberg, Ronzhin, Va'vra, Varner,Wetstein,Zinovev*
   (a) Set up test protocols for the various test facilities and make appropriate modifications to accomodate up to $8'' \times 8''$ plates.
   (b) With the Simulation Group, set up data-base for systematic codification of test results.
   (c) Expeditiously test the functionalized development units from the ALD and Photo-cathode Groups

6. **Simulation Group** *Ivanov,Beaulieu,Abrams,Genat,Insepov,Roberts,Tremsin,Tang*
   (a) With the Test Group, set up data-base for systematic codification of test results.
   (b) Systematically compile existing data on materials and define the needed measurements for characterization by the Emissive Materials Group;
   (c) Complete the MCP simulation code including space charge;
   (d) Validate the simulation with commercial tubes;
   (e) Complete a first-generation glass-substrate-based MCP-PMT simulation;
   (f) Complete a first-generation AAO/ALD-based MCP-PMT simulation;
   (g) Optimize funnel and pore shapes for an MCP-PMT with opaque photo-cathode.

7. **Mechanical Assembly Group** *Stanek,Northrop,Anderson,Forbush,Genat,Ronzhin,Sellberg,Siegmund, Tremsin,Wetstein,Zhao*
   (a) Identify candidate materials, vendors, and construction methods for the $8'' \times 8''$ and $4' \times 2'$ modules;
   (b) Complete an initial mechanical/electrical design for proto-type glass and ceramic $8'' \times 8''$ modules, and construct mechanical proto-types (no photo-cathode yet);
   (c) Measure the vacuum, residual gases, out-gassing rates, and surface chemistry of proto-type modules;
   (d) Assemble a complete Development(32.8mm) AAO/ALD or glass capillary MCP-PMT with conventional photo-cathode for testing.
   (e) Evaluate the process economics.

8. **Electronics Group** *Varner,Genat,Anderson,Bogdan,Drake,Frisch,Heintz,Kennedy, Nishimura,Rosen,Ruckman,Tang*
   (a) Construct and test a $8'' \times 8''$ proto-type transmission-line anode (e.g. velocity, time resolution, cross-talk, attenuation);
   (b) Construct a first-generation clock distribution system;
   (c) Construct a first-generation DAQ system;
   (d) Construct a first-generation anode PC card with existing sampling chips [23, 22];
   (e) Submit a first IBM-8RF chip with timing control, sampling capacitor chain, and ADC blocks.
9. **Integration Group** *Drake,Genat,Anderson,Byrum,Frisch,Ronzhin,Sanchez,Siegmund,Tremsin,Wetstein*
   (a) Install the first-generation clock distribution system and DAQ computer in the integration area;
   (b) Integrate the first-generation DAQ and MCP with first-generation front-end card with existing sampling chips;
   (c) Integrate the individual tests into a user-accessible system suite.
10. **Management Group** *Frisch,Siegmund,Byrum,Pellin,Weerts*
   (a) Identify the senior staff member at Argonne responsible for tracking costs, schedules, responsibilities, and reviews;
   (b) Identify co-leaders for each of the groups.
   (c) Establish the project in the appropriate project manager software;
   (d) Establish preliminary major decision points for photo-cathode, geometry, substrate, module size, mechanical assembly, and cost;
   (e) Select internal review committees and schedule reviews;
   (f) Survey and clarify IP and future production relationships with industry;
   (g) Evaluate the process economics for each major component.

9.2 Year 2

1. **Photo-cathode Group** *Siegmund,Attenkofer,Insepov,Pellin,Yusof*
   (a) Construct a facility for production and vacuum transfer of $8'' \times 8''$ conventional (bialkali) photo-cathodes with quantum-efficiency $\geq 25\%$.
   (b) Demonstrate advanced photo-cathode quantum efficiency >35%;
   (c) Continue and refine the development and characterization of novel materials for Photo-emission and Secondary Electron Emission (SEE): Higher quantum efficiency (QE), nano-structures, photon trapping usingwavelength tuning;
2. **Glass Substrate Group** *Tremsin,Frisch,Siegmund,Hau,Pellin,Sullivan*
   (a) Achieve open-area ratios $\geq 80\%$ and channel sizes ≤ 20 microns;
   (b) Optimize the process economics for large areas.
3. **Advanced Substrate Group** *Wang,Routkevitch,Pellin*
   (a) Achieve straight pores with diameter $\geq$1 micron, $40 \leq$ L/D$\leq$100, and open-area ratio $\geq$70% (no-funnel option) or $\geq$90% (funnel option)"
   (b) Demonstrate gain > 1000, non-uniformity to < 15% in an advanced plate.
   (c) Perform initial scale-up and develop cost projections for 8"x8" AAO with large pores.
4. **Atomic Layer Deposition Group** *Elam,Sullivan,Insepov,Libera,Wang*
   (a) Demonstrate gain > 1000, non-uniformity to < 15%
   (b) Optimize process economics for batch production
   (c) Develop multi-dynode stripe coating of channel SEE layers for narrowing gain and transit-time spreads;
5. **Testing Group** *Adams,Veryovkin,Attenkofer,Genat,May,Nishimura,Ramberg, Ronzhin,Va'vra, Varner,Wetstein,Zinovev*
   (a) Expeditiously test the functionalized development units from the ALD and Photo-cathode Groups
   (b) Set up to test completed MCP-PMT 's in development and $8'' \times 8''$ sizes in the Argonne laser test-stand and MTEST.
6. **Simulation Group** *Ivanov,Beaulieu,Abrams,Genat,Insepov,Roberts,Tremsin,Tang*
   (a) Validate simulation of morphology-based emissive materials
   (b) Include dynamic effects in MCP simulation
   (c) Completion of 'end-to-end' simulation package.
7. **Mechanical Assembly Group** *Stanek,Northrop,Anderson,Forbush,Genat,Ronzhin,Sellberg,Siegmund, Tremsin,Wetstein,Zhao*
   (a) Construct working glass and ceramic $8'' \times 8''$ MCP-PMT 's with gain $\geq 5 \times 10^5$
   (b) Finish design of $4' \times 2'$ module.
8. **Electronics Group** *Varner,Genat,Anderson,Bogdan,Drake,Frisch,Heintz,Kennedy, Nishimura,Rosen,Ruckman,Tang*
   (a) Construct and test 4-foot PC card with Varner and Ritt chips
   (b) Construct clock distribution system for MTEST test-beam
   (c) Construct DAQ system for MTEST test-beam
   (d) Construct second-generation front-end card for MTEST test-beam
   (e) Submit second IBM-8RF chip (4-channel)
9. **Integration Group** *Drake,Genat,Anderson,Byrum,Frisch,Ronzhin,Sanchez,Siegmund,Tremsin,Wetstein*
   (a) Integrate first-generation DAQ and $8'' \times 8''$ MCP with anode and front-end
   (b) Continue development of system test suite
10. **Management Group** *Frisch,Siegmund,Byrum,Pellin,Weerts*
    (a) Review of Progress
    (b) Review of Major Decision Points on Photo-cathode, Substrate, Module Size, Assembly, and Cost
    (c) Re-evaluate process economics for each component
    (d) Get another Program Director

9.3 Year 3

1. **Photo-cathode Group** *Siegmund,Attenkofer,Insepov,Pellin,Yusof*
   (a) Produce a $8'' \times 8''$ conventional photo-cathode with photo-cathode quantum efficiency. ≥ 35 % with acceptable dark current;
   (b) Continue the characterization survey of novel materials for Photo-emission and Secondary Electron Emission: higher quantum efficiency , nano-structures, wavelength tuning.

2. **Glass Substrate Group** *Tremsin,Frisch,Siegmund,Hau,Pellin,Sullivan*
   (a) Evaluate the process economics for large-area, psec timing, and medical applications.
   (b) Setup for industrial-scale production of plates optimized for the ALD coating process and robust mechanical assembly;

3. **Advanced Substrate Group** *Wang,Routkevitch,Pellin*
   (a) Evaluate the process economics for large-area, psec timing, and medical applications.
   (b) Fabricate scaled substrates in quantities and sizes sufficient for 6 working proto-type modules;
   (c) Continue exploring advanced processes and pore geometries for cheaper production and higher QE.

4. **Atomic Layer Deposition Group** *Elam,Sullivan,Insepov,Libera,Wang*
   (a) Evaluate the process economics for large-area, psec timing, and medical applications.
   (b) Achieve single-photo-electron resolution out to 4 pe's.
   (c) Continue the characterization survey of novel materials for Photo-emission and Secondary Electron Emission: higher quantum efficiency , nano-structures, wavelength tuning.

5. **Testing Group** *Adams,Veryovkin,Attenkofer,Genat,May,Nishimura,Ramberg, Ronzhin,Va'vra, Varner,Wetstein,Zinovev*
   (a) Transition to industrial-style testing.
   (b) Continue to test innovations on a small scale.

6. **Simulation Group** *Ivanov,Beaulieu,Abrams,Genat,Insepov,Roberts,Tremsin,Tang*
   (a) Continue development of codes for field-emission-based photo-cathode and secondary emission materials.

7. **Mechanical Assembly Group** *Stanek,Northrop,Anderson,Forbush,Genat,Ronzhin,Sellberg,Siegmund, Tremsin,Wetstein,Zhao*
   (a) Build a quantity of $8'' \times 8''$ and $4' \times 2'$ modules; [10]
   (b) Design and optimize quantity assembly procedures;
   (c) Continue to interface to applications through Psec Workshop Series [25] and mutual collaborators.

8. **Electronics Group** *Varner,Genat,Anderson,Bogdan,Drake,Frisch,Heintz, Kennedy,Nishimura,Rosen,Ruckman,Tang*
   (a) Design production generation clock distribution;
   (b) Design production FPGA DAQ/control card;
   (c) Submit 16(32)- channel IBM-8RF chip.

9. **Integration Group** *Drake,Genat,Anderson,Byrum,Frisch,Ronzhin,Sanchez,Siegmund,Tremsin,Wetstein*
   (a) Assemble a 4-module system;
   (b) Test 4-module system.

10. **Management Group** *Frisch,Siegmund,Byrum,Pellin,Weerts*
    (a) Establish production hand-off of modules to industry;
    (b) Establish paths to application-specific modifications of the generic devices;
    (c) Set up a lab/industry/university group charged with exploring other applications and transformational developments.

[10] Enough to establish quality control, uniformity, and enough to use in preliminary applications.

10 Budget

11 Budget Justification

References

[1] The Hamamatsu Ultra Bialkali photo-cathode has achieved a quantum efficiency of 43%. See http://jp.hamamatsu.com/resources/products/etd/eng/html/pmt_003.html

[2] For example, the Hamamatsu R9800 25-mm tube has a transit time spread (TTS) of 270 psec (FWHM). See www.hamamatsu.com.

[3] For example, see http://sales.hamamatsu.com/multianode/

[4] K. Arisaka et al., "Performance of a Prototype Aerogel Counter Readout", http://www.scientificcommons.org/40872582 (2008)

[5] Arisaka, K. et al., "XAX: a multi-ton, multi-target detection system for dark matter, double beta decay and pp solar neutrinos", ArXiv http://arxiv.org/abs/0808.3968 (2008)

[6] Photonis/Burle Industries, 1000 New Holland Ave., Lancaster PA, 17601. See http://www.photonis.com/industryscience/products/microchannel_plates_detectors/reference_list

[7] See http://sales.hamamatsu.com/en/products/electron-tube-division/detectors/microchannel-plates-mcps.php

[8] See http://www.photek.com/

[9] O.H.W. Siegmund, Barry Welsh, John Vallerga, Anton Tremsin, Jason McPhate, "High-performance microchannel plate imaging photon counters for spaceborne sensing", Proc. SPIE Vol. 6220 (2006) 622004

[10] Siegmund, O.; Vallerga, J.; Jelinsky, P.; Michalet, X.; Weiss, S.; Cross delay line detectors for high time resolution astronomical polarimetry and biological fluorescence imaging, Nuclear Science Symposium, 2005 IEEE, Volume 1, 23-29 Oct. 2005 Page(s):448 - 452

[11] P. Jelinsky, P. Morrissey, J. Malloy, S. Jelinsky, and O. Siegmund, C. Martin, D. Schiminovich, K. Forster, T. Wyder and P. Friedman, Performance Results of the GALEX cross delay line detectors, Proc. SPIE Vol. 4854, pp 233-240, 2003.

[12] In addition to the above references, see: O.H.W. Siegmund, John Vallerga, Anton Tremsin, Characterizations of microchannel plate quantum efficiency, Proc. SPIE Vol. 5898 (2005) 58980H.

[13] O. H. W. Siegmund, A. S. Tremsin, C. P. Beetz, Jr., R. W. Boerstler, D. R. Winn, "Progress on development of silicon microchannel plates", SPIE Proc., vol. 4497, 139-148, 2002.

[14] A.S. Tremsin, O.H.W. Siegmund, C.P. Beetz R.W. Boerstler, The latest developments of high gain Si microchannel plates. Proc. SPIE Vol. 4854, pp 215-224, 2003.

[15] High amplitude events in microchannel plates, O.H.W. Siegmund, J. Vallerga, and P. Lammert, IEEE Trans. Nucl. Sci., NS-36, 830-835 (1989).

[16] V. Ivanov, Computation Methods and Device Optimization in Electron Optics (2 volumes, in Russian), Moscow, 2005.

[17] See http://www.arradiance.com/, including a A. S. Tremsin, H. F. Lockwood, D. R. Beaulieu, N. T. Sullivan, E. Munro, J. Rouse, "3D microscopic model of electron amplification in microchannel amplifiers for maskless lithography", 7th International Conference on Charged Particle Optics, Cambridge, England, July 2006, Physics Procedia 1 (2008) 565.

[18] A.B. Berkin, V.V. Vasilyev, "Numerical simulation of the amplification regime for pulsed current in the channel of MCP", June 2007 (in Russian); A.B. Berkin, V.V. Vasilyev, "Numerical model of the amplification regime for the direct current in the channel of MCP", June 2007 (in Russian); A.J. Guest, "A computer model of channel multiplier plate performance", 1971

[19] J. Milnes and J. Howorth, (Photek Ltd.), "Picosecond Time Response Characteristics of Micro-channel Plate PMT Detectors"; SPIE USE V.8, 5880 (2004); "Advances in Time Response Characteristics of Micro-channel Plates", http:/www.photek.com/support/technical_papers.htm

[20] D. Breton, E. Auge, E. Delagnes, J. Parsons, W Sippach, V. Tocut, The HAMAC rad-hard Switched Capacitor Array. ATLAS note. October 2001. Breton

[21] E. Delagnes, Y. Degerli, P. Goret, P. Nayman, F. Toussenel, and P. Vincent. SAM : A new GHz sampling ASIC for the HESS-II Front-End. Cerenkov 2005

[22] S. Ritt. "The DRS chip: Cheap waveform digitizing in the GHz range."; Nucl.Instrum.Meth.A518:470-471,2004

[23] G. Varner, L.L. Ruckman, J.W. Nam, R.J. Nichol, J. Cao, P.W. Gorham, and M. Wilcox. The Large Analog Bandwidth Recorder And Digitizer with Ordered Readout (LABRADOR) ASIC, Nucl.Instrum.Meth.A583:447-460,2007.

[24] J.-F. Genat, G. Varner, F. Tang, H. Frisch; "Signal Processing for Pico-second Resolution Timing Measurements",To be published in Nucl. Instr. Meth., 2009; arXiv:0810.5590. We have noticed in our discussions with groups interested in applications that our natural translation of time resolution into space resolution along the distance of travel is not commonly shared; it takes some getting used to for the words 'time resolution of 10 psec' to naturally represent a resolution of 3 mm (or less if in a medium) in the direction the photon or charged particle came from.

[25] For the agendas and slides of the last 7 workshops, see http://psec.uchicago.edu/workshops.php

[26] Q. Xie, C.-M. Kao, X. Wang, N. Guo, C. Zhu, H. Frisch, W.W. Moses, C.-T. Chen; " Potential Advantages of Digitally Sampling Scintillation Pulses in Timing Determination in PET", Nuclear Science Symposium Conference Record, 2007. NSS '07; Vol. 6: 4271-4274

[27] H. Kim C.-M. Kao, Q. Xie, H. Frisch, W. W. Moses, W.-S. Choong, L. Zhou, F. Tang, J. Lin, O. Biris, and C.-T. Chen; "A Multi-Threshold Method for TOF-PET Signal Processing". Nucl. Instrum. Meth. A 602, 618-621(2009)

[28] D. Herbst, " Time of Flight in PET Using Fast Timing and Leading Edge Fit Optimization", Submitted to IEEE08, October, 2008; Dresden Germany

[29] J. Lin, O. Biris, C.-T. Chen, W.-S. Choong, H. Frisch, C.-. Kao, W. W. Moses, F. Tang, Q. Xie, L. Zhou; "Electronics development for fast-timing PET detectors: The multi-threshold discriminator Time of Flight PET system", Proceedings of SORMA, Berkeley CA, May, 2008.

[30] Q. Xie, C.-M. Kao, X. Wang, N. Guo, C. Zhu, H. Frisch, W.W. Moses, C.T. Chen;
"Potential Advantages of Digitally Sampling Scintillation Pulses in Time Determination in PET", NSSC/MIC IEEE, Honolulu, Hawaii, Oct 27-Nov 3, 2007.

[31] H. Nicholson, private communication. We are also grateful for the strong push toward developing much larger detector modules than we had envisioned.

[32] The surface area of the solenoidal magnet coil cryostats for both ATLAS and CDF is close to 30 m^2. The idea is to 'tile' the outside of the solenoidal coil, where magnetic fields are not a problem. We have performed simulations that show that interactions in the coil are not a problem for charged particles. The coil also can serve as a 'pre-converter' for photons, for which the system should provide excellent time (i.e. space) resolution.

[33] We thank Neville Harnew for guidance on the LHCb requirements. A typical design for an LHCb upgrade is a coverage of 5m x 6m (of order 10 m from the interaction point) to achieve charged-particle (K/pi) identification in the 1-10 GeV range. The system easily fits in the available longitudinal length of 30 cm.

[34] William Moses (LBNL), private communication. We thank Dr. Moses for also providing us with a rough cost estimate for a typical system.

[35] Patricia Dehmer, Deputy Director for Science Programs, DOE Office of Science, HEPAP, Feb. 2009, as quoted by H. Nicholson, The Development of Large Area Psec Photo-Devices; Workshop VII, Argonne National Laboratory, Lemont, IL; 26-27 February 2009; http://psec.uchicago.edu/workshops.php

[36] We thank Paul Hink (Photonis) for influential input to this section.

[37] Henry J. Frisch, Harold Sanders, Fukun Tang, and Tim Credo; United States Patent 7485872, "Large area, pico-second resolution, time of flight detectors".

[38] See, for just one example, http://www.industrial-lasers.com/display_article/330518/39/none/none/eat/Laser-glass-cutting-in-flat-panel-display-production. We have initiated contacts with a number of firms in the industry, and also have dedicated glass expertise on the staff at Argonne. We have started design work at Argonne and Chicago on the details of a glass solution, including the best way to connect to the HV and signals. What is shown is just a 'cartoon' illustrating the basic ideas.

[39] Masaki Ishitsuka, "L/E analysis of the atmospheric neutrino data from Super-Kamiokande"; Ph.D Thesis, University of Tokyo, Feb., 2004

[40] O. Siegmund, J. Vallerga, J. McPhate, J. Malloy, A. Tremsin, A. Martin, M. Ulmer and B. Wessels, Development of GaN photocathodes for UV detectors, Nuclear Instruments and Methods in Physics Research Section A: Vol. 567, Issue 1, 2006, Pages 89-92

[41] A.S. Tremsin, O.H.W. Siegmund, Quantum efficiency and stability of alkali halide UV photocathodes in the presence of electric field, Nuclear Instruments and Methods in Physics Research (sect. A), Vol. 504 (2003), 4-8.

[42] A.S. Tremsin and O.H.W. Siegmund, Polycrystalline diamond films as prospective UV photocathodes, Proc. SPIE, 4139, 16, (2000)

[43] Hellmut Fritszche, private communication.

[44] K. Attenkofer, talk Workshop on the Development of Large Area Psec Photo-Devices; Workshop VII, Argonne National Laboratory, Lemont, IL; Feb. 2009; http://hep.uchicago.edu/psec/

[45] I. Veryovkin, talk Workshop on the Development of Large Area Psec Photo-Devices; Workshop VII, Argonne National Laboratory, Lemont, IL; Feb. 2009; http://hep.uchicago.edu/psec/

[46] See http://www.arradiance.com/, including a link to: D. R. Beaulieu, D. Gorelikov, P. de Rouffignac, K. Saadatmand, K. Stenton, N. Sullivan, A. S. Tremsin; "Nano-engineered ultra high gain microchannel plates"

[47] J.W. Elam, G. Xiong, C.Y. Han, HH Want, J.P. Birrell, U. Welp, J.N. Hyrn, M.J. Pellin, T.F. Baumann, J.F. Poco, and J.H. Satcher, "Atomic Layer Deposition for the Conformal Coating of Nanoporous Materials", Journal of Nanomaterials, 2006, p. 1-5

[48] J.W. Elam, J. A. Libera, M.J. Pellin, and P.C. Stair, "Spatially Controlled Atomic Layer Deposition in Porous Materials", Applied Physics Letters, 2007 **91** (24)

[49] A. M. Dabiran, A. M. Wowchak, P. P. Chow, O. H.W. Siegmund, J. S. Hull, J. Malloy, A. S. Tremsin, "Direct deposition of GaN-based photocathodes on microchannel plates", Proc. SPIE, vol. 7212-38 "Optical Components and Materials VI", San Jose, CA January 2009.

[50] J.W. Elam, D. Routkevitch, S. M. George, "Properties of ZnO/Al_2O_3 Allow Films Grown Using Atomic La;yer Deposition Techniques, J. of the Electrochem. Soc 2003 150(6) G339

[51] A.B.F., J.W. Elam, J.T. Hupp, and M.J. Pellin, "ZnO Nanotube-Based Dye-Sensitized Solar Cells", Nano Letters, 2007(7), P.2183

[52] See http://www.synkera.com, including the links to "Self-organized Anodic Aluminum Oxide" and "Ceramic MEMS" sections.

[53] J. W. Elam, D. Routkevitch, P. Mardilovich, S. M. George, "Conformal Coating of Ultra-high Aspect Ratio Nanopores of Anodic Alumina by Atomic Layer Deposition"; Chem. Materials, 15 (2003) 3507-3517.

[54] This is the term used to describe the coating of the substrate with emittive materials to provide amplification.

[55] The direction of the field lines in the channel is a function of the bulk and surface resistances, and has been the subject of some controversy. In the devices we consider here the lines are parallel to the channel axis provided one is more than several channel diameters away from the ends.

[56] 'Trust but validate', R. R. Reagan, on signing the 1987 Intermediate Nuclear Forces treaty. (http://www.usemod.com/cgi-bin/mb.pl?TrustButVerify).

[57] A. Tremsin, private communication.

[58] Incom,Inc. Charlton Mass. http://www.incomusa.com/

[59] We thank Michael Minot (Incom) and Joseph Renaud from Incom,Inc for the pictures and information.

[60] K. Inami, Workshop on Timing Detectors, Institute of Nuclear Physics in Lyon (IPNL) France, Oct. 2008

[61] J. Va'vra, D.W.G.S Leith, B. Ratcliff, E. Ramberg, M. Albrow, A. Ronzhin, C. Ertley, T. Natoli, E. May, and K. Byrum, submitted to Nucl. Instr. & Meth., March 2009

[62] Hamann, T. W., A. B. F. Martinson, et al. (2008). "Atomic Layer Deposition of TiO2 on Aerogel Templates for Novel Photoanodes in Dye-Sensitized Solar Cells." Journal of Physical Chemistry C 112(27): 10303-10307.

[63] Hamann, T. W., A. B. F. Martinson, et al. (2008). "Aerogel Templated ZnO Dye-Sensitized Solar Cells." Advanced Materials 20(8): 1560-1564.

[64] O.H.W. Siegmund, private communication.

[65] B. W. Adams, K. Attenkofer, Rev. Sci. Instrum. 79, 023102 (2008)

[66] See http://www.arradiance.com/.

[67] K. Byrum, H. J. Frisch, J.-F. Genat, E. May, T. Natoli, F. Tang, "Pico-second Timing with Micro-Channel Plate Devices and Waveform Sampling Readout Electronics", submitted to Real Time 2009, Bejing, China, May 2009.

[68] The large and complex CDF detector at Fermilab was built by subgroups each with its own internal hardware 'god-parent' committee formed of experts from within the collaboration, and chaired by a senior member experienced in that area. These committees averted several major disasters and initiated several major innovations.

[69] F. Tang, C. Ertley, H. Frisch, J.-F. Genat; "Transmission-Line Readout with Good Time and Space Resolution for Large-Area MCP-PMTs", TWEPP, Naxos, Greece (2008); C. Ertley, "Development of Pico-second Resolution Large-Area Time of Flight Systems", SORMA West 2008, Berkeley CA, Poster 136, May 12, 2008; T. Credo, H. Frisch, H. Sanders, R. Schroll, and F. Tang; Proceedings of the IEEE, Rome, Italy, Oct. 2004; Nuclear Science Symposium Conference Record, 2004 IEEE, Volume 1.

[70] The University of Washington group has just joined during these final stages of preparing the proposal, and so is not represented in the budget tables. We will fund the expected (small) travel and M&S costs to support their effort in the alternative substrate and mechanical assembly groups with subcontracts from Argonne.

[71] Argonne National Laboratory, Fermi National Laboratory, Saclay/IRFU, Stanford Linear Accelerator Center, University of Chicago, University of Hawaii; Fermilab Experiment T979; H. Frisch, Spokesperson; Memorandum of Understanding, PSEC Collaboration; Fermilab, Batavia IL; Feb, 2008

[72] MANX project proposal; https://mctf.fnal.gov/meetings/2007-1/04_05/project-narrative-06ER86282-6Manx-v2-w-appendices.pdf/view

[73] C.-M. Kao, Q. Xie, Y. Dong, L. Wan and C.-T. Chen, "Development and Performance Evaluation of a High-Sensitivity Positron Emission Tomography Scanner Dedicated for Small-Animal Imaging" Submitted to IEEE Transaction on Nuclear Science, 2008.

[74] The LHC upgrade is described in: O. Bruning, "LHC challenges and upgrade options", J.Phys.Conf.Ser.110:112002,2008.

[75] M. Diwan, S. Kettell, L. Littenberg, W. Marciano, Z. Parsa, N. Samios, S. White, R. Lanou, W. Leland, K. Lesko, Karsten Heeger, W. Y. Lee, W. Frati, K. Lande, A. K. Mann, R. Van Berg, K. T. McDonald, D. B. Cline, P. Huber, V. Barger, D. Marfatia, T. Kirk, R. Potenza; "Proposal for an Experimental Program in Neutrino Physics and Proton Decay in the Homestake Laboratory"; BNL-76798-2006-IR; arXiv:hep-ex/0608023v2.

[76] H. Frisch, in Photo-Detectors in Water Cherenkov Neutrino Detectors; Workshop, Argonne National Laboratory, Lemont, IL; 20 December 2008; http://www.hep.anl.gov/mcsanchez/large-area-photodet-workshop/

[77] See, for example, D. Acosta et al. (CDF Collaboration); Nucl. Instrum. Meth. A, 2004, pp 605-608

[78] W. Klempt; Nucl. Instrum. Meth. A433: 542-553, 1999; An extensive list of references on timing measurements can also be found in: A. Mantyniemi, MS Thesis, Univ. of Oulu, 2004; ISBN 951-42-7460-I; ISBN 951-42-7460-X; http://herkules.oulu.fi/isbn951427461X/isbn951427461X.pdf

[79] J.L. Wiza, Micro-channel Plate Detectors. Nuclear Instruments and Methods 162, 1979, pp 587-601

[80] S. Cova et al. Constant Fraction Circuits for Picosecond Photon Timing with Micro-channel Plate Photomultipliers. Review of Scientific Instruments, Vol 64-1, 1993, pp 118-124.

[81] T. Credo, H. Frisch, H. Sanders, R. Schroll, and F. Tang; Proceedings of the IEEE, Rome, Italy, Oct. 2004; Nuclear Science Symposium Conference Record, 2004 IEEE, Volume 1.

[82] K. Inami, N. Kishimoto, Y. Enari, M. Nagamine, and T. Ohshima; Nucl. Instrum. Meth. A560, 303-308, 2006

[83] J. Va'vra, J. Benitez, J. Coleman, D. W. G. Leith, G. Mazaher, B. Ratcliff and J. Schwiening, Nucl. Instrum. Meth. A572, 459 (2007)

[84] For a detected photon, a time resolution of 1 psec allows the determination of a spherical shell of thickness ≈1 mm from which the photon originated. The resolution along the beam axis depends on the angle of the photon to the beam, but this will in general allow some confirmation that a photon came from a given vertex.

[85] See, for example, C.H. Chen and J. F. Gunion, Phys. Rev. D 58, 07005 (1998).

[86] T. Aaltonen et al (CDF Collaboration), ArXiv: 0804.1043 [hep-ex], Phys. Rev. D.78.032015 (2008); See also: M. Goncharov, T. Kamon, V. Khotilovich, V. Krutelyov, S.W. Lee, D. Toback, P. Wagner, H. Frisch, H. Sanders, M. Cordelli, F. Habbacher, and S. Miscetti; "The Timing System for the CDF Electromagnetic Calorimeters"; Nucl.Instrum.Meth.A565:538-542,2006;

[87] C.-M. Kao, J. S. Souris, S. Cho; B. C.Penney, C.-T. Chen; Nuclear Science Symposium Conference Record, 2005 IEEE Volume 4, Issue , 23-29 Oct. 2005 Page(s): 2081 - 2084

[88] The DUSEL-specific workshop slides and agenda are available at: http://www.hep.anl.gov/mcsanchez/large-area-photodet-workshop/

[89] We have already achieved the necessary timing resolution in the Fermilab test beam for a 1% momentum resolution for 210 MeV muons in a 10' field-free drift space. The one exception is the possible high magnetic field in the regions of TOF2 and TOF3, depending on the detailed layout.

[90] K.A. Jenkins, A.P. Jose, D.F Heidel; An On-chip Jitter Measurement Circuit with Sub-picosecond Resolution; Proceedings of the 31st European Solid State Circuits Conference, Vol 12, pp 157-160, 2005

[91] Systematic errors in sampling may be calibrated out with the use of extra calibration channels in the front-end readout.

12 Appendix A: Applications

12.1 Overview

The development of very cheap, robust, large-area photo-detectors with intrinsic position resolution would be transformative in a number of fields of science. It would also allow major transformations in societal areas such as health care and security.

The requirements for systems vary with the size of the system and the characteristics of the input signal. A system for the Fermilab MTEST test beam would consist of 4 stations totaling 0.01 m^2, with a resolution of better than 10 psec [71]. A system for measuring 6-dimensional cooling of 250-MeV muons would consist of 4 stations, totaling 1 m^2, also with 10 psec resolution [72]. An advanced micro-PET detector with TOF capability would require less than 0.5 m^2 [73], with resolution in the 30-100 psec range. A system for an upgrade to an existing collider detector such as ATLAS [74] at the LHC would require 30 m^2 at 1-psec resolution. Lastly, a detector system that fully covers the proposed water Cherenkov system for neutrino detection at the proposed NSF/DOE DUSEL laboratory [75] would require 30,000 m^2 at $\simeq$ 100 psec resolution.

The development of specific devices for applications is beyond the scope of this 3-year proposal. Our goal is to develop commercializable modules; the optimization of the design for a given application will involve details studies of the tradeoffs. Our model has been to interact with the practioners in several of the obvious applications, with the goal of encouraging them to do detailed simulations and studies of the new opportunities that would arise. As the development would be transformative, one has to think 'outside the box' to understand the cost savings and opportunities, and this is best left to the practioners themselves, as they have the detailed tools.

For example, in the application of large-area photo-detectors as replacements for conventional PMT's in a water Cherenkov detector in DUSEL, a second-generation hermetic detector (100% photo-coverage) can measure events much closer to the detector wall with good efficiency, and so the ratio of fiducial volume to total volume can be much larger, with a significant savings in excavation, tank, and photo-detector cost for the same fiducial volume. The limit in span of the cavern wall is also significantly different in the vertical and horizontal directions, and so removing the constraint on height due to water pressure on the PMT's allows a change in the aspect ratio of the cavern, with possible additional large savings for the same volume [11]. The MCP-PMT devices do not need photo-multiplier bases, magnetic shielding, or implosion protection, changing the support and infrastructure requirements. A speculative but interesting thought is that a different geometry allowed by hermetic coverage and tracking ability might allow the addition of magnetic field for lepton sign determination [76]. Lastly, and perhaps most difficult to quantify without extended simulation with a sophisticated package like the Super-K monte carlo program, the addition of space and time information transform the detector into a tracking device, with reconstruction capability, allowing smaller uncertainties on measurements of things that exist, or more stringent limits on things that don't, for the same running time (big savings). [12]

The 5 areas below are all ones for which the development of large-area fast photo-detectors would be what Paul Horn of IBM has called 'a disruptive technology'. Within each of the two general categories of societal or scientific they are listed in order of economic importance.

12.2 Collider Physics: Strange, Charm, Bottom, Top Quark, and Tau Lepton Identification; Photon Vertexing

An enormous investment in effort and money goes into probing the most fundamental underpinnings of our universe, space/time, symmetries, forces, and constituents of matter. For example, a fully-reconstructed top-quark event costs on-the-order-of 10M$. [13] Consequently investments that substantially increase the amount or quality of the information per event should be judged against the ongoing cost of not doing them. For example,

[11] These two effects are clearly inter-dependent, as the latter depends on how close to the photo-surface one can work.

[12] This too is related to the overall geometry of the device, as a tall, thin, deep detector has much better properties with respect to scattering of the light, and may even be able to support a magnetic field for sign determination. All of which needs detailed study by simulation.

[13] We note that this fundamental research has a huge return on investment- the World-Wide-Web and Medical Imaging alone provide returns in one year many orders-of-magnitude larger than the total investment in HEP over the life-time of the field. Economically we have been a bargain almost as good as Manhattan.

an upgrade to a detector that decreases the amount of accelerator running time by 30% to achieve a given precision on a measurement needs to be measured against the cost of running for 4 months/year over the life of the experiment.

Present detectors at hadron colliders measure 3-momenta of particles produced in the collisions very precisely due to the inventions of sophisticated wire drift chambers and silicon strip detectors. However there is one more quantity for each track to be measured, and one that carries essential information about the underlying fundamental (parton-level) collision. That quantity is the mass of the particle, which for hadrons carries the information about the flavor of the quarks inside. Present practice at the Tevatron and (in simulated data) at the LHC is to treat all tracks in a jet as 'hadrons', and, with only a few exceptions beyond the b- and c-quarks, to classify jets as the generic objects produced. There is, however, a level of precision that could be reached by identifying the quarks inside the hadrons. For almost all cases the resulting list of 4-vectors is all the information that is present in the event [14]. Two example applications of flavor identification are: 1) the precision measurement of the top mass, in which one W-boson decays to either $u\bar{d}$ or $c\bar{s}$, with different calorimeter responses, and 2) possible separation of the b-quark and bbar-quark in top decay based on the sign of K mesons. A more general application is in signature-based searches, in which the well-defined texture of the CKM matrix implies the existence of Cabibbo-suppressed channels such as $\gamma bc\not{E}_t$, in which the Standard Model contributions are expected to be very small, and hence a good place to look for new physics from models with different flavor textures (much as one looks for parity violation in atomic physics in forbidden channels).

The typical resolution for measuring time-of-flight of charged particles achieved in large detector systems in high energy physics has not changed in many decades, being on the order of 100 psec [77, 78]. This is set by the characteristic scale size of the light collection paths in the system and the size of the drift paths of secondary electrons in the photo-detector itself, which in turn are usually set by the transverse size of the detectors, characteristically on the order of one inch (100 psec). However, a system built on the principle of Cherenkov radiation directly illuminating a photo-cathode followed by a photo-electron amplifying system such as a Micro-Channel Plate Photo-Multiplier (MCP) [79, 80] with characteristic dimensions of 10 microns or less, has a much smaller characteristic size, and consequently a much better intrinsic time resolution [81, 82, 83]. Figure 22 shows the separation at 1σ and 3σ for pions, kaons, and protons. Figure 23 shows a 'cartoon' of tiling the outside of a typical solenoid of a collider detector.

Time-of-flight techniques with resolution of less than several picoseconds would allow the measurement of the mass, and hence the quark content, of relativistic particles at upgraded detectors at high energy colliders such as the Fermilab Tevatron, the LHC, Super-B factories, and future lepton-colliders such as the ILC or a muon-collider, and the association of a photon with its production vertex in a high-luminosity collider [84]. Other new capabilities would be in disentangling the many vertices produced at the LHC at high luminosity by associating charged particles and photons with separate vertices in the 2-dimensional time-vs-position plane, and searching for new heavy particles with short lifetimes [85, 86].

[14] It is no accident that the fundamental particles that *can* be identified, electrons and muons, are highly prized at hadron colliders, as they can often be traced up the chain of parentage to the gauge bosons that produced them.

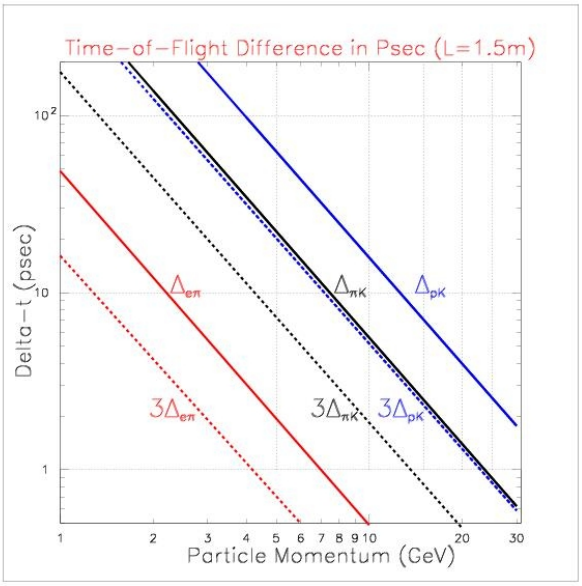

Figure 22: The time-difference over a 1.5m path length vs momentum for pions and kaons (black), protons and kaons (blue), and pions and electrons (red) at a 1-sigma (solid) and 3-sigma (dashed) separation.

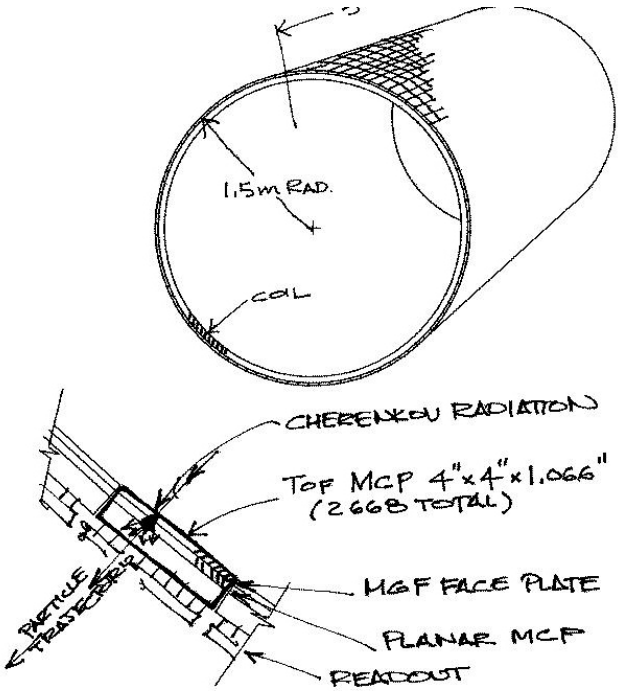

Figure 23: An example 'tiling' of the outer surface of a solenoidal magnet coil such as that of CDF or Atlas.

12.3 Medical Imaging

We have been working closely with colleagues at the University of Chicago and LBNL in Medical Imaging to develop an all-digital readout, using time-of-flight to add a third-coordinate for faster reconstruction, for Positron Emission Tomography [26, 27, 28, 29, 30]. The expertise we have from our work in HEP on large trigger systems, enormous data volumes, real-time reconstruction seem very well matched to solving similar problems in PET. There is also a great deal of interest in medical imaging from our physics students, who work with us and our medical colleagues. The development of transmission line readout enables the development of new and cheaper PET detectors, as the transmission line readout has a much smaller number of electronics channels, resulting in a lower cost.

The development of cheap planar photo-detectors with good time and space resolution would be transformational for PET, allowing much cheaper crystal arrays, much cheaper electronics, and a much faster reconstruction, allowing either lower dose or faster throughput. In addition the planar nature of the detector allows designs with better energy, space, and time-of-flight (TOF) resolution. Figure 24 shows a possible 'Sampling Calorimeter' design, in which sheets of polished crystal are interspersed with planar MCP-PMT 's instrumented with transmission-line readout and cheap waveform sampling on both ends. Each crystal is measured in x and y by the transmission lines on either side; addition spatial resolution in the orthogonal direction from the strips is obtained from the timing on the ends, so that the position of a cluster is over-constrained to eliminate noise from multiple clusters.

This design solves the 'depth-of-interaction' problem, as each crystal can be thin and viewed from the side. Only light within the Snell's-Law transmission cone crosses the air gap to the MCP close to the point of interaction, limiting the transverse spread. The depth is limited by the thickness of the crystal. We propose to put wave-shifter or scintillator bars with embedded optical fibers to collect the light on the 4 edges of the crystal, providing better energy resolution and also a fast Level-1 (deadtime-less) trigger for the DAQ.

We have tested the concept with a 2-crystal PMT setup provided by Bill Moses (LBNL). A Photonis MCP was placed in front of the crystal, and the energy resolution and coincidence efficiency were measured. The change in resolution is shown in Figure 25; the efficiency dropped by less than 5%.

Our UC collaborators have recently simulated a two-plane sampling-calorimeter 'micro-PET' detector for small animal research [87] based on the design of Figure 24. The energy resolution and time resolution show a great deal of promise. A full-size PET camera could be made out of similar modules.

In addition to having better spatial and time resolution, a flat panel MCP optical readout based on a single MCP panel has a cost advantage over a typical conventional PET detector. As an example of costing, we consider a rough comparison of the cost for a 4-photo-tube array reading out a $2'' \times 2''$ crystal block, versus the cost of a single plane of MCP with transmission-line anodes [34] reading out an 8" by 8" array of pixelated blocks. A conventional block detector covers a 2"x2" area and uses four 1" diameter PMTs that cost \$100 each, i.e. \$400 for PMTs. A rough estimate is another \$200 for readout electronics, and \$50 for each photo-multiplier base, leading to a total of about \$650 per 4 square inches, i.e. about \$160/in^2. We presently estimate \$1000 as a conservative upper limit for a fully implemented $8'' \times 8''$ MCP, or about \$16/in^2, an order-of-magnitude cheaper. The system would be also be more compact than conventional cameras, with possible associated savings.

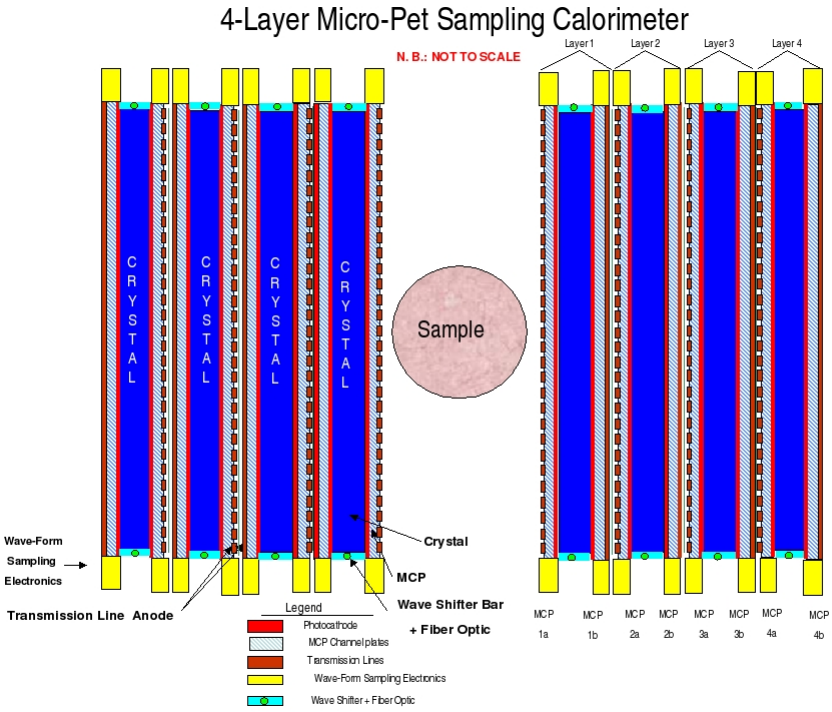

Figure 24: A design for a micro-PET detector that uses thin cheap transmission-line readout MCP's to solve the depth-of-interaction problem, and that has excellent energy, position, and time resolution. Air-gaps between the crystals and the MCP's localize the light transmitted to the MCP's; light that is internally reflected is collected along the edges of each crystal sampler for energy measurement. The electronics consists of cheap, low-power, wave-form sampling that locally converts hits into energy, time, and chisquared, and provides a Level-1 trigger for readout.

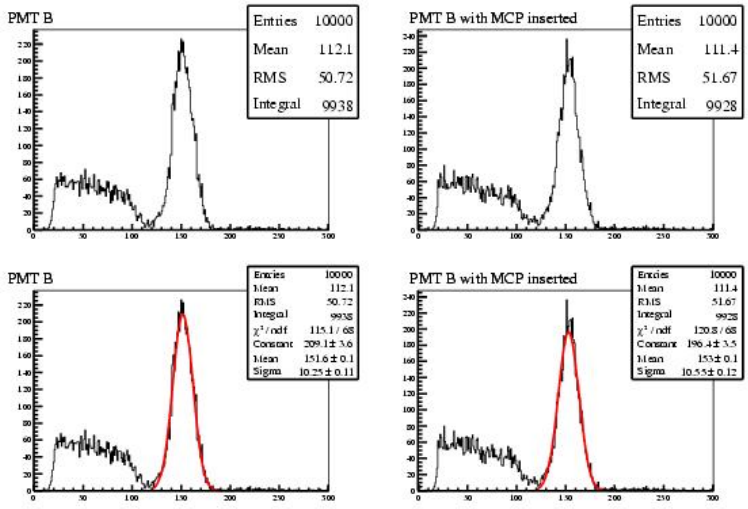

Figure 25: Actual data on the effect of an MCP between the source and the crystal. The net loss is less than 5%, and one can see from the figure that the effect on the energy resolution is minimal. (Heejong Kim, with the LBNL PET setup of W. Moses and S. Choong.)

12.4 Neutrino Physics

The pioneering work on very large water Cherenkov counters for neutrino detection culminated in the beautiful results from the Super-K experiment in Japan. An extremely large water detector modeled on Super-K is one possibility for the DUSEL facility. Here we propose the development of a detector technology for a 'next-generation' water Cherenkov counter, with close to 100% coverage, 3D reconstruction of track directions, and resolution at the event vertex small compared to a radiation length for π^0/electron separation. The time-of-arrival of the Cherenkov ring photons is measured with a resolution of better than a cm in the transverse coordinate directions and a few cm in the orthogonal direction, allowing a measurement of the track direction, and possibly the momentum (from fitting the multiple scattering). It may be possible to discriminate against π^0 backgrounds to electrons with this resolution near the vertex. The system would have a resolution for each detected photon much less than a radiation length in all three space dimensions, a significant new capability whose implications we are just starting to explore, but one which is likely to significantly increase rejection of pizero backgrounds to electron appearance by differentiating between 2 and 1 vertices and 4 and 1 particles, in the background and signal, respectively. The resolution in time and space may also provide tracking capability by the evolving time-projection of the Cherenkov ring on the walls, as sketched in Figure 26. One may even (again, a question for simulation) obtain momentum resolution from the width of the fitted Cherenkov ring.

Understanding the new capabilities from the time and space resolution will take detailed simulation; we are trying to get a serious effort on this started by other interested parties, beginning with a workshop on the subject we held at Argonne in October [88] for DUSEL proponents.

Cavity excavation costs are dependent on the aspect ratio, with walls being appreciably cheaper per linear foot than ceilings. Planar detectors would be physically robust as well, able to withstand high pressures, allowing a taller detector. A correlated consideration is the ratio of fiducial volume to total volume; a hermetic detector has a higher ratio, as acceptances are more uniform closer to the walls. This has the secondary benefit that the cost optimum moves toward a taller less-wide detector. An unexplored area is whether one could add a weak magnetic field across a deep, tall, and (relatively) narrow detector to do sign determination for precision studies of CP violation and searches for rare processes [15]

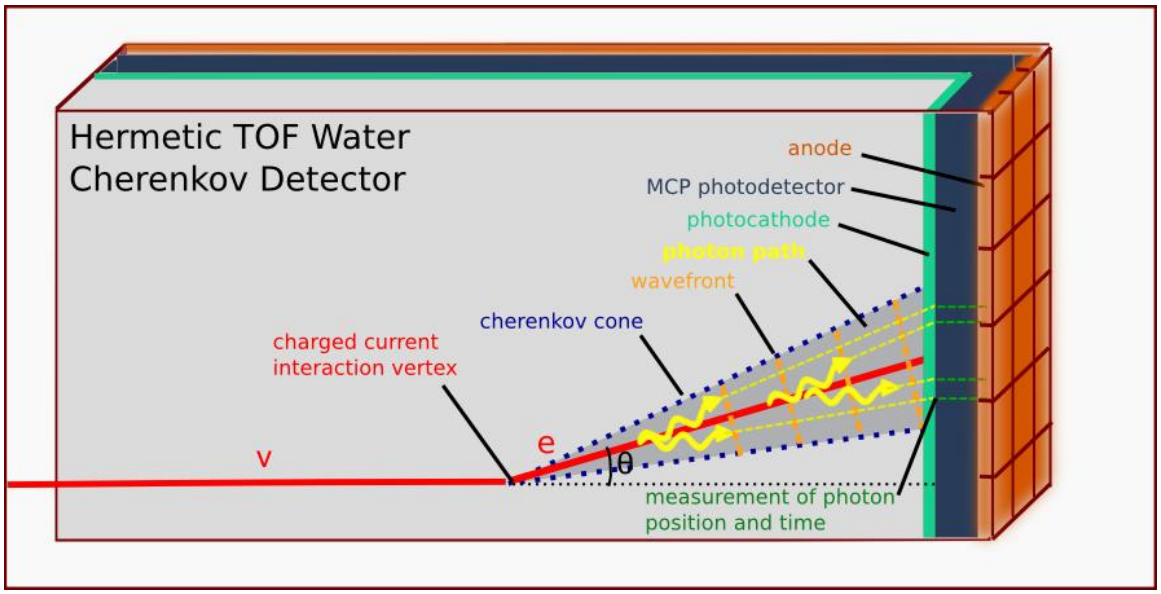

Figure 26: A 'cartoon' of one wall of a large 'hermetic' water Cherenkov neutrino detector, with the wall covered in large photo-detector panels. The time and space resolution allows reconstruction of the Cherenkov photons as an evolving ring collapsing onto the wall, so that the angle of the track, and possibly the origin, may be reconstructable (to be simulated).

[15] We do not make these arguments in support of this proposal *per se*, but instead to encourage the growing simulation effort on optimizating the parameters of a water Cherenkov counter if freed from the constraints of using conventional PMT's. It will take simulation to know if these opportunities are real.

12.5 Non-proliferation and Transportation Security

Measuring at high precision the time-coordinate in addition to the transverse coordinates in a large-area photo-detectors gives a 3-dimensional picture, as the time-coordinate gives the distance from the plane to the origin of the photon. This leads to shorter exposure and reconstruction times, advantageous for radiation-sensitive scanners used in transportation.

We have not explored this beyond casual conversations. However, there is expertise in transportation security at Argonne, and we will include the present efforts in our next workshop, which will return to having a strong component on applications.

12.6 Accelerator Diagnostics

The MANX 6-dimensional cooling experiment has expressed interest in using psec timing to augment or replace expensive magnetic spectrometers for the measurement of the momentum of the muons before and after passing through a cooling channel. The longitudinal component of the momentum (Pz) determines the longitudinal emittance of the beam. This could be an ideal first serious use of the technique in a system, as it saves money, has relatively forgiving specifications [89], and is out in the open where one can work on it. Detailed simulations are in progress to understand the effects of multiple scattering and fringe fields. The layout of the MANX spectrometer is shown in Fig. 27.

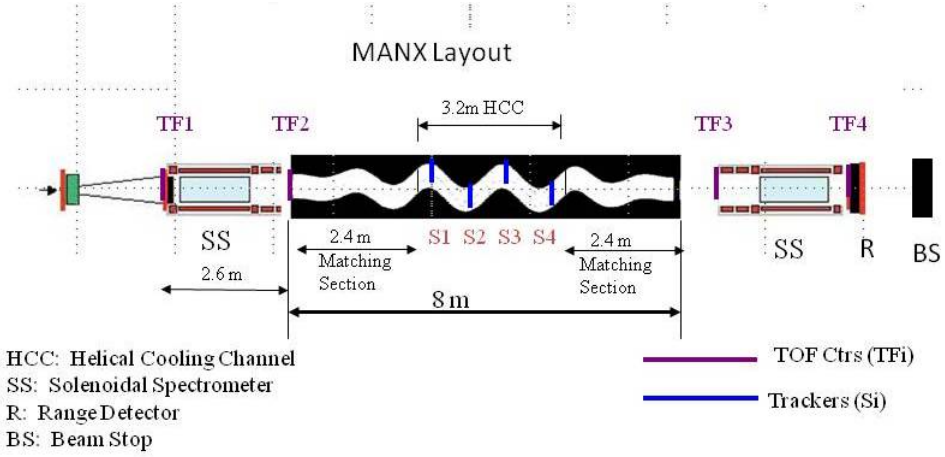

Figure 27: The layout of the MANX muon cooling experiment. The Helical Cooling Channel (HCC) is a 3.2m-long helical solenoidal magnet filled with liquid helium, with matching section magnets filled with helium at STP. Four stations with 5-10 psec resolution to measure velocity are under consideration by the MANX collaboration to augment or replace the two existing MICE solenoidal spectrometers (SS).

Another application is the measurement of longitudinal emittance in accelerators; we have had expressions of interest from the Advanced Photon Source at Argonne, the Accelerator Division at Fermilab, and the LHC.

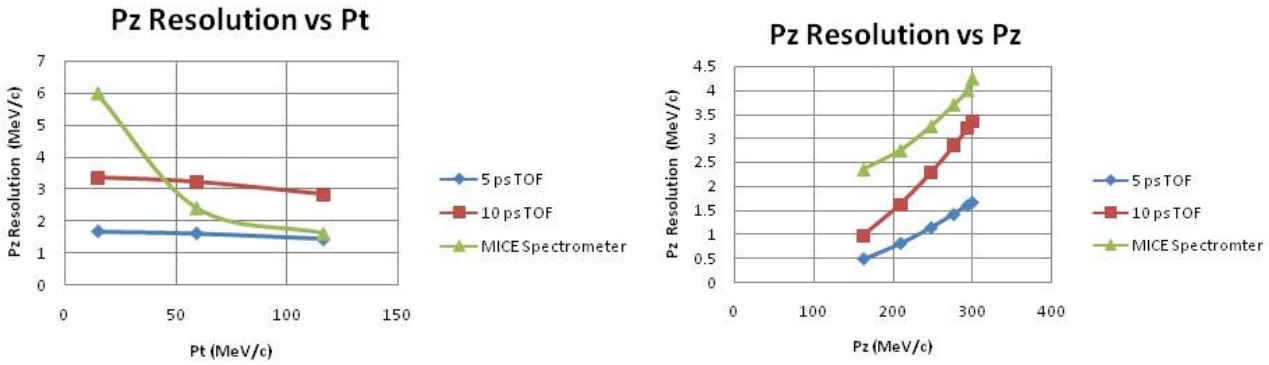

Figure 28: The resolutions in longitudinal momentum, Pz, vs transverse momentum, Pt, (Left) and vs Pz (Right), calculated using time-of-flight (TOF), assuming a 2.6m separation between two TOF planes, and a 300 MeV muon momentum. Results for TOF resolutions of 5 and 10 psec are shown, however calculated ideally without considering effects of material or stochastics. The reported MICE spectrometer resolutions are shown for comparison.

13 Appendix B: Simulation of Front-End Electronics

We have developed a simulation package based on MATLAB to model the time resolution for fast pulses from photo-detectors [24]. Using the parameters measured from commercial micro-channel plate photo-multipliers, we have simulated and compared the time-resolutions for four signal processing techniques: leading edge discriminators, constant fraction discriminators, multiple-threshold discriminators and pulse waveform sampling. We find that timing using pulse waveform sampling gives the best resolution in the presence of white noise and a substantial signal, such as fifty photo-electrons. With micro-channel plate photo-detectors, our simulations predict that it should be possible to reach a precision of several picoseconds or better with pulse sampling given large-enough input signals. At high sampling rates of the order of 40 GHz, a relatively low precision digitization (8-bit) can be used. For large-area photo-detectors a lower sampling rate and longer buffer, such as in existing sampling chips [23, 22, 20, 21] are a developed economical and low-risk solution.

The left-hand panel in Figure 29 shows the time-resolution versus the number of photo-electrons for the four timing techniques. The number of photo-electrons is varied between between 10 and 110; the sampling rate is 40 GHz, with no sampling jitter. The analog bandwidth is assumed to be 1 GHz, and the digitization is 16 bits.

The pulse sampling technique performs best of the four techniques, particularly for lower numbers of photo-electrons. Note that the sampling technique is relatively insensitive to (random) clock jitter; at 40 GHz sampling; jitters smaller than 5 psec do not introduce significant degradation in the resolution [90, 91].

We have simulated the dependence of the time resolution with the analog bandwidth for the baseline sampling rate of 40 GS/s, as shown in the left-hand plot of Figure 29. The degradation of the time resolution at high analog bandwidths is due to the fact that fewer points participate to the timing extraction, since the signal gets shorter. The time resolution versus analog bandwidth for a sampling rate proportional to the analog bandwidth is shown in the right-hand plot of Figure 29, and shows the resolution improving with analog bandwidth/sampling rate, as expected.

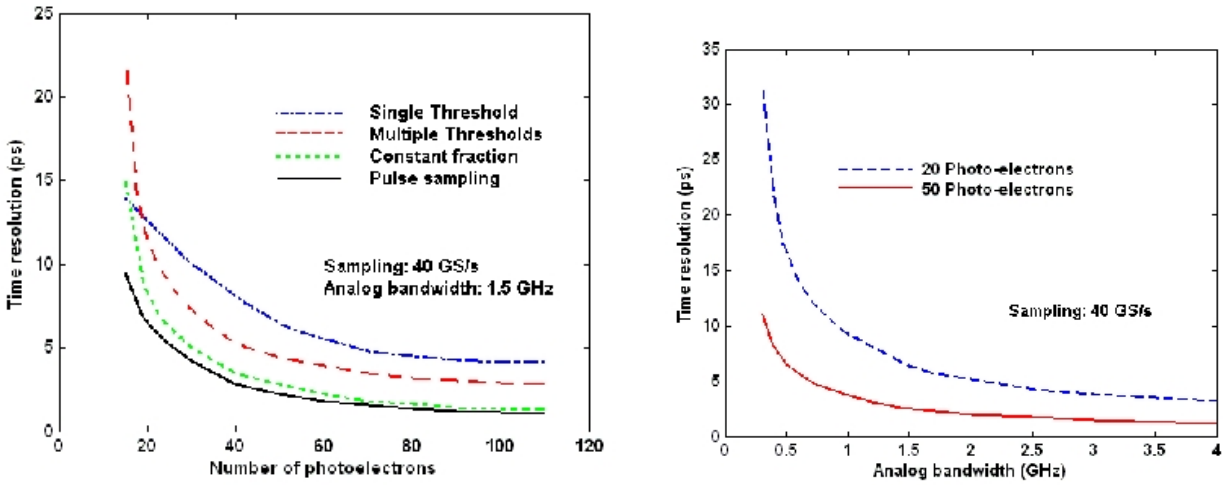

Figure 29: Left: Time resolution versus the number of primary photo-electrons, for the four different timing techniques: one-threshold (blue), constant fraction (black), multiple threshold (red), and pulse sampling (green) at 40 GHz. The analog bandwidth of the input to the sampling is taken to be 1 GHz, no sampling jitter added. Right: Time resolution versus analog bandwidth for a fixed sampling rate of 40 GS/s, for input signals of 20 and 50 photo-electrons and an 8-bit A-to-D precision.

14 Appendix C: Advanced Photo-cathodes

Photocathode Technology for the Near UV – Visible Regime

Alkali photocathodes have been employed for many decades as the principal detection method for visible photon wavelengths in photo multiplier tubes (PMT) (Sommer, 1980) due to their high quantum efficiency (QE) and economical production with high yields. The photocathode is responsible for converting the optical photons to free electrons, which are then accelerated into an amplifying structure to achieve gain. A perfect cathode will show a very high absorption in the spectral range of interest, a high electron yield, low thermal noise, low reflection losses, and fast time response. The optimum photocathode has also to meet a wide variety of engineering, process and materials compatibility, and lifetime requirements. To a large degree these properties will determine the demands on the vacuum system, the complexity of the mechanical detector assembly, and therefore the cost efficiency of the full detection system. The project will have to meet additional challenges by scaling up the production processes to large areas and ensuring the necessary quality control.

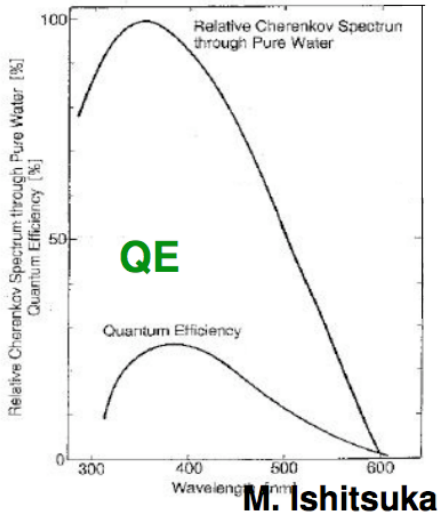

Fig. 1 Cherenkov emission spectrum for pure water, compared with the bialkali photocathode response curve for a Hamamatsu PMT.

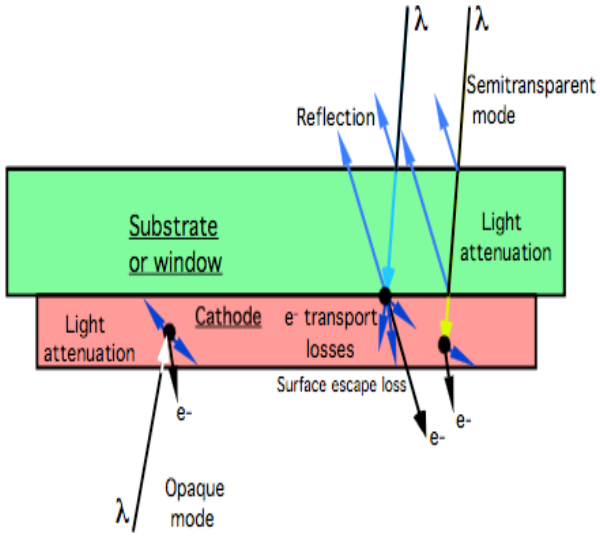

Fig. 2 Schematic of opaque and semitransparent alkali photocathode geometries for optical photon detection.

To convert photons to free electrons the cathode has to provide a high absorption probability for photons, a fast and low loss path for photoelectron(s), and a minimal surface escape barrier for electrons to escape from the surface. Over the years a wide range of materials has been discovered which fulfill these three tasks. Bialkali cathodes (for example Na_2KSb), Multialkali photocathodes ($Na_2KSb(Cs)$), and GaAs type photocathodes with various dopants (P, In) are typical for the near UV, visible and near IR regimes. For alkali photocathodes operating through the simple photoelectric effect, a fraction of the produced primary photoelectrons can leave if their residual kinetic energy is larger than the work function (the energy barrier between the surface state and the free vacuum levels). The lowest photon energy which can be principally detected must be higher than band gap plus the work

function of the cathode material. One substantive difference between cathode types is the noise, expressed in terms of a dark counting rate. Bialkali cathodes are comparatively quiet at room temperature (Fig. 5) (10 to 100 events cm^{-2} sec^{-1}) compared with semiconductor or multialkali cathodes (1000 to 50000 events cm^{-2} sec^{-1}). This means <10,000 events cm^{-2} sec^{-1} for an 8"-square panel using bialkali, versus >4 MHz for a "red" cathode.

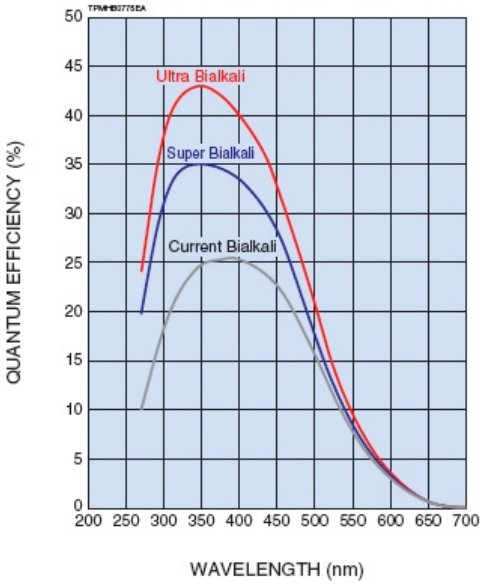

Fig. 3. High efficiency bialkali cathode results from the Hamamatsu catalog.

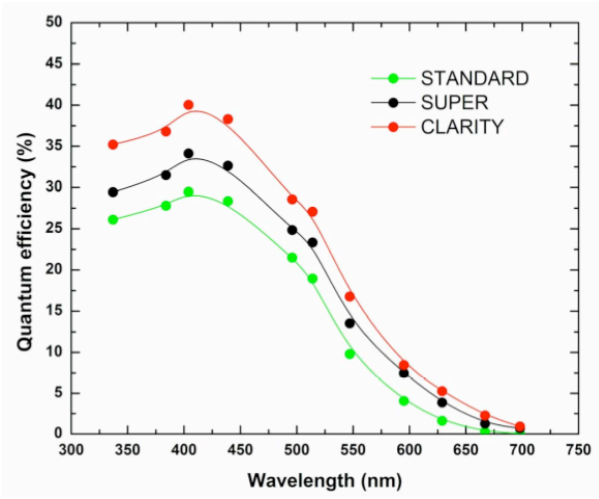

Fig. 4. High efficiency bialkali photocathodes developed by Photonis (Kapusta, et al 2007).

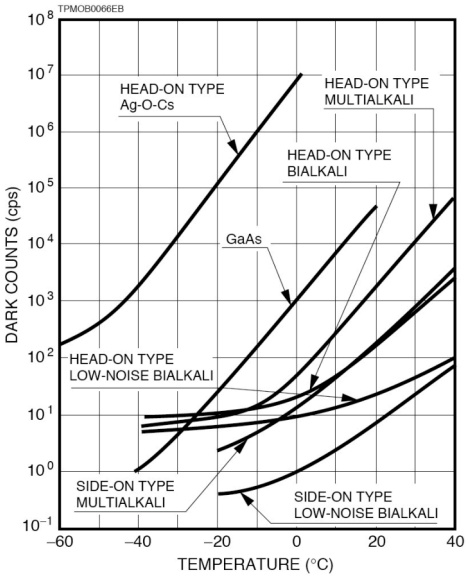

Fig. 5. Background event rates for various photocathode types as a function of temperature.

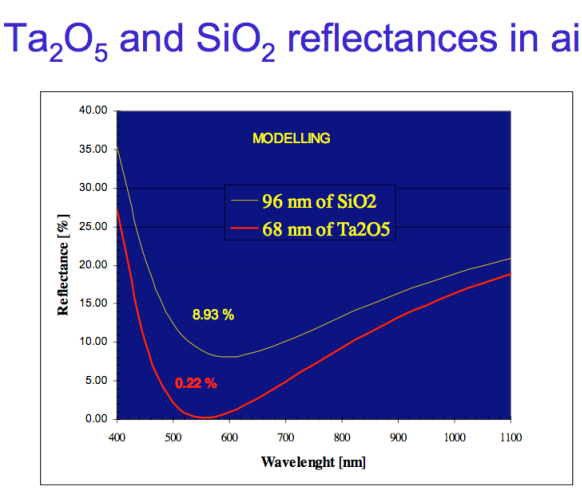

Fig. 6. Effects of anti-reflective coatings on entrance window reflectivity in a water medium, optimized for 530nm light.

The spectrum of Cherenkov light in pure water is shown in Fig. 1. This closely matches the response curve of bialkali photocathodes, which is also shown. Recent state-of-the-art bialkali cathode technology provides at least 20%-25% electron efficiency over the visible spectral range. Present state-of-the-art bialkali cathodes, developed by Photonis and Hamamatsu a few years ago (Mirzoyan et al. 2006), have reached peak levels in excess of 40% (Figs. 3, 4). A combination of recapturing transmitted photons, the optimization of the thickness and composition of the cathode efficiency during the production process, and the use of anti-reflective layers under the cathode (Fig. 6) are responsible for these improvements.[1, 2]

Standard bialkalis fabricated in the Space Science Center (SSL) facilities have similar efficiency (20%) to those that have been traditionally produced. These types of cathode have been made on substrates up to 4" in diameter (Fig. 7, 8). Increasing the size and efficency of bialkali photocathodes in the geometry desired for our project requires somewhat different implementation than used for the Hamamatsu and Photonis PMTs, as a large planar geometry is uniquely different from `tulip' shaped PMT enclosures. A program of optimization, and accommodation can be envisaged which addresses the needs of this program. Small standard size (25mm cathode) and 32.8mm MCP tubes can be employed to establish the correct cathode implementation techniques, and then large test articles can be made to investigate the scale-up issues such as cathode uniformity.

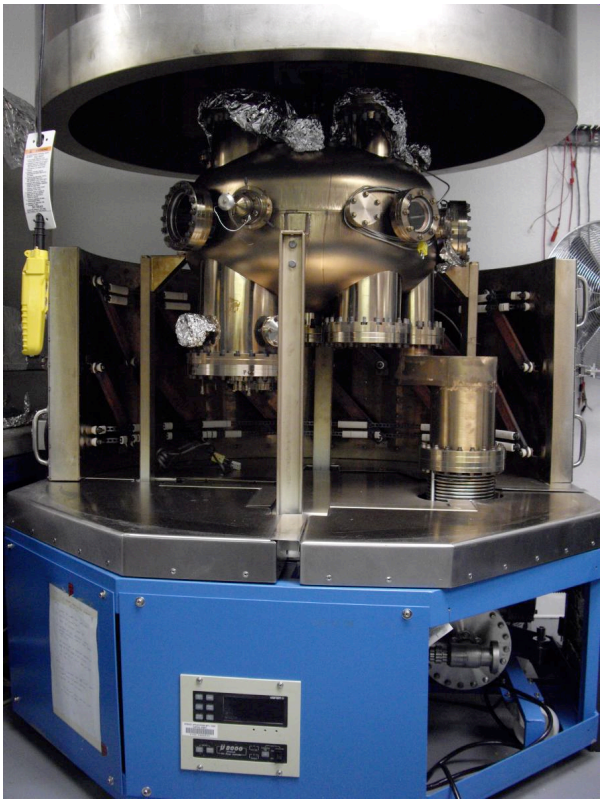

Fig. 7. Large ultrahigh vacuum process tank capable of accommodating 10" photocathodes at SSL.

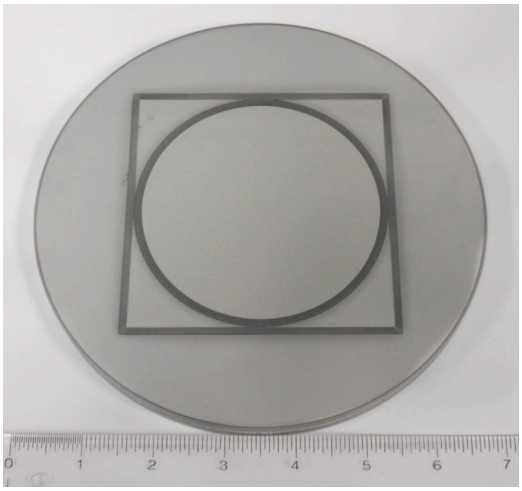

Fig. 8. Large 7" fiber optic used for the entrance window of a bialkali cathode tube.

The choice of the correct input window is part of this process, where borosilicate glass is acceptable but not as good as fused silica for transmission concerns. Application of anti-reflective coatings is extremely important (Fig. 6) to minimize losses over the wavelength

range of interest, and if used under the cathode must be applied before the cathode processing. In situ manipulation of the cathode material deposition follows fairly well defined rules, although optimization of the metals deposition can have substantial effect on the end result. Recapture of transmitted photons requires geometrical design considerations. In our case a flat geometry can be enhanced by the use of highly reflective coatings of electrode material on the top of the MCP, which is directly below the window/cathode. Lastly, attempts were made a number of years ago to deposit bialkali cathodes directly onto MCPs to provide an "opaque" cathode. Opaque cathodes generally have higher efficiencies than semitransparent cathodes because the absorption depth can be made far deeper than the photoelectron emission depth, though use of acute angle surfaces and/or rough surfaces. Normal MCPs are poor substrates as they contain many contaminants. However, the MCP substrates under consideration for this program are chemically inactive. Therefore tests of bialkali photocathodes directly deposited onto the MCP (glass/AAO) surface and down several pore diameters will be investigated. Once these techniques have been investigated in small format geometry, we can apply the results to larger areas and evaluate the efficiency, stability and uniformity of large area (8") substrates and geometries.

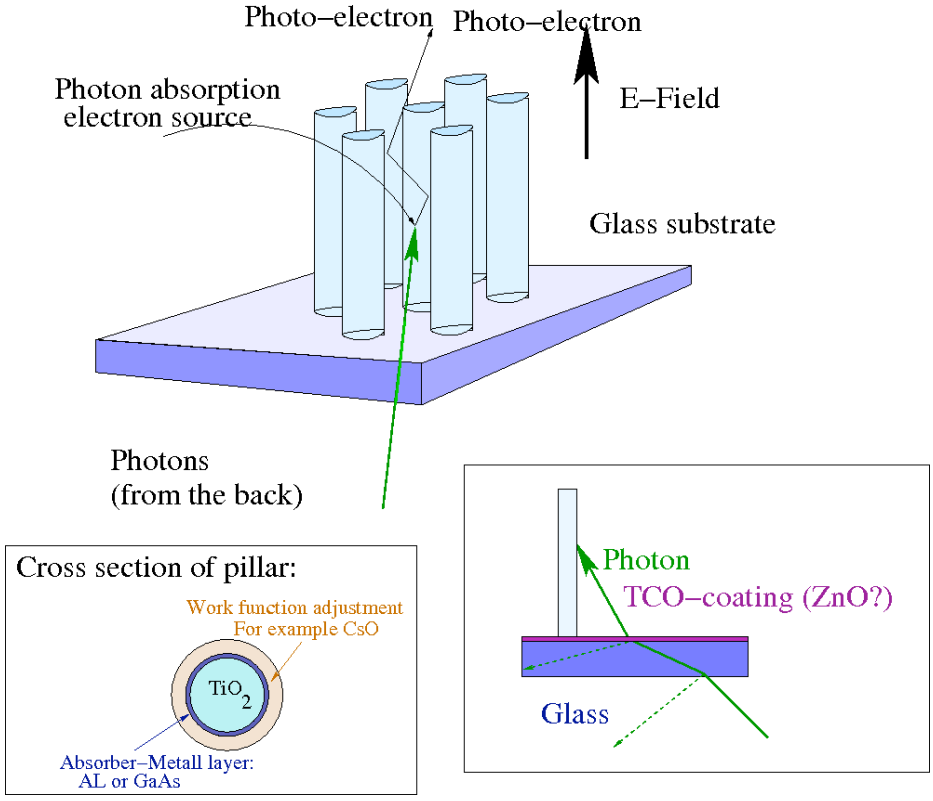

Figure 8: Schematic structure of a morphology-based photo-cathode; the glass substrate (quartz) is coated on one side with a transparent conductive oxide (TCO) which will ensure an equipotential surface. This surface is covered by pillars, each working as an individual NEA-cathode. The structure will act like a photon trap reducing reflection losses and increasing the effective absorption thickness of the cathode.

In parallel to this established route we want to explore a novel photocathode concept based on a nano-structured morphology. This morphology will increase significantly the surface-to-volume ratio, allows a wide range of band-structure engineering tools to optimize noise/efficiency for a given spectral range, reduce optical reflection losses, and to improve the lifetime of the cathode under relaxed vacuum conditions by reducing ion-etching effects.

By changing the cathode from a flat film to a structured morphology such as pillars, the effective thickness of the cathode will be increased and the reflection losses minimized.[3] One example for such new technologies is the so-called "moth-eye" technology developed for solar cells[4] where the insects' eyes are covered by nanostructured coatings. This creates layers in which the refractive index gradually changes from one to the value of the insects' optical nerve. The resulting effect is very little light is reflected out of the eye. This technology can be transferred to cathode technology. In our case the support structure forming the morphology of the cathode should be transparent and slightly p-doped to avoid charging effects. Each pillar is coated with a nearly intrinsic optically dense semiconductor layer 50-100nm thick, which is terminated with 5-10nm of negative electron affinity (NEA) material. The semiconductor structure of the pillar follows a PIN-diode structure, creating a strong radial electric field in the active area of the pillar resulting in effective electron emission. For similar structures field strengths of about 4V/μm are reported.[5] As shown in Figure 8, the light will penetrate the glass substrate from the backside, and hit one of the pillars. Either the photon will be absorbed in the active area and converted in a photoelectron or it penetrates the pillar and will be absorbed on the backside or on a neighboring pillar. We want to emphasize that the photon will be mainly absorbed in active areas since the support structure is transparent. A moderate field perpendicular to the cathode surface (along the pillar main axis) will extract the electrons from the cathode. Preliminary simulations, shown in Figure 9 based on a not-yet-optimized geometry, show that the transient time of the electron through the cathode is insensitive to the emission angle of the electron. Therefore the timing characteristics will be only slightly broadened (by less than 3.5ps for the given simulation). An interesting aspect of this geometry is that the active area of the cathode is not directly exposed to the positive ion bombardment from the MCP channels since the surface is parallel to the electric field lines. Due to the electric field distribution most of the ions will hit the non-active top of the pillars resulting in no damage.

To design the photocathode coating we will utilize knowledge from planar cathode design. The optical absorption layer, for example 300nm GaAs, is combined with a second strongly *n*-doped thin semiconductor layer. This negative electron affinity (NEA) layer has a reduced work function in comparison to the bare absorption layer and, similar to a *pn*-transition of a diode, introduces an electric field perpendicular to the surface.[6, 7] This field breaks the symmetry and creates a force on the thermalized electrons. The carriers are pushed towards the surface, increasing the electron emission.[6] Typically the NEA layer is formed from a Cs-O thin film of about 10nm-50nm. By changing the stoichiometry of Cs and O the defect concentration can be optimized to result in a strongly n-doped film.[8] The optimization process requires an in-situ measurement of the cathode efficiency during the production process.[9] The introduced electric field permits increasing the absorption layer thickness of the cathode. In addition, the oxide layer is insensitive against oxidation. Over a wide spectral range (250nm-700nm) efficiencies of 20%-26% are reported for planar GaAs-CsO cathodes.[10] The bandgap

of the intrinsic-absorption layer can be widely tuned from 0.4eV to nearly 2.2eV by changing the composition of GaAs to $In_xGa_{(1-x)}As$ or $Al_xGa_{(1-x)}As$ compositions. The layer can be built up either homogeneously or in a layered structure to allow optimization for multiple wavelengths. The noise behavior will depend mainly on the bandgap for intrinsic materials. A comparison with Si-PIN detector technology shows that a bandgap of about 1.2eV results in a negligible noise behavior at a temperature of about 0C. In the case of real materials it will mainly depend on defect densities and interface reconstruction effects, which yield to n-doping creating free electrons. This effect can be minimized by growing excellent film structures and by compensation doping, as it is done in PIN-diode and Si-drift detector technology.

The development of the morphology-based NEA-cathode is based on extensive efforts using nano-technology to create cathodes for other applications like solar cells, and light emitting devices. We propose to develop the structures on the basis of TiO_2-nano rods. TiO_2 based materials provide a large variety of morphologies. Various low and high temperature processes have been reported which results in well-defined morphologies on various

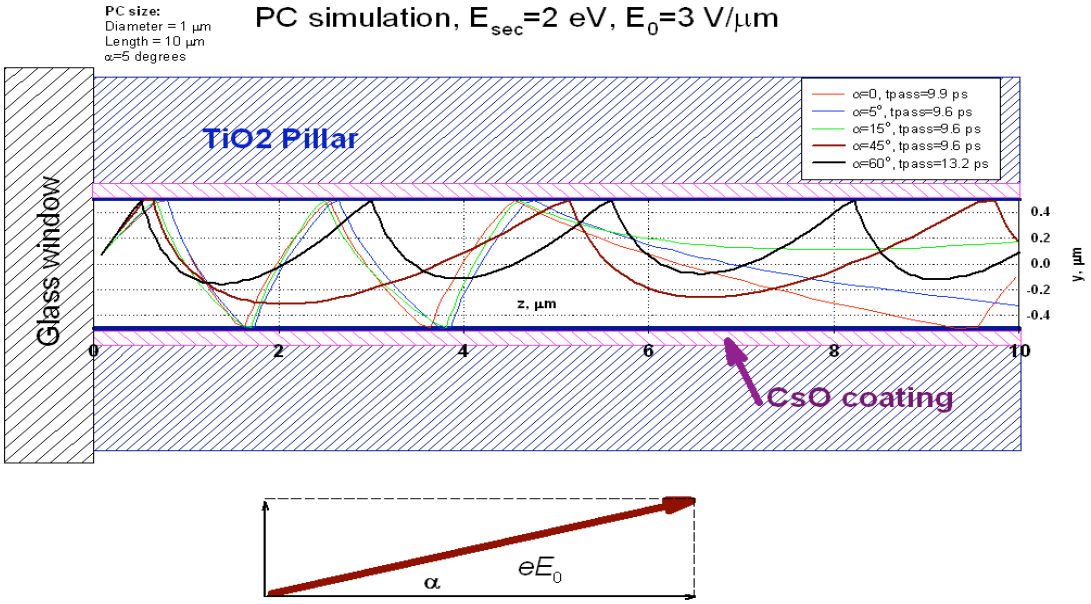

Figure 9: Simulation of the electron path through pillars dependent on various emission angles; the geometry is not optimized. The simulations show that the transient time is insensitive to the emission angle of the electron.

substrates.[11, 12] This material is compatible with atomic layer deposition (ALD) which permits growing a Cr-doped TiO_2 top layer.[13] The ability of coating complex morphologies homogeneously makes ALD an enabling technology. The TiO_2/Cr layer will be p-doped to provide the necessary optical transparence, conductivity to avoid charging effects, and the first layer of the PIN-structure. Alternative p-doped layers may be AlGaAs doped with Si. Multiple variations exist for the growth of the optical absorption and the NEA layer. Following state of the art NEA-flat-cathodes designs, we will use GaAs and CsO layers.[14] We will also explore alternatives such as Ge-based optical absorption layers with Si/Cs/O NEA layers.[15, 16] For highly UV-sensitive cathodes we suggest an Au-CsO combination.[17] All these

layer combinations will be compatible with ALD or similar deposition techniques.[18-21] We want to emphasize that these activities will fully utilize the materials sciences competency of Argonne National Laboratory's Center for Nano-scale Materials, Material Science Division and Electron Microscope Center, as well as the test facilities of the Advanced Photon Source and the computational facilities of the Mathematics and Computer Science Division.

References:

1 M. Kapusta, P. Lavoute, F. Lherbet, et al., 2007 IEEE Nuclear Science Symposium Conference Record, 73 (2007).

2 R. Mirzoyan, M. Laatiaoui, and M. Teshima, Nuclear Instruments & Methods in Physics Research Section a-Accelerators Spectrometers Detectors and Associated Equipment **567**, 230 (2006).

3 W. F. Bogaerts and C. M. Lampert, Journal of Materials Science **18**, 2847 (1983).

4 G. V. Silke L. Diedenhofen, Rienk E. Algra, Alex Hartsuiker, Otto L. Muskens, George Immink, Erik P. A. M. Bakkers, Willem L. Vos, Jaime Gómez Rivas, Advanced Materials **Volume 21**, 973 (2009).

5 J. J. Zou, Z. Yang, L. Qiao, et al., Optoelectronic Materials and Devices Ii **6782**, R7822 (2007).

6 L. N. Dinh, W. McLean, M. A. Schildbach, et al., Physical Review B **59**, 15513 (1999).

7 L. N. Dinh, W. McLean, M. A. Schildbach, et al., Flat-Panel Displays and Sensors - Principles, Materials and Processes. Symposium (Materials Research Society Symposium Proceedings Vol.558)|Flat-Panel Displays and Sensors - Principles, Materials and Processes. Symposium (Materials Research Society Symposium Proceedings Vol.558), 533 (2000).

8 J. S. Huang, Z. Xu, and Y. Yang, Advanced Functional Materials **17**, 1966 (2007).

9 L. Liu, Y. J. Du, B. K. Chang, et al., Applied Optics **45**, 6094 (2006).

10 L. Liu and B. Chang, Advanced Materials and Devices for Sensing and Imaging II **5633**, 339 (2005).

11 X. Chen and S. S. Mao, Chemical Reviews **107**, 2891 (2007).

12 X. B. Chen and S. S. Mao, Journal of Nanoscience and Nanotechnology **6**, 906 (2006).

13 G. H. Takaoka, T. Nose, and M. Kawashita, Vacuum **83**, 679 (2008).

14 B. K. Chang, W. L. Liu, R. G. Fu, et al., Apoc 2001: Asia-Pacific Optical and Wireless Communications: Optoelectronics, Materials, and Devices for Communications **4580**, 632 (2001).

15 J. X. Wu, M. S. Ma, J. S. Zhu, et al., Applied Surface Science **173**, 8 (2001).

16 Goldstei.B and Martinel.Ru, Journal of Applied Physics **44**, 4244 (1973).

17 H. Jinsong, X. Zheng, and Y. Yang, Advanced Functional Materials, 1966 (2007).

18 H. Kim, S. Sohn, D. Jung, et al., Organic Electronics **9**, 1140 (2008).

19 S. Won, S. Go, W. Lee, et al., Metals and Materials International **14**, 759 (2008).

20 H. Kim, H. B. R. Lee, and W. J. Maeng, Thin Solid Films **517**, 2563 (2009).

21 A. I. Persson, B. J. Ohlsson, S. Jeppesen, et al., Journal of Crystal Growth **272**, 167 (2004).

15 Appendix D: Anodized Aluminum Oxide Plates

15 Appendix D: Anodized Aluminum Oxide Plates

15.1. Introduction

A microchannel plate (MCP) is a solid-state electron amplifier that contains an array of micropores (channels) typically imbedded in a lead silicate glass. The surface is chemically treated to enhance secondary electron emission from the walls of the channels.[1] A typical commercially available MCP is built with a channel diameter between 6 and 25 microns, and a channel aspect ratio, i.e. the ratio of length to diameter, between 40 and 100 . The smallest channel diameter of which we are aware in a commercial MCP has a channel diameter of 2.3 microns, as shown in Figure 1a.[2]

The typical lead glass MCP is fabricated through a multi-step process starting with melting of new glass materials, fiber drawing , slicing, polishing, and chemical processing.[2] It is elaborate and expensive, and does not seem suited to scaling up for large-area detection applications. New approaches to MCP fabrication that bypass the limitations of glass technologies and enable scalable low-cost manufacturing of larger-area MCPs with high spatial/temporal resolution and improved lifetime are needed.

Nanoporous anodic aluminum oxide (AAO) has been identified as a possible alternative for glass as the substrate for MCPs, due to its similar hexagonally close packed arrays of cylindrical and uniform pores that are perpendicular to the surface (Figure 1b). The diameter of the pores in typical AAO fabrication can be controlled in the range from ~10 nm to ~ 250 nm, with corresponding pore-to-pore spacing from 30 to 600 nm. Contrary to glass MCPs, AAO can be prepared in a simple wet chemistry process, attracted further interest as a candidate for new MCP design and development.

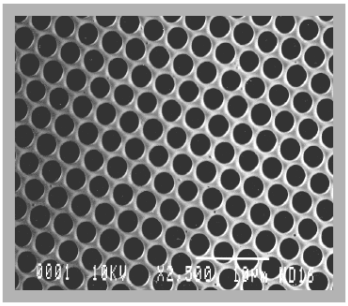

Figure 1a. 2.3 microns commercial MCP from Burle Electro-Optics.

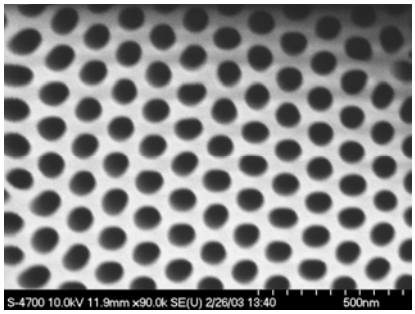

Figure 1b. SEM image of an AAO template with 80 nm pore diameter and 143 nm pore-to-pore distance

AAO has been used as a protective layer over aluminum surfaces in very large scale applications for corrosion prevention as well as metal finishing and decoration. Due to the interest from the areas of nanoscience and technology, starting in 1990-s AAO has been recognized and widely used as templates for nanoscale material synthesis [3-9] In addition, the control of AAO nanostructures has reached a new level recently.[10] Synkera has been using AAO extensively as a nano/microfabrication platform for the development of a variety of products, from membranes for gas separation and nano/ultrafiltration to gas microsensors, BioMEMS and energy conversion materials [11] and has significant related experience.

Although the promise of using AAO for MCP development was recognized in the late 1960-s [12] and further explored in the 1990-s [13], it has not been fully implemented for a number of reasons. ***First***, the typical AAO pore diameter (10 to 250 nm) is too small for creating functional MCPs: (i)

in channels <0.5 μm, the space charge would be excessive for achieving the required gain and high local count rate, (ii) in small pores the electron path is too short to acquire the energy sufficient for secondary electron generation. ***Second***, even for 250 nm channels, the MCP would have to be thin for common aspect ratios and thus unable to withstand the required voltage and too fragile. ***And finally***, no reproducible and controllable processes for uniform modification of the resistance and secondary emission properties were available for high aspect ratio nanopores.

15.2. Challenges in realizing large area low cost MCPs from AAO

The general challenges in realizing large area MCPs for targeted large-area, low-cost detectors are:

- Scaling substrate to large sizes in a batch process to keep the cost down
- Achieving a channel diameter in the range where adequate amplification occurs
- Enabling processing temperatures up to 900°C if photocathodes are to be integrated directly onto the MCP surface

Although several alternative technologies could be considered for this task (including capillary-based glass substrates, porous Si-based, microsphere, and fiber mat plates, etc), using intrinsic pores of AAO is highly attractive due to a number of inherent advantages, such as low cost, scalability, uniformity and thermal range. However, for AAO to be the substrate of choice for functional large area ceramic MCPs, several specific challenges listed below have to be addressed with our approaches outlined in parentheses.

- Developing AAO with a pore diameter ≥ 0.5 μm. (The largest pore diameter demonstrated in the open literature is 250 nm; Synkera has demonstrated feasibility of 0.4 - 0.6 μm channels in small prototypes. New electrolytes and anodization methods need to be developed for achieving larger diameters).
- Retaining a channel structure satisfactory for electron amplification and minimized spontaneous field emission. (Increasing pore size often leads to a heavily distorted and convoluted network of pores. Surface patterning demonstrated by ANL, and stable anodization regimes under development at Synkera could be used to alleviate this issue).
- Maximizing the open area ratio and achieving a funnel shape to maximize the efficiency of the first strike. (Controlled anodization and etching approaches).
- Realizing required channel resistance and secondary emission coefficient. (ALD was confirmed to be the method of choice, Section 14 appendix E).
- Scaling the processes involved in large pore formation to the required size (8”x8”). (Scale-up of the AAO with large pores is far from trivial; issues of uniform current density distribution, heat dissipation and others will be addressed).
- Achieving mechanical integrity in the scaled 8”x8” size for a given MCP thickness. (Will require proper support in the detector body; an Al rim and internal frame structure could be used).
- Demonstrating targeted cost saving

While there are significant challenges remaining in the development of AAO-based MCPs, if realized, it would represent a technical breakthrough and a significant market opportunity for a new generation of large-area ceramic MCPs at a cost below that of other methods.

15.3. Current Status

Conventional AAO has been prepared in sulfuric acid (10-30 nm pores), oxalic acid (40-100 nm pores), and phosphoric acid (larger than 100 nm pores). These pore diameters are one to two orders of magnitude smaller than those of the current MCP. In order not to deviate too much away from a region of the channel sizes that is known to be working very well in MCPs, we plan to bring the AAO pore size closer to the micron and sub-micron region. The prior work related to overcoming the challenges in achieving required AAO channel dimensions, ordered structure and scale, is described in the following subsections.

15.3.1. The bottom-up approach to achieve large Pore Sizes

In order to prepare pores in the 100 to 500 nm region, we will take the hard anodization approach recently reported in the literature.[10] Although the method has been used in industry for surface coating, it is not common in the research community. The reason is that the pore structure is not well-ordered and is difficult to control. This method utilizes a DC anodization potential between 110 and 160 V. Temperature control during anodization is very important to avoid melt-down of the Al surface. Using this approach (hard anodization), ANL has shown a highly ordered pore array with a pore diameter of 240 nm and a pore distance of 350 nm and have successfully prepared an 1" diameter AAO membrane (Figure 2).

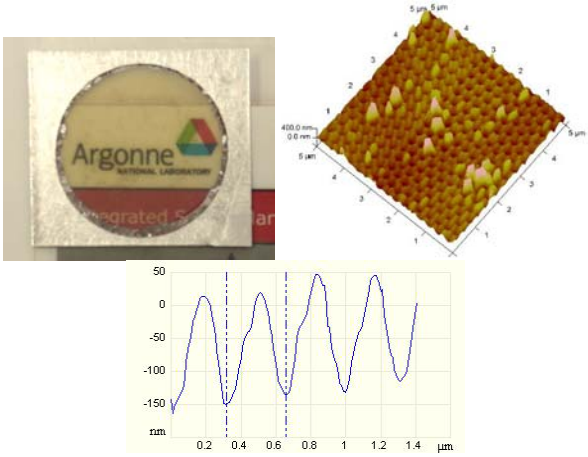

Figure 2. AAO after second anodization at 140 V with Al removed: photograph (left), AFM image of 5x5 μ^2 scan (right), and pore size measurements (bottom).

We plan to utilize our newly explored methods to design and develop new AAO based microchannel plates with larger (0.5-1 µm) pores. To address the challenge of the large pore size for the application of AAO for MCPs, Synkera has been developing new anodization electrolytes and anodization methods that allow significantly expanded boundaries of AAO pore dimensions. To date, Synkera has demonstrated feasibility of channels with diameter up to 0.5-0.6 µm and pore-to-pore distance as high as 1.2 µm (Figure 3a, left). The surface of this AAO has a cone-shaped entrance, a 'funnel' , which when enhanced by chemical etching, can be exploited to create a surface that would increase the efficiency of the "first strike". AAO of this type withstands processing temperatures up to 1100°C without loss of integrity and is being used for the development of the preliminary prototypes of 25 mm MCPs.

15.3.2. AAO Scale-Up

In related prior work on AAO-based gas separation membranes, Synkera successfully scaled the processes and produced free-standing AAO membranes with active areas as large as 8" x 14", on an Al rim (11"x18") for mechanical support (Figure 3b). We will use this relevant AAO scale-up approach and experience to scale the large-pore anodization processes to support the fabrication of scaled 8"x8" MCP substrates.

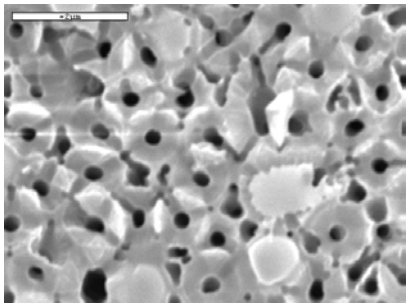

Figure 3a. Surface view of the AAO with pore diameter in the 0.4–0.6 μm range (Synkera). Note the funnels surrounding each pore opening (the circular areas covering most of the surface).

Figure 3b. The world largest AAO membrane (with conventional pores) supported on an Al rim, produced at Synkera Technologies Inc.

15.3.3. Pore Ordering

To complement the bottom-up approach and to reach required pore ordering with a pore-to-pore distance in the 0.5-5 micron region, we propose to combine novel anodization processes that intrinsically support a large pore period, with patterning of the surface of Al to guide the pore initiation process. Pore ordering in AAOs is desirable because device testing results may be readily compared with that from simulation.

We have access to sophisticated facilities that allow exploration of pore ordering. The 2-10 micron pore diameter is where the current MCP operates, and it will be useful to get into this region so that in-depth comparison between porous lead silicate and ALD coated AAO membranes can be done. The following techniques for surface patterning are available to us at the Argonne Center for Nanoscale Materials (CNM): 1) Focused ion beam (FIB), 2) Photolithography, 3) Laser writer, 4) Nanoimprint and indentation techniques. These methods are briefly discussed here.

1) The FIB is a patterning tool. One can generate nearly any patterns in three-dimensions. A hexagonally closed packed (hcp) pattern has been generated over Al (Figures 4a and b) with use of FIB to drill holes on the surface. These holes on the surface will then be used to develop pores through anodization with pore-to-pore distance at exactly 0.5 micron. The pattern is perfect but the main drawback is that FIB is a serial technique and it is expensive and time consuming for a large area. However, for a small area (cm^2), this is a perfect tool for making a prototype for initial testing and proof of concept experiment.

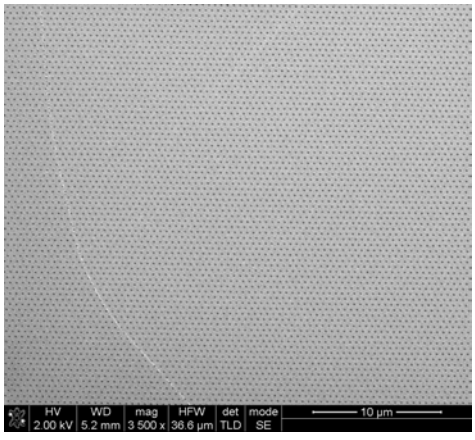

Figure 4a. hcp pattern fabricated at ANL/CNM over Al with use of FIB, 10 μm scale bar.

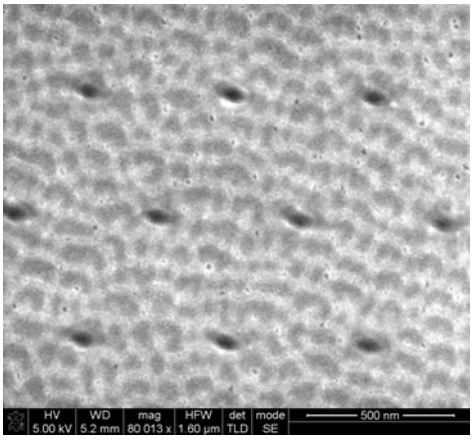

Figure 4b. Same hcp pattern over Al showing 500 nm pore distance, 500 nm scale bar.

2) Photolithography. This is a very good

tool for large areas. To prepare the desired pattern, one needs to first develop a photomask. For large scale applications, once the desired pattern is set, this technique will be very useful.
3) Laser writer. This is a fast prototyping tool. No photomask is needed. One can generate a set of patterns with variable parameters quickly. For our current exploratory research, the laser writer is a useful tool.
4) Nanoindentation. We will first generate a set of patterns with use of a laser writer. After developing the pattern, the features can be coated with a layer of ultra-nano-crystalline diamond (UNCD) to prepare a hardened stamp. The pattern can be repeated over a large area with such a stamp. Other bottom-up approaches, such as nanosphere imprint [14], could be also used for this purpose. The textured surface will then be anodized in the conditions that match the pore period of the pattern to fabricate the desired pore structure. We have all these top-down fabrication processes available to us. In addition to the use of a single piece of equipment, new processes will be developed to utilize several techniques together in order to achieve the goal of making large area detectors.

15.3.4. Pore shape design and development

According to simulation, a funnel shaped pore opening is beneficial to enhance the initial photoconversion and secondary electron emission. Work along this direction has not been reported in the literature. The desired pore configuration for this proposed work is a funnel shaped opening followed with a narrow straight pore. It should be noted that the pore opening in AAO has naturally conical shape, especially if pre-anodization step described above was used to pre-organize the pore lattice. This shape could be further enhanced during the pore widening by chemical etching. Thus, early in the project we will further explore this effect in order to form the desired surface topology. Additional approaches to pore shaping can be explored as well, if needed.

References

[1] J.L. Wiza, "Microchannel plate detectors", *Nuclear Instruments and Methods*, *162* 587-601 **1979**.

[2] B. Laprade and R. Starcher, "The 2 micron pore microchannel plate development of the world's fastest detector", **2001**, http://www.burle.com/cgi-bin/byteserver.pl/pdf/2micron2.pdf

[3] D. Routkevitch, T. Bigioni, M. Moskovits, J. M. Xu, Electrochemical Fabrication of CdS Nano-Wire Arrays in Porous Anodic Aluminum Oxide Templates, *J. Phys. Chem*., *100*(33), 14037-14047 **1996**.

[4] D.Routkevich, A. Tager, J. Haruyama, D. Al-Mawlawi, M. Moskovits and J. M. Xu, Nonlithographic Nanowire Arrays: Fabrication, Physics and Device Applications, Special Issue of *IEEE Trans. Electron Dev.* on "Present and Future Trends in Device Science and Technologies", *43*(10), 1646-1658 **1996**.

[5] Z. L. Xiao, C. Y. Han, U. Welp, H. H. Wang, W. K. Kwok, G. A. Willing, J. M. Hiller, R. E. Cook, D. J. Miller, G. W. Crabtree, "Fabrication of Alumina Nanotubes and Nanowires by Etching Porous Alumina Membranes", *Nanoletters* 2(11), 1293-1297, **2002**.

[6] H.H. Wang, C.Y. Han, G.A. Willing, Z. Xiao, "Nanowire and Nanotube Syntheses Through Self-assembled nanoporous AAO Templates", *Mat. Res. Soc. Symp. Proc.*, *775*, 107, **2003**.

[7] C.Y. Han, Z.L. Xiao, H.H. Wang, G.A. Willing, U. Geiser, U. Welp, W.K. Kwok, S.D. Bader, G.W. Crabtree, "Porous anodic aluminum oxide membranes for nanofabrication" *ATB Metallurgie*, *43*, 123, **2003**.

[8] G. Xiong, J. W. Elam, H. Feng, C. Y. Han, H.-H. Wang, L. E. Iton, L. A. Curtiss, M. J. Pellin, M. Kung, H. Kung, P. C. Stair, "Effect of Atomic Layer Deposition Coatings on the Surface Structure of Anodic Aluminum Oxide Membranes", *J. Phys. Chem.B*. *109*, 14059-14063, **2005**.

[9] C.Y. Han, G.A. Willing, Z. Xiao, and H.H. Wang, "Control of the Anodic Aluminum Oxide Barrier Layer Opening Process by Wet Chemical Etching", *Langmuir 23,* 1564-1568 **2007**.

[10] W. Lee, R. Ji, U. Gösele, and K. Nielsch, "Fast fabrication of long-range ordered porous alumina membranes by hard anodization", *Nat. Mater.* 5, 741-747, **2006**.

[11] See http://www.synkera.com, including links to "Self-organized Anodic Aluminum Oxide" and "Ceramic MEMS" sections; also A. Govyadinov, P. Mardilovich, D. Routkevitch, et al, Anodic Alumina MEMS: Applications and devices, Microelectromechanical Systems (MEMS) 2000, *Proc. ASME Int. Mech. Eng. Congress*, Nov. 5-10, 2000, Orlando, Florida, Vol. 2, ASME, New York, 313-318 **2000**.

[12] US Patents ## 362633, 3724066, 3760216.

[13] A. Govyadinov et. al., *Nucl. Instr. Methods Phys. Res.*, A 419, 667-675 **1998**; F. Emel'yanchik, A. Govyadinov et al., *Appl. Surf. Sci*., ,*111*, 295-301 **1997**.

[14] S. Fournier-Bidoz, V. Kitaev, D. Routkevitch, I. Manners, G. A. Ozin, Highly Ordered Nanosphere Imprinted Nanoporous Anodic Alumina (NINA), *Adv. Mater., 16* (23-24), 2193-2196 **2004**.

16 Appendix E: Atomic Layer Deposition for the Fabrication of Microchannel Plates

Atomic Layer Deposition for the Fabrication of Microchannel Plates

In this portion of the project we will use atomic layer deposition (ALD) thin film techniques to modify anodic aluminum oxide (AAO) membrane templates to fabricate microchannel plate (MCP) detectors. The ALD will be used to apply resistive coatings to the inner surfaces of the AAO membranes to allow the MCP pores to recharge following an amplification event. In addition, we will use ALD to deposit a thin layer of material with high secondary electron coefficient (SEC) on the inner walls of the pores to improve the gain. This layer may be applied uniformly throughout the AAO nanopores to produce a continuous dynode device as is utilized in conventional MCPs. Alternatively, we will apply the high SEC layer at well-controlled depth locations along the AAO nanopores to produce a discrete dynode structure similar to the structure of photomultiplier tubes that may yield a narrower pulse width. Finally, ALD will also be used to apply a photocathode layer on the input side of the MCP device.

Atomic layer deposition (ALD) is a thin film growth technique that is currently used for the mass production of semiconductor electronics[1]. ALD uses alternating, saturating reactions between gaseous precursor molecules and a substrate to deposit films in a layer-by-layer fashion[2]. By repeating this reaction sequence in an ABAB… pattern, films of virtually any thickness (atomic monolayers to microns) can be deposited with atomic layer precision (Fig 1).

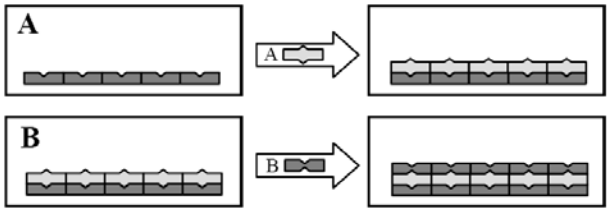

Figure 1. Illustration of AB sequence for atomic layer deposition of one monolayer. Notches in the starting substrate for reaction A represent discrete reactive sites. Exposing this surface to reactant A results in the self-limiting chemisorption of a monolayer of A species. The resulting surface becomes the starting substrate for reaction B. Subsequent exposure to molecule B covers the surface with a monolayer of B species. Consequently, one AB cycle deposits one monolayer of compound AB and regenerates the initial surface.

This alternating reaction strategy eliminates the “line of site” or “constant exposure” requirements that limit conventional thin film methods such as physical- or chemical-vapor deposition, and offers the unique capability to coat complex, 3-dimensional objects with precise, conformal layers. These attributes make ALD an ideal method for applying precise, conformal coatings over porous or high-aspect ratio substrates including AAO membranes[3, 4].

As an example of the ALD process, consider the following binary reaction sequence for Al_2O_3 in which the surface species are designated by asterisks[5]:

A) $OH^* + Al(CH_3)_3 \rightarrow O\text{-}Al(CH_3)_2^* + CH_4$

B) $O\text{-}Al\text{-}CH_3^* + H_2O \rightarrow O\text{-}Al\text{-}OH^* + CH_4$

In reaction A, the substrate surface is initially covered with hydroxyl (OH) groups. The hydroxyl groups react with trimethyl aluminum vapor ($Al(CH_3)_3$, TMA) to deposit a monolayer of aluminum-methyl groups and give off methane (CH_4) as a byproduct. Because TMA is inert to the methyl-terminated surface, further exposure to TMA yields no additional growth beyond one monolayer. In reaction B, this new surface is exposed to water vapor regenerating the initial hydroxyl-terminated surface and again releasing methane. The net effect of one AB cycle is to deposit one monolayer of Al_2O_3 on the surface. Despite the atom-by-atom growth approach, thick films can be applied efficiently on planar surfaces since the individual AB cycles can be performed in less than 1 second. For nanoporous surfaces, the AB cycle time is increased to allow the gaseous precursors to diffuse into the nanopores[3].

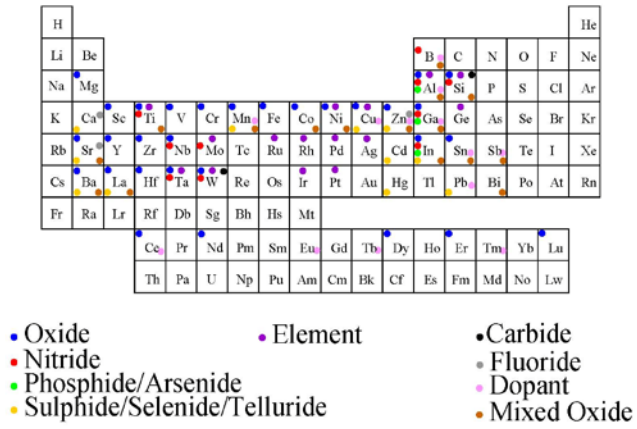

Figure 2: Materials that can be prepared using ALD.

A broad range of materials can be deposited by ALD including most metal oxides, as well as metal nitrides, phosphides and selenides, and many elemental materials (Fig. 2). This flexibility makes ALD a very attractive since a rich variety of transparent conducing materials can be prepared using the same equipment. It is also straightforward to make multilayered films, as well as doped, blended, and graded materials.

ALD of Controlled-Resistance Layers

As shown in Figure 2, ALD can be used to prepare thin film coatings of a broad range of materials. Additionally, by depositing alternating layers of two or more different materials, the resulting physical, chemical, and electronic properties of the compound material can be tuned between those of the components. In particular, ALD can be used to prepare thin film coatings with controlled resistance by blending together materials with high and low resistance such as Al_2O_3 and ZnO. Al_2O_3 ALD is accomplished using alternating exposures to TMA and H_2O while ZnO uses alternating exposures to diethyl zinc (DEZ) and H_2O. By controlling the relative number of TMA/H_2O and DEZ/H_2O cycles, $AlZn_xO_y$ alloy films can be deposited with precise control over both composition and thickness and the resistivity can be adjusted over a very wide range from 10^{-3} to 10^{16} Ohm cm (Figure 3)[6, 7]. By depositing conformal layers of these $AlZn_xO_y$ alloy films inside of the AAO nanopores, the resistance across the MCP can be controlled.

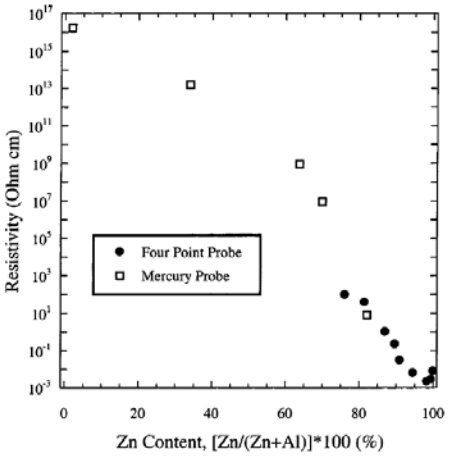

Figure 3: Resistivity of ZnO/Al2O3 alloy films prepared on glass surfaces determined using four-point probe and mercury probe measurements.

ALD in AAO

Figure 4 shows an example of where we have used ALD of Al_2O_3 to tune the pore diameter of AAO membranes. In this applications, the AAO membranes are to be used as nanoporous catalytic membranes for the selective oxidation of hydrocarbons[8, 9]. AAO membranes having an initial pore

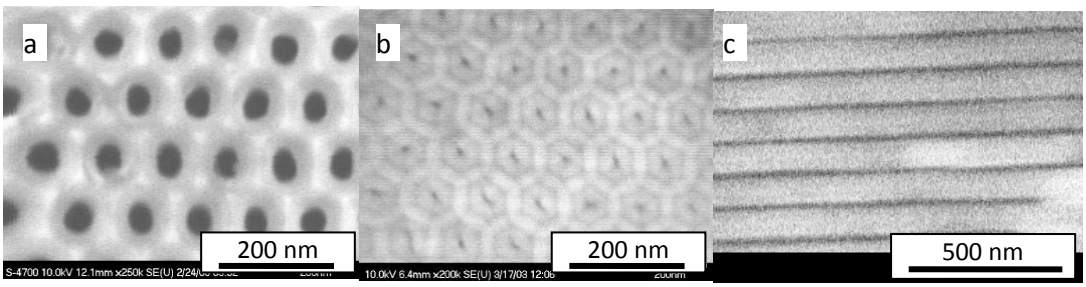

Figure 4: Plan view SEM images of AAO membrane before (a) and after (b) 15 nm ALD Al_2O_3 coating. (c) Cross-sectional SEM image after coating recorded from middle of membrane. Conformal Al_2O_3 coating extends to middle of AAO.

diameter d=40 nm and pore length L=70 micron were coated by 15 nm ALD Al_2O_3 to achieve a final pore diameter of d=10 nm. By tuning the AAO pore diameter, we can control the contact time between the reactants and the catalyst. An additional function of the Al_2O_3 coating is to cover up the aluminum oxalate and other impurities in the AAO that are introduced during the anodization step. These impurities may cause a different initial reactivity of the AAO surface towards the Al_2O_3 ALD precursors. Plan view and cross sectional SEM images (Fig. 4) demonstrate that the very high aspect ratio ($L/d \sim 10^4$) pores are conformally coated using ALD. We have used similar techniques to apply conformal coatings of transparent conducting oxide layers such as aluminum-doped zinc oxide and tin-doeped indicum oxide inside of AAO membranes to fabricate high surface area electrodes for dye-sensitized solar cells[10, 11].

ALD Stripe Coating

Recently we have developed an ALD method for depositing materials at specific depth locations within nanoporous templates such as AAO membranes[12]. We will use this method to fabricate a discrete dynode structure inside of the AAO. This method uses the passivating effect of one ALD precursor to prevent the chemisorption of a second precursor applied in a subsequent exposure. For instance, after a hydroxylated surface has been exposed to trimethyl aluminum (TMA), this surface will be unreactive towards the chemisorption of diethyl zinc (DEZ). Infiltration of nanoporous materials occurs via Knudsen diffusion so that the reactive sites tend to fill in order starting from the pore entrance[3]. Consequently, the pore entrance can first be reacted using a sub-saturating TMA exposure. During the subsequent DEZ exposure, the DEZ will only adsorb on the interior pore surfaces further down from where the TMA was applied. The TMA and DEZ exposures can be followed by a saturating H_2O

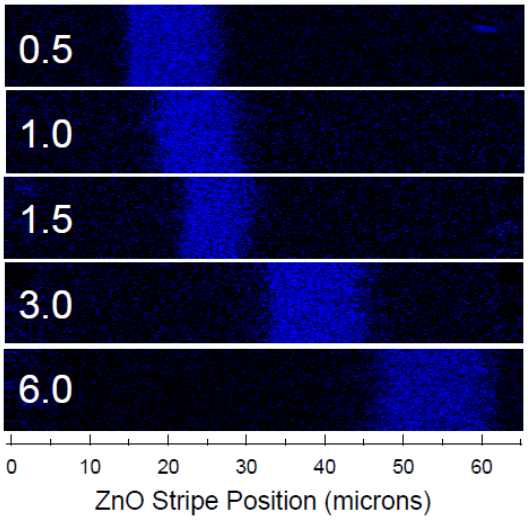

Figure 5: (a) Zn elemental distibution in cross-sectional specimens of AAO membranes determined using EDAX versus the TMA exposure time. Increasing TMA exposure time shifts ZnO stripe to greater depth.

exposure to form the corresponding metal oxides and repopulate the surfaces with hydroxyl groups. By repeating this TMA/DEZ/H_2O sequence, a ZnO "stripe" is formed in which the depth location and width are controlled by the durations of the TMA and DEZ exposures, respectively. This effect is illustrated in Figure 5. In addition to ZnO, we have demonstrated this stripe coating capability for a range of other ALD materials including MgO and TiO_2 and we also have deposited multiple stripes within AAO pores. By applying these methods to materials with high secondary electron coefficients, we intend to fabricate discrete dynode structures within the AAO pores.

Past Experience and Expertise: Elam and Pellin have pioneered the use of ALD technology to modify AAO templates for applications in catalysis and photovoltaics. Together with Libera, they have developed ALD stripe coating methods.

Facilities: Argonne has three ALD coating systems located in two well-equipped laboratories (Figure 6). These novel viscous flow atomic layer deposition (ALD) reactors are capable of depositing films of any thickness with atomic layer precision. These reactors utilizes a hot-wall tube furnace design to accommodate a variety of substrates including porous membranes, aerogels, and powders and are equipped with ten separate chemical precursor introduction channels enabling the fabrication of a host of single component and composite films. The Argonne ALD reactors are equipped with an in-situ quartz crystal microbalance configured for high temperature operation in an ALD environment allowing real time film growth measurements with sub-monolayer precision, and also a mass spectrometer for in-situ monitoring. We are in the currently building a fourth ALD coating system for plasma enhanced atomic layer deposition that will be operational when this project commences and available for completing the

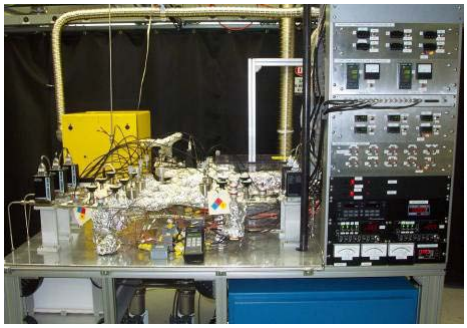

Figure 6: ALD coating system at Argonne

project tasks. In addition, we have nearly completed a scaled-up ALD coating system capable of coating 100g of high surface area powders for catalysis.

At Argonne we have a host of analytical tools suitable for analyzing the thin film coatings in this project. These tools include a variable angle spectroscopic ellipsometer (J. A. Woolam M2000V), stylus profiler (Ambios XP1), Raman microprobe spectrometer (Renishaw RM2000), UV-Vis spectrophotometer with diffuse reflection/absorption capabilities (Cary 5000), x-ray fluorescence spectrometer (Oxford ED2000), x-ray photoelectron spectrometer (Perkin-Elmer), powder x-ray diffractometer (Rigaku Miniflex), and BET surface area measurement systems. We also have access to world-class scanning- and transmission-electron microscopy analysis at the Argonne Electron Microscopy Center, including a well-equipped specimen preparation laboratory, and a dual-beam FIB system. We also have a complete chemical preparation laboratory.

1. Ritala, M. and M. Leskela, *Atomic Layer Deposition*, in *Handbook of Thin Film Materials*, H.S. Nalwa, Editor. 2001, Academic Press: San Diego. p. 103.
2. George, S.M., A.W. Ott, and J.W. Klaus, *Surface Chemistry for Atomic Layer Growth.* Journal of Physical Chemistry, 1996. **100**: p. 13121-13131.
3. Elam, J.W., D. Routkevitch, P.P. Mardilovich, and S.M. George, *Conformal Coating on Ultrahigh-Aspect-Ratio Nanopores of Anodic Alumina by Atomic Layer Deposition.* Chemistry of Materials, 2003. **15**(18): p. 3507-3517.
4. Elam, J.W., G. Xiong, C.Y. Han, H.H. Wang, J.P. Birrell, U. Welp, J.N. Hryn, M.J. Pellin, T.F. Baumann, J.F. Poco, and J.H. Satcher, *Atomic Layer Deposition for the Conformal Coating of Nanoporous Materials.* Journal of Nanomaterials, 2006. **2006**: p. 1-5.
5. Ott, A.W., J.W. Klaus, J.M. Johnson, and S.M. George, *Al2O3 thin film growth on Si(100) using binary reaction sequence chemistry.* Thin Solid Films, 1997. **292**(1-2): p. 135-144.
6. Elam, J.W. and S.M. George, *Growth of ZnO/Al2O3 Alloy Films Using Atomic Layer Deposition Techniques.* Chemistry of Materials, 2003. **15**: p. 1020-1028.
7. Elam, J.W., D. Routkevitch, and S.M. George, *Properties of ZnO/Al2O3 Alloy Films Grown Using Atomic Layer Deposition Techniques.* Journal of the Electrochemical Society, 2003. **In Press**.
8. Pellin, M.J., P.C. Stair, G. Xiong, J.W. Elam, J. Birrell, L. Curtiss, S.M. George, C.Y. Han, L. Iton, H. Kung, M. Kung, and H.H. Wang, *Mesoporous catalytic membranes: Synthetic control of pore size and wall composition.* Catalysis Letters, 2005. **102**(3-4): p. 127-130.
9. Stair, P.C., C. Marshall, G. Xiong, H. Feng, M.J. Pellin, J.W. Elam, L. Curtiss, L. Iton, H. Kung, M. Kung, and H.H. Wang, *Novel, uniform nanostructured catalytic membranes.* Topics In Catalysis, 2006. **39**(3-4): p. 181-186.
10. Martinson, A.B.F., J.W. Elam, J.T. Hupp, and M.J. Pellin, *ZnO Nanotube Based Dye-Sensitized Solar Cells.* Nano Letters, 2007(7): p. 2183-2187.

11. Martinson, A.B.F., J.W. Elam, J. Liu, M.J. Pellin, T.J. Marks, and J.T. Hupp, *Radial electron collection in dye-sensitized solar cells.* Nano Letters, 2008. **8**(9): p. 2862-2866.
12. Elam, J.W., J.A. Libera, M.J. Pellin, and P.C. Stair, *Spatially controlled atomic layer deposition in porous materials.* Applied Physics Letters, 2007. **91**(24).

17 Appendix F: Biographical Sketches